

# **3D Debris Mobility Assessment Using LS-DYNA**

**GEO Report No. 325**

**R.C.H. Koo**

**Geotechnical Engineering Office  
Civil Engineering and Development Department  
The Government of the Hong Kong  
Special Administrative Region**

# **3D Debris Mobility Assessment Using LS-DYNA**

**GEO Report No. 325**

**R.C.H. Koo**

**This report was originally produced in August 2015  
as GEO Special Project Report No. SPR 4/2015**

© The Government of the Hong Kong Special Administrative Region

First published, February 2017

Prepared by:

Geotechnical Engineering Office,  
Civil Engineering and Development Department,  
Civil Engineering and Development Building,  
101 Princess Margaret Road,  
Homantin, Kowloon,  
Hong Kong.

## **Preface**

In keeping with our policy of releasing information which may be of general interest to the geotechnical profession and the public, we make available selected internal reports in a series of publications termed the GEO Report series. The GEO Reports can be downloaded from the website of the Civil Engineering and Development Department (<http://www.cedd.gov.hk>) on the Internet. Printed copies are also available for some GEO Reports. For printed copies, a charge is made to cover the cost of printing.

The Geotechnical Engineering Office also produces documents specifically for publication in print. These include guidance documents and results of comprehensive reviews. They can also be downloaded from the above website.

These publications and the printed GEO Reports may be obtained from the Government's Information Services Department. Information on how to purchase these documents is given on the second last page of this report.



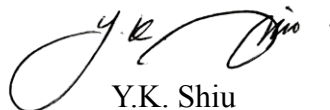
W.K. Pun  
Head, Geotechnical Engineering Office  
February 2017

## Foreword

This report presents a series of back analyses of notable landslide case histories of Hong Kong and several well documented laboratory flume tests using the 3-dimensional advanced numerical program LS-DYNA. Results of a benchmarking exercise between the performance of LS-DYNA and other debris flow simulation programs including 3d-DMM, MADflow and TOCHNOG are also presented.

The initial phase of this study was carried out by Arup (Hong Kong) as part of the Agreement No. 10/2009(GE) - Landslide Investigation Consultancy for Landslides Occurring in Kowloon and the New Territories in 2010 and 2011 under the technical support and supervision of the S&T Division. More recently, Mr R.C.H. Koo has repeated independently the analyses undertaken by Arup under the supervision of Dr J.S.H. Kwan. He also carried out a further study to identify the ranges of key parameters that are suitable for debris mobility assessment.

Dr Carlos Lam assisted in reviewing the derivation of the Drucker-Prager Constitutive model by Arup. Mr C.H. Poon, Mr W.K. Ho and Ms Cherie Cheung provided technical assistance in undertaking the LS-DYNA numerical analyses. Their effort in developing a number of spreadsheets for pre- and post-processing is much appreciated. Contributions from all parties are gratefully acknowledged.



Y.K. Shiu

Chief Geotechnical Engineer/Standards & Testing

## **Abstract**

Debris mobility model has been developed using an advanced finite element package LS-DYNA with a view to facilitating coupled analysis of debris mobility and structural response of debris-resisting barriers subject to debris impact. The coupled analysis may assist in establishing optimised design of debris-resisting structures. The debris mobility model is equipped with a new user-specified module to calculate the resistance to debris motions following Voellmy rheology. A series of back analyses of notable landslide case histories of Hong Kong and several laboratory flume tests using the model of LS-DYNA has been carried out to identify the suitable constitutive model of debris flows and the ranges of key parameters for analysing the landslide mobility. The performance of the LS-DYNA debris mobility model has also benchmarked against other advanced programs including 3d-DMM, TOCHNOG and MADflow.

## Contents

	Page No.
Title Page	1
Preface	3
Foreword	4
Abstract	5
Contents	6
List of Tables	8
List of Figures	9
1 Introduction	10
2 LS-DYNA Numerical Modelling	11
2.1 LS-DYNA Package	11
2.2 Debris Mobility Modelling Using LS-DYNA	11
3 Debris Mobility Back Analysis	12
4 Benchmarking with Other Advanced Programs	13
5 Discussion	16
5.1 Key Parameters Adopted for Back Analysing Landslide Case Histories in Hong Kong	16
5.2 Other Observations	17
6 Further Work	18
7 Conclusions	18
8 References	19
Appendix A: Laboratory Flume Test	22
Appendix B: Open Hillslope Failures	49
Appendix C: Channalised Debris Flows	61
Appendix D: Benchmarking with Other Advanced Programs	78

	Page No.
Appendix E: Yield Function Coefficients of Drucker-Prager Constitutive Model	87



**List of Tables**

Table No.		Page No.
3.1	Back Analysis Cases	13
5.1	Summary of Key Parameters Used	16

## List of Figures

Figure No.		Page No.
1.1	Numerical Framework of Debris-barrier Interaction	10
4.1	Val Pola Landslide (extracted from Crosta et al, 2004)	14
4.2	Simulated Debris Frontal Locations against Time	15
4.3	Val Pola Landslide - LS-DYNA's Simulations	16
6.1	LS-DYNA Simulation on Interaction between Debris Flow and Rigid Barrier (Kwan et al, 2015)	19

## 1 Introduction

Experience shows that landslide debris-resisting structures can provide practical and effective means for mitigating the natural terrain landslide risk. While state-of-the-art engineering approach is being adopted, design of such structures involves a certain degree of uncertainty. There is a need for enhancing the understanding of the dynamic interaction between landslide debris and debris-resisting structures as well as the performance of landslide debris-resisting structures.

Suitable and calibrated numerical models can help the study of the interaction between landslide debris and debris-resisting structures. The numerical models should be able to perform analyses which couples debris mobility modeling and simulation of structural responses of debris-resisting structures (see Figure 1.1).

Depth-averaged continuum numerical models, viz 2d-DMM (Kwan & Sun, 2007; Law & Ko, 2015) and DAN/W (Hung, 1995), provide a practical means to assess the landslide debris runout parameters for routine design of debris-resisting barriers where free field conditions are considered. However, these models are not suitable for incorporation into coupled analysis for the study of debris-barrier interaction. In the depth-averaged formulations, landslide debris mass is discretised into a series of inter-connected slices or columns. The connectivity requirement imposes constraints on the simulations of turbulent mixing and deposition taking place when landslide debris impacts on barriers.

Development of a new debris mobility model using advanced numerical tools was therefore initiated. In 2012, Arup (Hong Kong) was commissioned by Geotechnical Engineering Office (GEO) to study the feasibility of using LS-DYNA for debris mobility analysis. As part of the study, Arup back-analysed some selected landslide cases and laboratory flume tests. In addition, a module of user-specified codes for modeling Voellmy rheology was developed.

Recently, the Standards and Testing (S&T) Division has carried out additional numerical analyses to identify the range of key modelling parameters suitable for the analysis of debris mobility, and benchmarked the performance of LS-DYNA against other well calibrated advanced programs including 3d-DMM, MADflow and TOCHNOG.

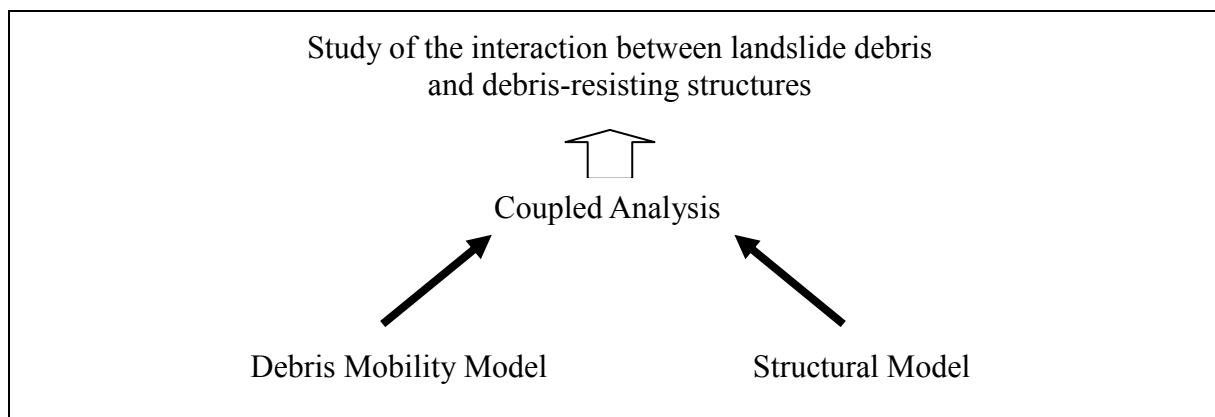


**Figure 1.1 Numerical Framework of Debris-barrier Interaction**

## 2 LS-DYNA Numerical Modelling

### 2.1 LS-DYNA Package

LS-DYNA is a multi-purpose finite element program for analysing the nonlinear response of structures. It has been adopted in different sectors of industry for analysing car crash, metal forming, buildings subject to seismic load, structural damage due to blasting, etc. The program is equipped with calculation modules for modelling dynamic impacts between structures and deformable materials. Arup (2014) carried out a comprehensive review on LS-DYNA and the other software, such as Plaxis 3D, FLAC 3D, MIDAS-GTS, ANSYS and ABAQUS and recommended that LS-DYNA is a program potentially suitable for simulation of debris-structure interaction.

### 2.2 Debris Mobility Modelling Using LS-DYNA

The debris mobility model developed using LS-DYNA carries out continuum analysis. Landslide debris is considered as an undrained, elasto-plastic material. Drucker-Prager (DP) yield criterion (Drucker & Prager, 1952) is assumed to describe the internal rheology of the landslide debris. The DP yield criterion is a pressure-dependent model for determining whether a material has failed or undergone plastic yielding. A conical yield surface is adopted in the DP model to allow for a stable numerical computation (Crosta et al, 2003).

The ground surface of the debris runout path is modelled using rigid shell elements. The resistance to debris runout included in the model comprises (i) basal friction at the interface of the landslide debris and the ground surface, and (ii) damping force proportional to the debris velocity. The Coulomb type basal friction, proportional to the normal stress acting at the debris/ground interface, is assumed. The proportional constant, basal friction coefficient ( $\tan\phi_b$ ), same as the conventional debris mobility analysis, such as 2d-DMM, is adopted. This type of friction has been adopted to establish the basal friction of a rigid block sliding down a ramp (Pudasaini & Hutter, 2007).

In the present LS-DYNA model, in addition to the Coulomb type basal friction, the resistance to debris motion comprises a damping force which is proportional to the velocity squared. The damping force models the resistance brought about by the energy loss due to turbulence of the debris flow, similar to the velocity-dependent term in the Voellmy model adopted by depth-averaged analysis. The damping force ( $F_d$ ) is calculated as per Equation 2.1:

$$F_d = \zeta_d m v^2 \dots\dots\dots (2.1)$$

where  $F_d$  = damping force (in kN)  
 $m$  = mass of debris (in t)  
 $v$  = debris velocity (in m/s)  
 $\zeta_d$  = damping coefficient (in  $m^{-1}$ ).

This damping force is applied to simulate the energy dissipation due to turbulence. In depth-averaged calculations, similar resistance, proportional to  $v^2$ , is considered in the Voellmy rheology (Hungr, 1995). The turbulence resistance ( $F_{turb}$ ) in the Voellmy rheology is defined as:

$$F_{\text{turb}} = m g v^2 / \zeta h \quad \text{.....} \quad (2.2)$$

where  $F_{\text{turb}}$  = turbulence resistance (in kN)  
 $g$  = gravitational acceleration (in  $\text{m/s}^2$ )  
 $h$  = debris thickness (in m)  
 $\zeta$  = turbulence coefficient (in  $\text{m/s}^2$ ).

Voellmy rheology has proven to produce reasonable simulations of channelised debris flows (GEO, 2011). The damping force applied in LS-DYNA analysis is therefore established with reference to the Voellmy rheology. The accelerations (or decelerations) resulted from  $F_d$  is pegged to that of  $F_{\text{turb}}$  (i.e.  $F_d / m = F_{\text{turb}} / m$ ). It follows that:

$$\zeta_d = g / \zeta h \quad \text{.....} \quad (2.3)$$

A user-specified module to implement the above calculations of the damping resistance was developed by Arup (2014) and has been incorporated into LS-DYNA. The above equations are derived from the Voellmy rheological model, which is empirical in nature.

The LS-DYNA debris mobility model handles scalar advection in an Eulerian grid and solves equations of motion based on an Arbitrary Lagrangian-Eulerian (ALE) description of finite-element method. ALE is a finite element formulation in which the computational system is not a priori fixed in space or attached to material. When using the ALE technique in engineering simulations, the computational mesh inside the domains can move arbitrarily to optimize the shapes of elements, while the interfaces of the domains can move along with materials to precisely track the interfaces of a multi-material system (Arup, 2014). Therefore, it can be used to perform comprehensive engineering simulations, including heat transfer, fluid flow and fluid-structure interactions. The computational domain is discretised into an array of hexahedral elements. The elements record the variables, e.g. velocity, strain, etc., of landslide debris mass at various positions within the computational domain. Debris mass transport between elements follows the results of the ALE descriptions.

The model cannot simulate explicitly ground surface erosion in the entrainment process and the subsequent changes in the ground profile after the entrainment. However, entrainment can be simulated by means of releasing additional debris materials at specified locations. No entrainment is considered in this study for simplicity.

### 3 Debris Mobility Back Analysis

A series of back analyses of notable landslide case histories of Hong Kong and the other laboratory flume test studies using the LS-DYNA based debris mobility model has been carried out. The cases for the back analyses can be classified into 3 categories viz. (i) laboratory tests, (ii) open hillslope failures, and (iii) channelised debris flows (see Table 3.1).

Dynamics of dry sand flows were studied in the laboratory flume tests. Friction rheology is therefore used in the back analyses. The measured internal friction angle and basal friction angle reported by the researchers who conducted the experiments have been adopted. It is shown that LS-DYNA model is capable of replicating tests numerically with satisfaction. The calculated debris velocity and debris thickness match well with the

laboratory measurements (see Appendix A).

Friction rheology and Voellmy rheology have been used in the back analyses of the open hillslope failures and the channelised debris flows respectively. The rheological parameters recommended in previous studies (see references listed in Table 3.1) are adopted in the present study. The internal friction angle ( $\phi_{\text{int}}$ ) is back calculated based on the debris velocity records, if available, and the run-out distance observed from field mapping studies. The back analyses of the open hillslope failure cases are presented in Appendix B. Appendix C documents the analyses of the channelised debris flow cases.

**Table 3.1 Back Analysis Cases**

Case No.	Category	Name	Reference
1	Laboratory Flume Test (Dry Sand Flow)	USGS Flume Test	Iverson et al (2004)
2		Deflected Sand Flow	Manzella (2008)
3		HKUST Flume Test	Choi et al (2014)
4	Open Hillslope Failure	1995 Shum Wan Road Landslide	Knill & GEO (2006a)
5		1995 Fei Tsui Road Landslide	Knill & GEO (2006b)
6	Channelised Debris Flow	2008 Yu Tung Road Debris Flow	GEO (2012)
7		2005 Kwun Yam Shan Debris Flow	MGS (2008)
8		1999 Sham Tseng San Tsuen Debris Flow	FMSW (2005)

#### 4 Benchmarking with Other Advanced Programs

The LS-DYNA model has been benchmarked with two advanced debris mobility models viz. TOCHNOG and MADflow. Crosta et al (2003 & 2004) used the two programs to back analyse the 1987 Val Pola Landslide in Italy. The Landslide involved a source volume of about 40 million m<sup>3</sup>. Ground mass detached from the landslide source traveled down into a valley and ran up to the opposite bank of the valley. The reported run-up height is 300 m. The total runout distance on plan is over 1.5 km. Flow separation at the southern flank was observed as indicated in Figure 4.1.

TOCHNOG can carry out two-dimensional or three-dimensional continuum landslide mobility analyses, which is developed based on an Eulerian-Lagrangian finite element code. Eulerian approach is adopted for the analysis in which state variables (e.g. material strain, velocity, etc.) are transported through a stationary mesh. In contrast, MADflow adopts a Lagrangian numerical strategy. It solves depth-averaged shallow water flow equations. Landslide debris mass is discretised into an array of the debris columns. Connectivity between those debris columns is required. MADflow uses adaptive mesh technique to cope with the large distortions of the debris column geometry during simulations.

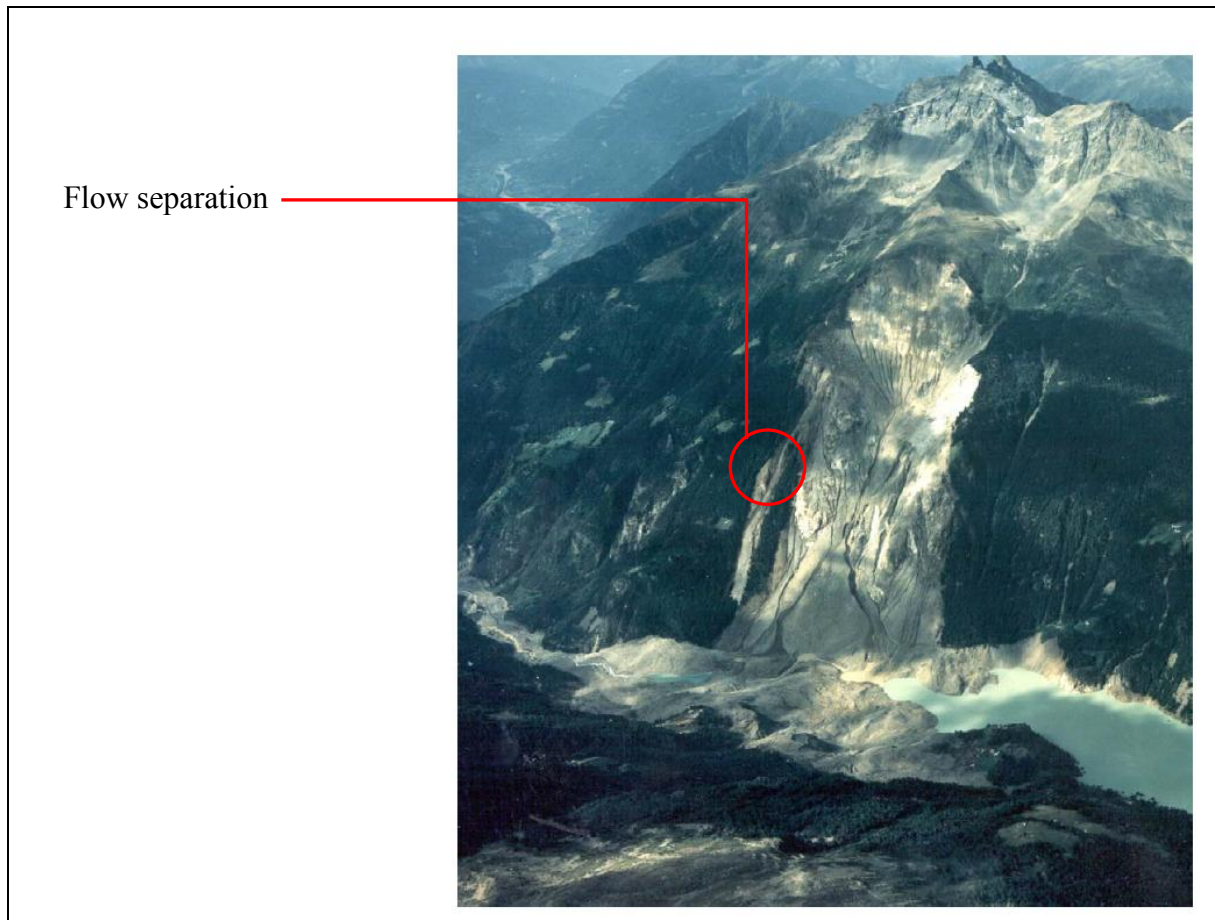


**Figure 4.1 Val Pola Landslide (extracted from Crosta et al, 2004)**

Crosta et al (2003) modelled the 1987 Val Pola Landslide using TOCHNOG. A plain strain analysis (i.e. two-dimensional analysis) was conducted. The landslide debris was assumed to be an elasto-plastic material. Drucker-Prager yield criteria were applied. An internal friction angle of  $45^\circ$  was assumed. A friction model was adopted in the analysis (Voellmy rheology is not included in the TOCHNOG package). The friction angle at the debris-ground interface was taken as  $18^\circ$  (i.e.  $\tan \phi_b = 0.32$ ).

The Lagrangian finite element model used by Crosta et al (2004), namely MADflow as referred by Chen & Lee (2007), does not require the specification of a soil constitutive model, instead, an equivalent pressure coefficient to describe the internal pressure within the debris mass is required. Voellmy rheology was assumed in the calculation of the resistance to debris motion. According to Crosta et al (2004), the MADflow analysis produced the results that best fit site observations when  $\tan \phi_b = 0.1$  and  $\xi = 200 \text{ m/s}^2$ . The calculated mean debris velocity is about 31.4 to 34.6 m/s before the debris reached the valley. The corresponding mean debris thickness was estimated to be in the order of 40 m. The equivalent basal friction coefficient can be estimated as  $0.25 (= \tan \phi_b + v^2 / \xi h = 0.1 + 35^2 / (200 \times 40))$ , which is in the same order of magnitude of that used by Crosta et al (2003), i.e. 0.32.

In the present benchmarking exercise, LS-DYNA model has been used to carry out a three-dimensional analysis of the Val Pola Landslide. The input parameters same as the TOCHNOG analysis are adopted because both models simulate the internal rheology of the landslide debris using Drucker-Prager yield criteria.

Figure 4.2 compares the debris frontal location calculated by LS-DYNA, TOCHNOG and MADflow. It shows that results of LS-DYNA and MADflow are similar. Both programs conduct three-dimensional analysis. They estimated that landslide debris front could have arrived at the bottom of the valley at 34 seconds after the onset of the landslide. This compares well with the estimation of Crosta et al (2004) of which the arrival time could be around 35 seconds. However, TOCHNOG estimates that the arrival time is 50 seconds. This could be due to the over-estimation on the basal friction by the plain strain analysis of TOCHNOG.

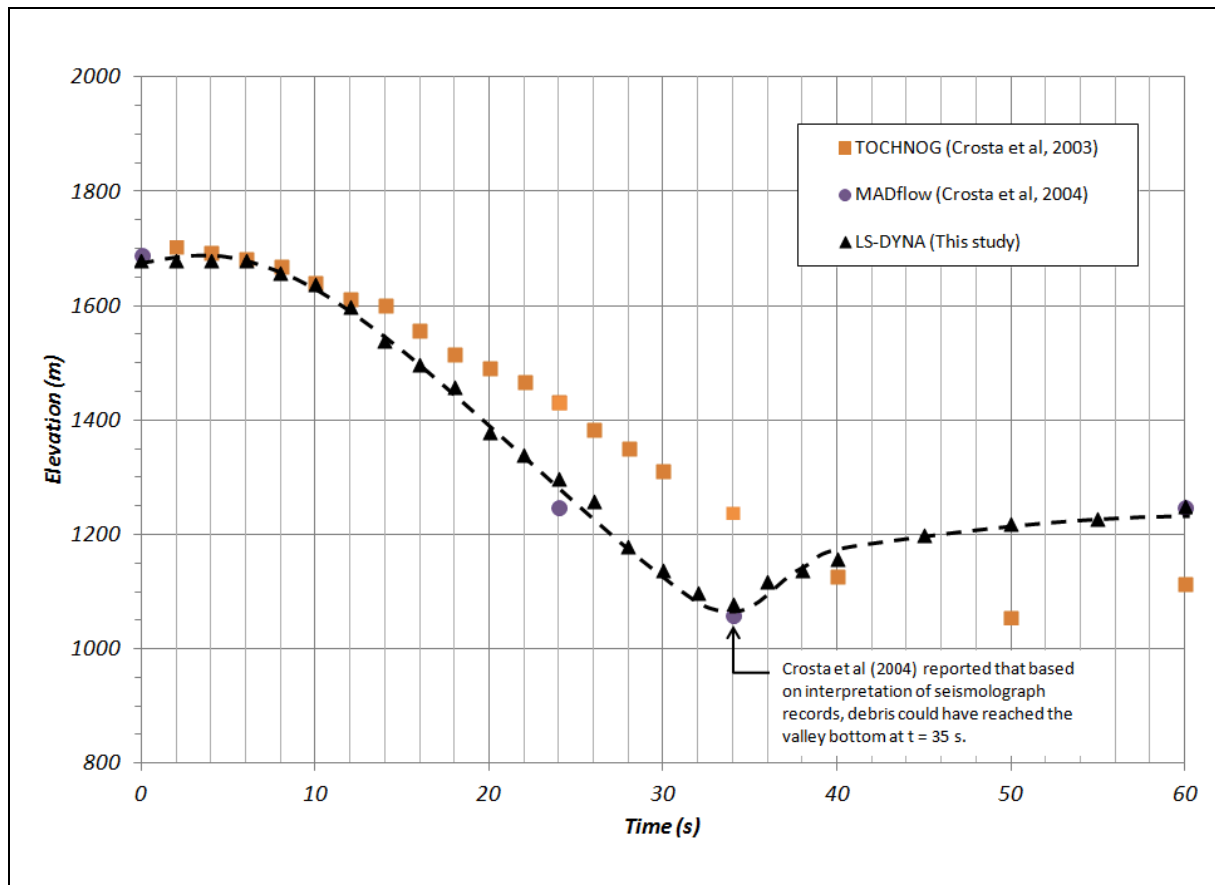


**Figure 4.2 Simulated Debris Frontal Locations against Time**

LS-DYNA reproduces the flow separation observed at the southern flank of the landslide (see Figure 4.3). However, MADflow could not capture this salient feature due to the constraint of depth-averaged formulations. Appendix D presents details of the benchmarking exercise.



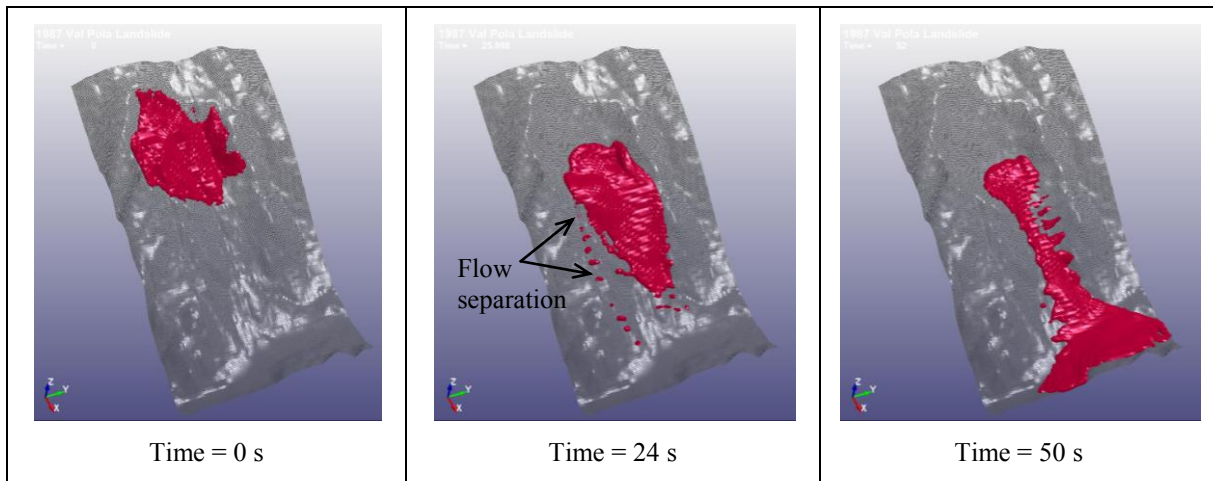


**Figure 4.3 Val Pola Landslide - LS-DYNA's Simulations**

## 5 Discussion

### 5.1 Key Parameters Adopted for Back Analysing Landslide Case Histories in Hong Kong

Case Nos. 4 to 8 in Table 3.1 pertain to the local landslide case histories. The LS-DYNA back analysis of those landslides adopted the same basal friction and turbulence coefficient recommended by previous studies (see references listed in Table 3.1). Typical values of debris density of 1,900 to 2,000 kg/m<sup>3</sup>, shear modulus of 6 MPa, bulk modulus of 12 MPa and Poisson ratio of 0.3 are assumed. The internal friction angle has been back calculated for each of the case histories. Table 5.1 summaries the parameters used and the internal friction angle obtained. The internal friction angles of open hillslope failures are in the range of 25° to 30°, and the internal friction angles of channelized debris flows are between 15° and 20°.

**Table 5.1 Summary of Key Parameters Used**

Case No.	Type	Name	Basal Friction Angle, $\phi_b$	Turbulence Coefficient, $\xi$	Internal Friction Angle, $\phi$
4	Open Hillslope Failure	Shum Wan Road Landslide	20°	-	25°
5		Fei Tsui Road Landslide	22° (failure scar) 35° (road)	- -	30°
6	Channelised Debris Flow	Yu Tung Road Landslide	8°	500	15°
7		Kwun Yam Shan Landslide	15°	500	20°
8		Sham Tseng San Tsuen Landslide	9°	250	15°

## 5.2 Other Observations

Other noteworthy items are summarised below:

- (a) The results of the LS-DYNA mobility analyses are not sensitive to debris density, shear modulus, bulk modulus and Poisson ratio. The exact value of debris density does not affect the debris mobility calculation, since the effects of the body force that drives the debris runout motions are counter-balanced by the resistance calculated proportional to the mass of the landslide debris. The debris flow material undergoes significant deformations and is yielded during almost the entire runout process. Hence the shear and bulk moduli are not sensitive to the analyses. The Poisson ratio is taken as a typical value of soil and it is also not sensitive to the results of mobility associated with large material deformations.
- (b) Attention should be made to the need for internal stress initialisation within the landslide debris materials before commencement of the mobility analysis.
- (c) Spacing of ALE grids for the analysing debris flow can be optimised for enhancing the computational efficiency. It is noted that the optimum grid size is dependent on the scale of the computational domain. For the flume tests studied in the back analysis, grid sizes in the range of 2 to 50 mm are found suitable. For landslide case histories, larger grid size in the order of 1 m should be used to facilitate efficient analysis without compromising the resolution of the results. The grid size should be comparable with the dimensions of the shell elements which model the runout path.
- (d) For forward prediction purposes, iteration runs to identify a suitable representative debris thickness for establishing the damping coefficient ( $\zeta_d$ ) would be needed.
- (e) A nominal value of cohesion of 1 kPa should be specified for the debris material in the analysis to avoid unreasonable dispersion of the debris flow during the simulation.
- (f) Yield function parameters of  $a_0$ ,  $a_1$  and  $a_2$  to define the Drucker-Prager constitutive model should be calculated following the guidelines given in Appendix E. The tension cut-off of the model has been assumed to be  $-10^{-5}$  kPa for back analysing the local landslide case histories.

## 6 Further work

Koo & Kwan (2014) demonstrated the capability of LS-DYNA for simulation of dynamic responses of flexible barriers subject to impacts of drop weights and replication of full-scale rockfall tests. Further study to examine the performance of LS-DYNA for carrying out coupled analysis of debris impacting flexible barriers should be carried out. An example of using LS-DYNA to simulate debris flow impacting a rigid barrier (see Figure 6.1) prepared by Kwan et al (2015) can serve as a basis for the further study. Figure 6.1 shows a LS-DYNA simulation of a debris flow impacting on a rigid barrier (Kwan et al, 2015). The velocity vector plots of the debris flow reveal the dynamics involved in the debris-barrier interaction. When debris flow reaches the barrier, it is impeded by the obstruction of the barrier. Debris at the frontal portion runs up against the barrier. A plug is then formed by the debris stopped and trapped behind the barrier. The extent of the plug enlarges when more debris is brought to rest behind the barrier. The debris flow subsequently rides on the plug and overtops the barrier.

## 7 Conclusions

LS-DYNA has been used to carry out debris mobility analysis of dry sand flows in experiments, and several notable landslide case histories including open hillslope failures and channelised debris flows. Performance of the LS-DYNA has also been benchmarked against other advanced numerical models for debris mobility assessment.

The results of this study indicate that LS-DYNA can produce reasonable simulations of landslide dynamics including landslide runout distance and velocity. The ranges of key parameters required for the LS-DYNA analysis have been identified. This facilitates the use of the LS-DYNA model for coupled analysis which simulates explicitly landslide debris impacting on debris-resisting structures in the next phase of study in future.

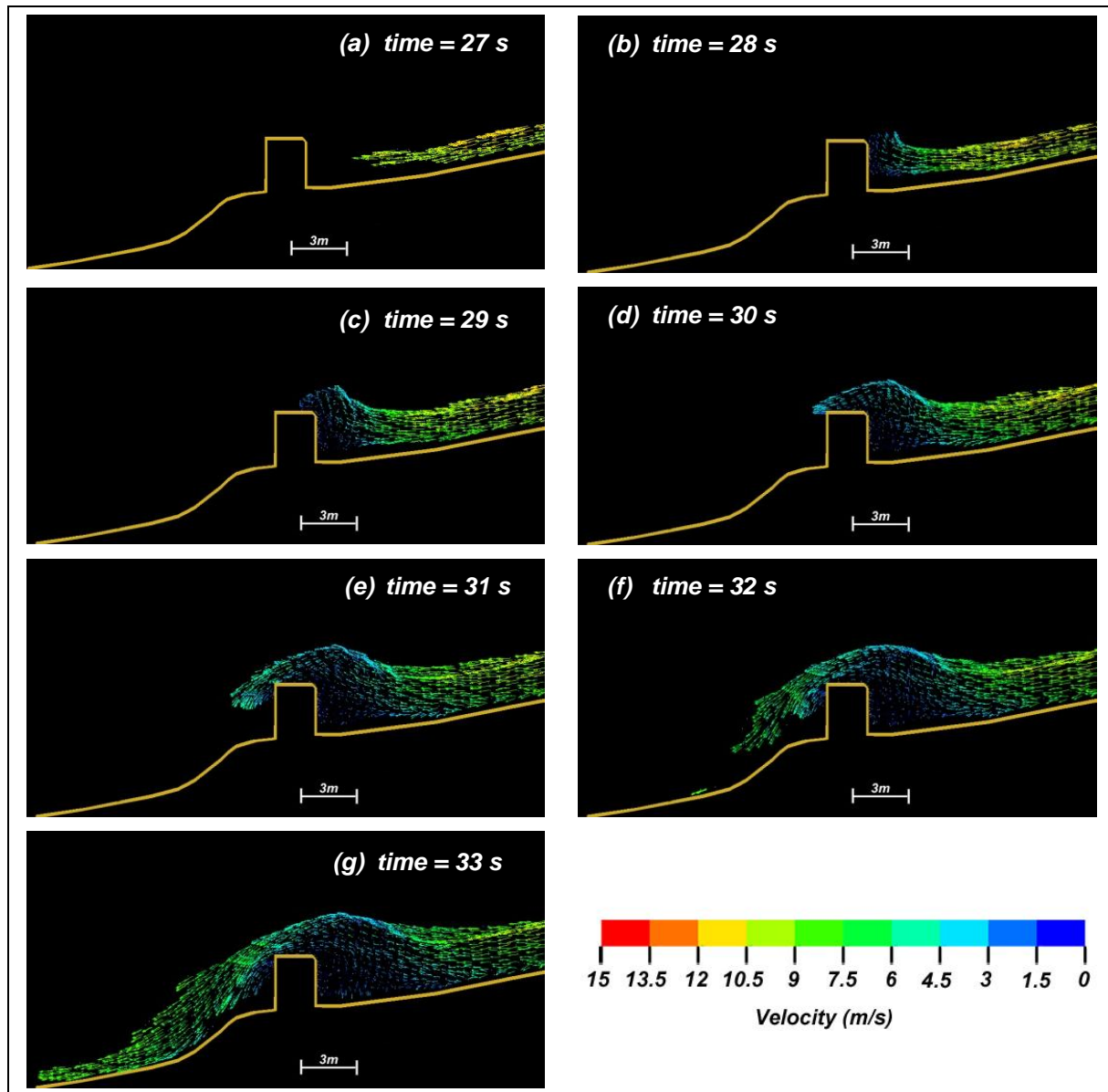


**Figure 6.1 LS-DYNA Simulation on Interaction between Debris Flow and Rigid Barrier (Kwan et al, 2015)**

## 8 References

- Arup (2014). *Pilot Numerical Investigation of the Interactions between Landslide Debris and Flexible Debris-resisting Barriers, Final Report*. Report prepared for Geotechnical Engineering Office, Hong Kong, 143 p.
- Chen, J.H. & Lee, C.F. (2007). Landslide mobility analysis using MADflow. *Proceedings of the 2007 International Forum on Landslide Disaster Management*, vol. II, pp 857-874.

- Choi, C.E., Ng, C.W.W., Song, D., Kwan, J.S.H., Shiu, H.Y.K., Ho, K.K.S. & Koo, R.C.H. (2014). Flume investigation of landslide debris-resisting baffles. *Canadian Geotechnical Journal*, vol. 51(5), pp 540-553.
- Crosta, G.B., Chen, H. & Lee, C.F. (2004). Replay of the 1987 Val Pola Landslide, Italian Alps. *Geomorphology*, vol. 60, pp 127-146.
- Crosta, G.B., Imposimato, S. & Roddeman, D.G. (2003). Numerical modelling of large landslides stability and runout. *Natural Hazards and Earth System Sciences*, vol. 3, pp 523-538.
- Drucker, D.C. & Prager, W. (1952). Soil mechanics and plastic analysis for limit design. *Quarterly of Applied Mathematics*, vol. 10, no. 2, pp 157-165.
- FMSW (2005). *Report on the Debris Flow at Sham Tseng San Tsuen of 23 August 1999, Findings of the Investigation (GEO Report No. 169)*. By Fugro Maunsell Scott Wilson Joint Venture. Geotechnical Engineering Office, Hong Kong, 92 p.
- GEO (2011). *Guidelines on the Assessment of Debris Mobility for Channelised Debris Flows (Technical Guidance Note No. 29)*. Geotechnical Engineering Office, Hong Kong, 6 p.
- GEO (2012). *Detailed Study of the 7 June 2008 Landslides on the Hillside above Yu Tung Road, Tung Chung, by AECOM Asia Company Limited (GEO Report No. 271)*. Geotechnical Engineering Office, Hong Kong, 124 p.
- Hungr, O. (1995). A model for the runout analysis of rapid flow slides, debris flows and avalanches. *Canadian Geotechnical Journal*, 32: 610-623.
- Iverson, R.M., Logan, M. & Denlinger, R.P. (2004). Granular avalanches across irregular three-dimensional terrain: 2. Experimental tests. *Journal of Geophysical Research*, vol. 109, F01015, doi:10.1029/2003JF000084, 16 p.
- Knill, J. & GEO (2006a). *Report on the Shum Wan Road Landslide of 13 August 1995 (GEO Report No. 178)*. By Sir John Knill & Geotechnical Engineering Office. Geotechnical Engineering Office, Hong Kong, 177 p.
- Knill, J. & GEO (2006b). *Report on the Fei Tsui Road Landslide of 13 August 1995 (GEO Report No. 188)*. By Sir John Knill & Geotechnical Engineering Office. Geotechnical Engineering Office, Hong Kong, 147 p.
- Koo, R.C.H. & Kwan, J.S.H. (2014). *A Numerical Study of Dynamic Responses of Two Selected Flexible Rockfall Barriers Subject to Punching and Areal Loads (Technical Note No. TN 4/2014)*. Geotechnical Engineering Office, Hong Kong, 47 p.
- Kwan, J.S.H. & Cheung, R.W.M. (2012). *Suggestions on Design Approaches for Flexible Debris-resisting Barriers (Discussion Note No. DN 1/2012)*. Geotechnical Engineering Office, Hong Kong, 90 p.

- Kwan, J.S.H., Koo, R.C.H. & Ng, C.W.W. (2015). Landslide mobility analysis for design of multiple debris-resisting barriers. *Canadian Geotechnical Journal*, dx.doi.org/10.1139/cgj-2014-0152.
- Kwan, J.S.H. & Sun, H.W. (2007). Benchmarking exercise on landslide mobility modeling – runout analysis using 3dDMM. *Proceedings of the 2007 International Forum on Landslide Disaster Management*, vol. II, pp 945-966.
- Law, R.P.H. & Ko, F.W.Y. (2015). *Validation of Geotechnical Computer Program “2d-DMM (Version 2.0)” (Technical Note No. TN 1/2015)*. Geotechnical Engineering Office, Hong Kong, 68 p.
- Manzella, I. (2008). *Dry Rock Avalanche Propagation: Unconstrained Flow Experiments with Granular Materials and Blocks at Small Scale*. PhD Thesis, École Polytechnique Federale de Lausanne, 220 p.
- MGS (2008). *Detailed Study of the 22 August 2005 Landslide and Distress on the Natural Hillside at Kwun Yam Shan, below Tate’s Ridge (GEO Report No. 239)*. By Maunsell Geotechnical Services Limited. Geotechnical Engineering Office, Hong Kong, 124 p.
- Pudasaini, S. & Hutter, K. (2007). *Avalanche Dynamics - Dynamics of Rapid Flows of Dense Granular Avalanches*. Springer-Verlag Berlin Heidelberg, 569 p.

## Appendix A

### Laboratory Flume Test

## Contents

	Page No.
Contents	23
List of Tables	24
List of Figures	25
A.1 USGS Flume Test	27
A.1.1 Physical Test Setup	27
A.1.2 LS-DYNA Model Setup	27
A.1.3 Simulation Results	30
A.2 Deflected Sand Flow	37
A.2.1 Physical Test Setup	37
A.2.2 LS-DYNA Model Setup	38
A.2.3 Simulations and Results	40
A.3 HKUST Flume Test	42
A.3.1 Physical Test Setup	42
A.3.2 LS-DYNA Model Setup	44
A.3.3 Simulation Results	46
A.4 References	46



### List of Tables

Table No.		Page No.
A1	Testing Parameters of the Flume Experiments A and B (extracted from Iverson et al, 2004)	28
A2	Input Parameters Adopted for the Sand Flow in the LS-DYNA Models of the USGS Experiments	30
A3	Details of the Deflected Sand Flume Experiment	38
A4	Input Parameters Adopted in the LS-DYNA Models of the HKUST Tests	46

## List of Figures

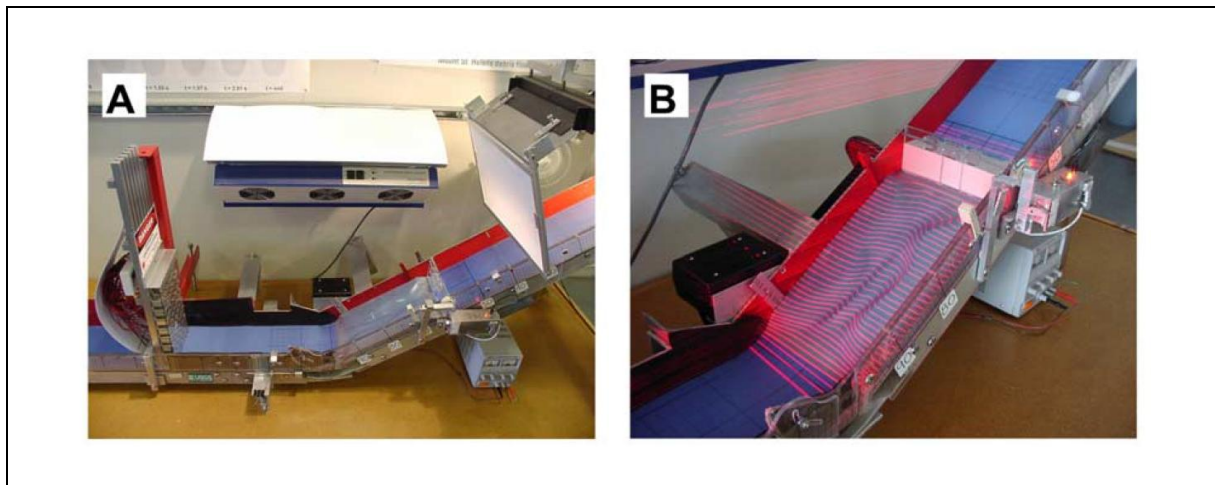
Figure No.		Page No.
A1	Photographs of the Miniature Flume Used in the Experiments (Iverson et al, 2004)	27
A2	LS-DYNA Models of Experiments A and B	28
A3	ALE Container Mesh for Experiment A	29
A4	Sand Flow LS-DYNA Simulation for Experiment A	31
A5	Side-by-side Comparison of the Flume Test Experiment Result and LS-DYNA Simulation for Experiment A	32
A6	Side-by-side Comparison of the USGS Flume Test Experiment Results and LS-DYNA Simulation for Experiment B	33
A7	Frontal Displacement-Time Curves of the Sand Flow Obtained from the Experiment Results and LS-DYNA Simulation for Experiment A	34
A8	Frontal Displacement-Time Curves of the Sand Flow Obtained from the Experiment Results and LS-DYNA Simulation for Experiment B	34
A9	Final Deposition of the Sand Flow Obtained from the LS-DYNA Simulation for Experiment A	35
A10	Final Deposition of the Sand Flow Obtained from the LS-DYNA Simulation for Experiment B	36
A11	Setup of the Deflected Sand Flow Experiment (extracted from Manzella, 2008)	37
A12	Depth Contours of the Final Deposition of Sand	38
A13	Setup of the LS-DYNA Model of the Deflected Sand Flow Test	39
A14	Final Deposition of the Sand Flow of LS-DYNA Simulation	40

Figure No.		Page No.
A15	Comparisons of the Deposition Profiles between the Experiment Results and the LS-DYNA Simulations	41
A16	The HKUST Flume Setup	42
A17	The Debris Flow Images Captured by the High Speed Camera at the Observation Point of 1.0 m Downstream from the Source	43
A18	Velocity and Thickness Hydrographs at 1.0 m Downstream from the Source	44
A19	Setup of the LS-DYNA Model for HKUST Flume Test	45
A20	Simulations of the LS-DYNA Model	47
A21	Frontal Velocity of the HKUST Test	48
A22	Velocity and Thickness Hydrographs of the HKUST Test	48

## A.1 USGS Flume Test

### A.1.1 Physical Test Setup

Iverson, et al (2004) carried out two small scale flume experiments in a bench top flume of 0.2 m wide and approximately 1 m long (see setup in Figure A1). A head gate was installed at the upslope portion for storage of dry sand source. The upper portion of the flume basal surface behind the head gate was lined with Formica and the steep part of the flume was coated with an urethane to form an irregular basal surface. The two experiments were carried out using different irregular topography, named Experiment A and Experiment B respectively.



**Figure A1 Photographs of the Miniature Flume Used in the Experiments (Iverson et al, 2004)**

Two types of sand materials were used for the flume tests. Their internal friction angles and basal friction on flume basal surface i.e. Formica and urethane, were measured using a series of tilt table tests. Other parameters such as sand mass and bulk density were also reported. A summary of the experimental conditions and sand properties, reproduced from Iverson et al (2004), is presented in Table A1.

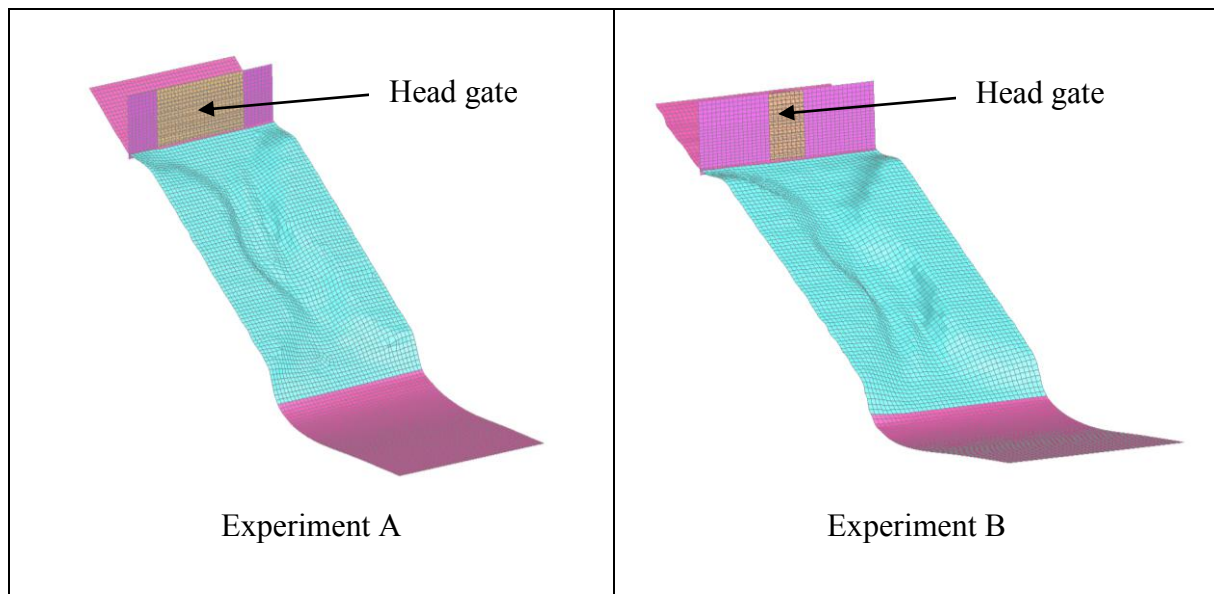
Digital photography and laser cartography were used for capturing the movement of the sand flow at an interval of 0.2 second.

### A.1.2 LS-DYNA Model Setup

The topography mesh was made up of 5,655 nos. quadrilateral rigid shell elements. The resolution of the topography mesh is approximately 5 mm by 5 mm. In the flume tests there was a small step of ~0.2 mm in height at the interface of Formica and the urethane coating at the upslope side. For simplicity this step is not included in the LS-DYNA model. Figure A2 shows the LS-DYNA models.

**Table A1 Testing Parameters of the Flume Experiments A and B (extracted from Iverson et al, 2004)**

Conditions/Properties	Experiment A	Experiment B
Orientation of flume topography	“regular”	“inverted”
Aperture width of flume head gate, cm	12	4
Ambient relative humidity, %	36	66
Ambient temperature, °C	21	17
Shape of sand grains	Angular	Rounded
Diameter of sand grains, mm	0.5 - 1	0.25 - 0.5
Sand volume, cm <sup>3</sup>	308	308
Sand mass, g	388.2	476.5
Sand bulk density, g cm <sup>-3</sup>	1.26	1.55
Basal friction angle, and on Formica, $\phi_{bed}$ , deg	$23.47 \pm 0.35$	$25.60 \pm 5.60$
Basal friction angle, sand on urethane, $\phi_{bed}$ , deg	$19.85 \pm 1.11$	$22.45 \pm 2.45$
Internal friction angle of sand, $\phi_{int}$ , deg	43.99 al fri	$39.39 \pm 9.39$

**Figure A2 LS-DYNA Models of Experiments A and B**

Vertical rigid shell elements were assigned at the upslope of the flume to model the head gate attached to the sand storage box. The gate width was specified in accordance with the reported experimental setup. The dry sand flow was modelled in LS-DYNA as ALE material. An array of grids (or “ALE container mesh”) comprising regular tetrahedral solid elements was setup in the computational domain. The resolution of the ALE container mesh

is approximately 5 mm by 5 mm on the planes parallel to the topography and 2 mm in the direction perpendicular to the runout plane. Rigid boundaries were assigned on the two sides of the sand storage box to prevent the ALE material from flowing out sideways. Figure A3 shows the layout of the ALE container mesh for Experiment A.

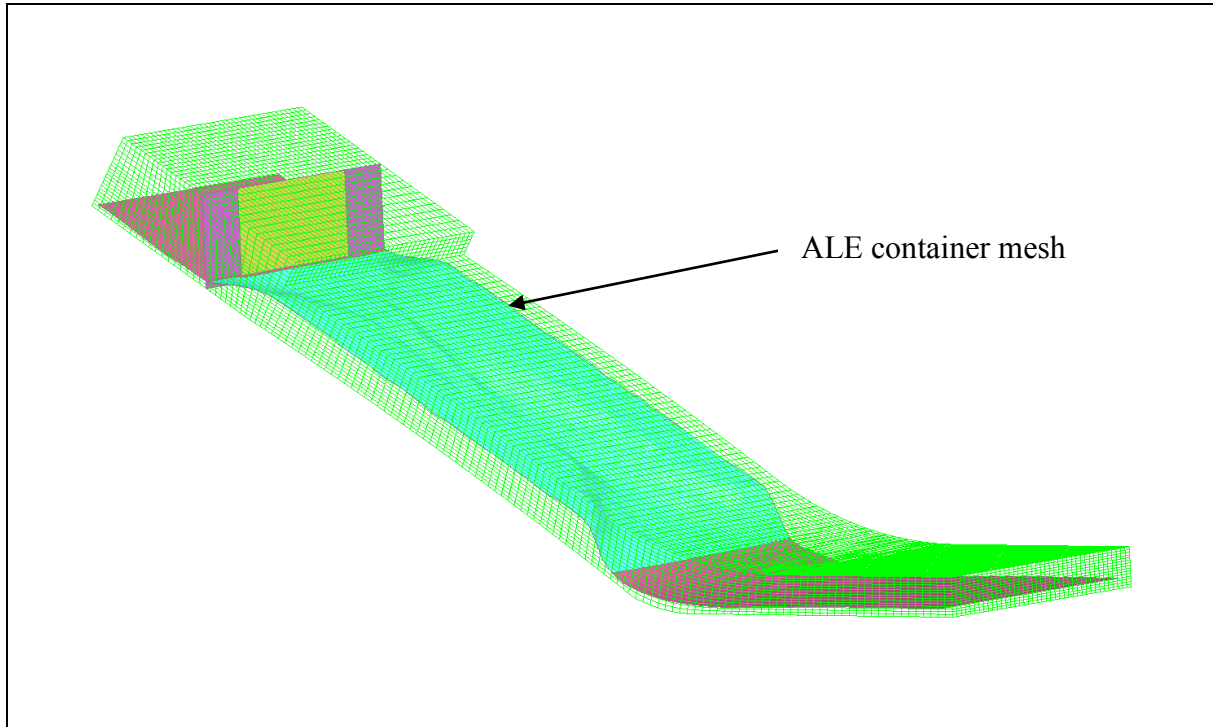


**Figure A3 ALE Container Mesh for Experiment A**

The topography and the head gate were modelled as rigid materials. The density and stiffness properties are not relevant to the analysis. Reasonable values that allow the simulation to proceed would suffice. The most important parameter required for an accurate modelling of debris mobility is the coefficient of the contact friction between the sand flow and the ground topography. The modelling of the topography material in LS-DYNA followed the descriptions in Iverson et al (2004) that the base behind the head gate was made of Formica whereas the floor of the irregular terrain was made of urethane. Table A2 summarises the input parameters adopted for modelling the materials.

Drucker-Prager constitutive model was well-tested for simulating sandy material in the ALE environment in LS-DYNA (Arup, 2014). This yield surface model provides a better smooth yield surface than the commonly used Mohr-Coulomb model. In the present study, the input property parameters for the ALE material representing the sand flow follow the parameters reported by Iverson et al (2004) as presented in Table A1. Stiffness of the dry sands was not given by Iverson (op cit), therefore typical values had been selected and adopted for the analysis. Sensitivity analysis was carried out, which indicates that results of the mobility assessment are not sensitive to stiffness parameters of the soil model. A reasonable assumption of shear modulus equals to 500 kPa can be adopted. In addition to the above, a small cohesion value of 1 kPa had been specified on top of the friction angle to

avoid unreasonable dispersion of the sand flow during the simulation. Table A2 summarises the input parameters adopted for the sand flows in the model.

**Table A2 Input Parameters Adopted for the Sand Flow in the LS-DYNA Models of the USGS Experiments**

Material Property	Adopted Input Parameters
Contact friction of urethane with the sand	Experiment A = 19.85° Experiment B = 22.45°
Contact friction of Formica with the sand	Experiment A = 23.47° Experiment B = 25.60°
Internal friction angle	Experiment A = 44.39° Experiment B = 39.39°
Material density of sand	Experiment A = 1,260 kg/m <sup>3</sup> Experiment B = 1,550 kg/m <sup>3</sup>
Shear modulus of sand	500 kPa
Bulk modulus of sand	1,000 kPa

### A.1.3 Simulation Results

The LS-DYNA model is first initialised by applying gravity load to the ALE material while the head gate is still closed. The gravity acceleration is increased gradually from 0 to 9.81 m/s<sup>2</sup> in 1 second. After full gravity load had been applied, the centre portion of the head gate is set to move forward by approximately 0.5 m to simulate the sudden release of the sand in the flume tests (See Figure A4). Velocity and internal pressure of the sand flow have been captured throughout the computation.

Figures A5 and A6 provide a side-by-side comparison of the LS-DYNA simulation results and the experimental data of the thickness of the sand flows. The LS-DYNA simulation generally reproduces the test results very well for both Experiment A and Experiment B in terms of the movement with respect to time and the deposition extent. In addition, the simulation is able to correctly predict the development of the sand prisms remain in the sand storage box. Flow discontinuity is observed in the simulation, for examples, in the mid-slope region at  $t = 1.97$  s in Experiment A, and  $t = 1.11$  s,  $t = 2.99$  s and  $t = 3.83$  s in Experiment B. This is a graphical illustration issue rather than calculation error. As seen in the corresponding flume test experiment results, the sand flow at those locations were very thin. Under the current resolution setting in the LS-DYNA simulation, i.e. the density of the ALE container mesh, such thin layer of sand is not correctly depicted. Nevertheless, the actual calculations of sand flow movement and deposition are not grossly affected.

It has been observed that the LS-DYNA simulation slightly overestimates the thickness of the sand prisms behind the head gate, and underestimates the maximum thickness of the deposition at the distal end. This could be caused by the difference in the head gate opening direction considered in the analysis. In the simulation, the gate is open instantly, while in the experiment the gate was probably lifted up in a more gradual manner. Also, friction coefficient of the head gate used in the simulation may deviate from that in the experiment.

The displacements of the sand flow front obtained from the experiment and the LS-DYNA simulation are compared. The displacement-time curves have been plotted and shown in Figures A7 and A8 for Experiment A and Experiment B respectively. Whilst for both Experiments A and B the predicted values and experiment measurement match reasonably, it can be seen that LS-DYNA under-predicts the frontal displacement starting from about  $t = 0.5$  s in Experiment B. It is probably because the phenomenon of dispersion of the sand flow is more evident in this case. Spherical sand grains used in the Experiment has a relatively strong tendency to saltate as observed by Iverson et al (2004). The saltated sand is much diffused at the front and therefore has not been simulated.

The final deposition plan and cross-section profiles are presented in Figures A9 and A10. The maximum thickness of the deposits predicted by LS-DYNA and measured values are in good agreement, with a difference of not more than 3 mm. The final deposition profiles between the LS-DYNA simulations and experimental results are comparable.

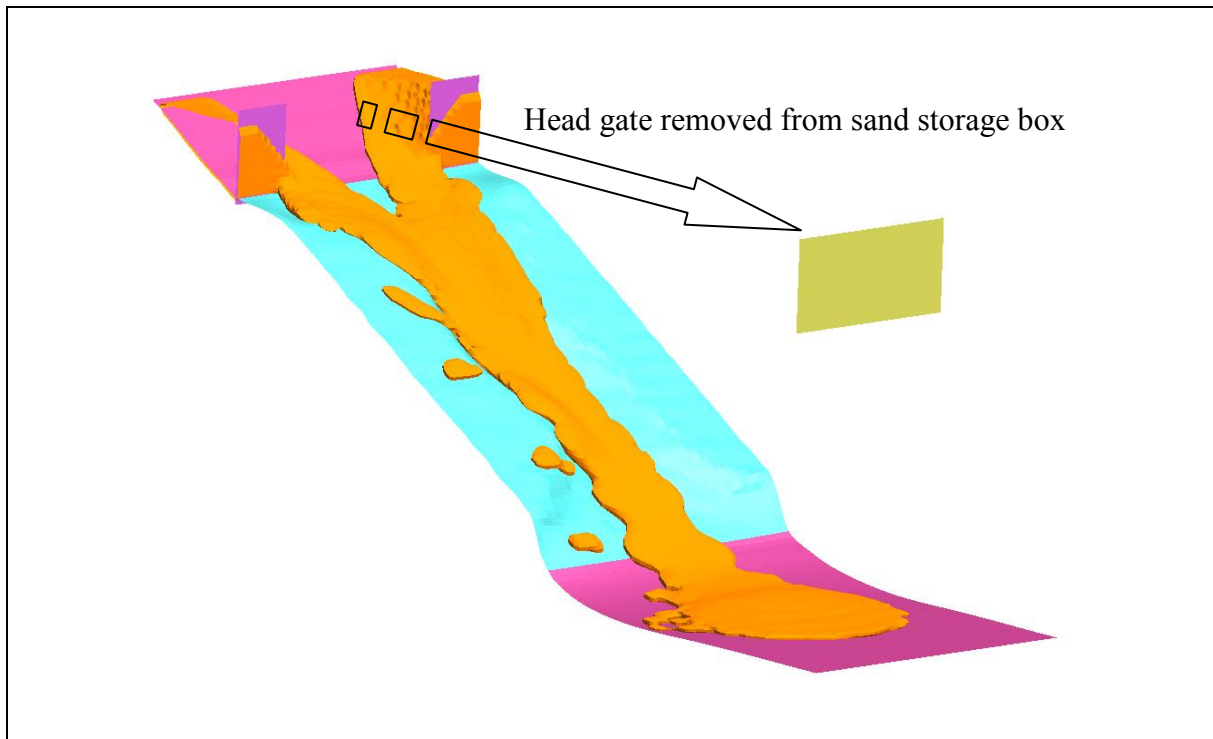


**Figure A4 Sand Flow LS-DYNA Simulation for Experiment A**



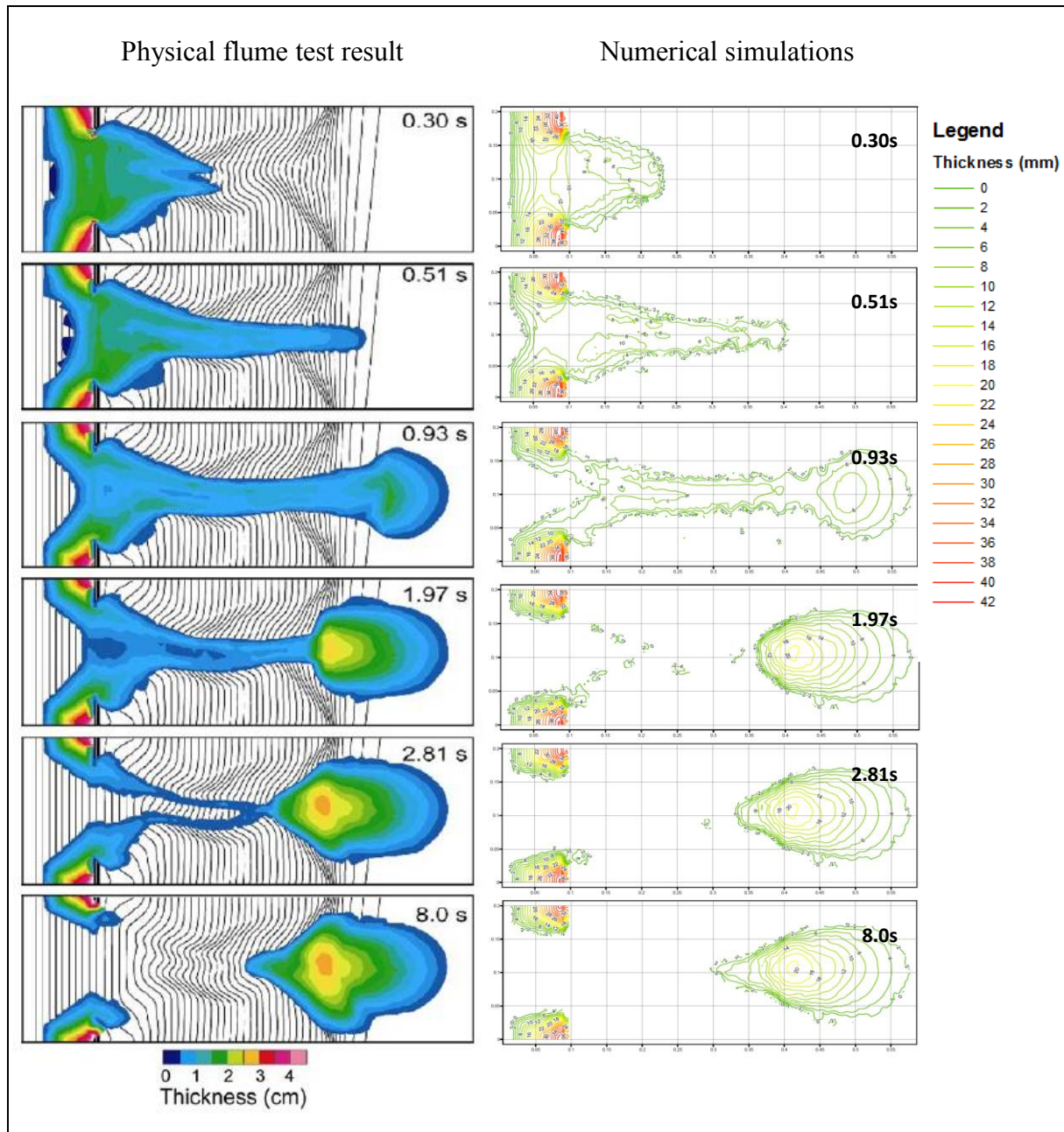


**Figure A5 Side-by-side Comparison of the Flume Test Experiment Result and LS-DYNA Simulation for Experiment A**

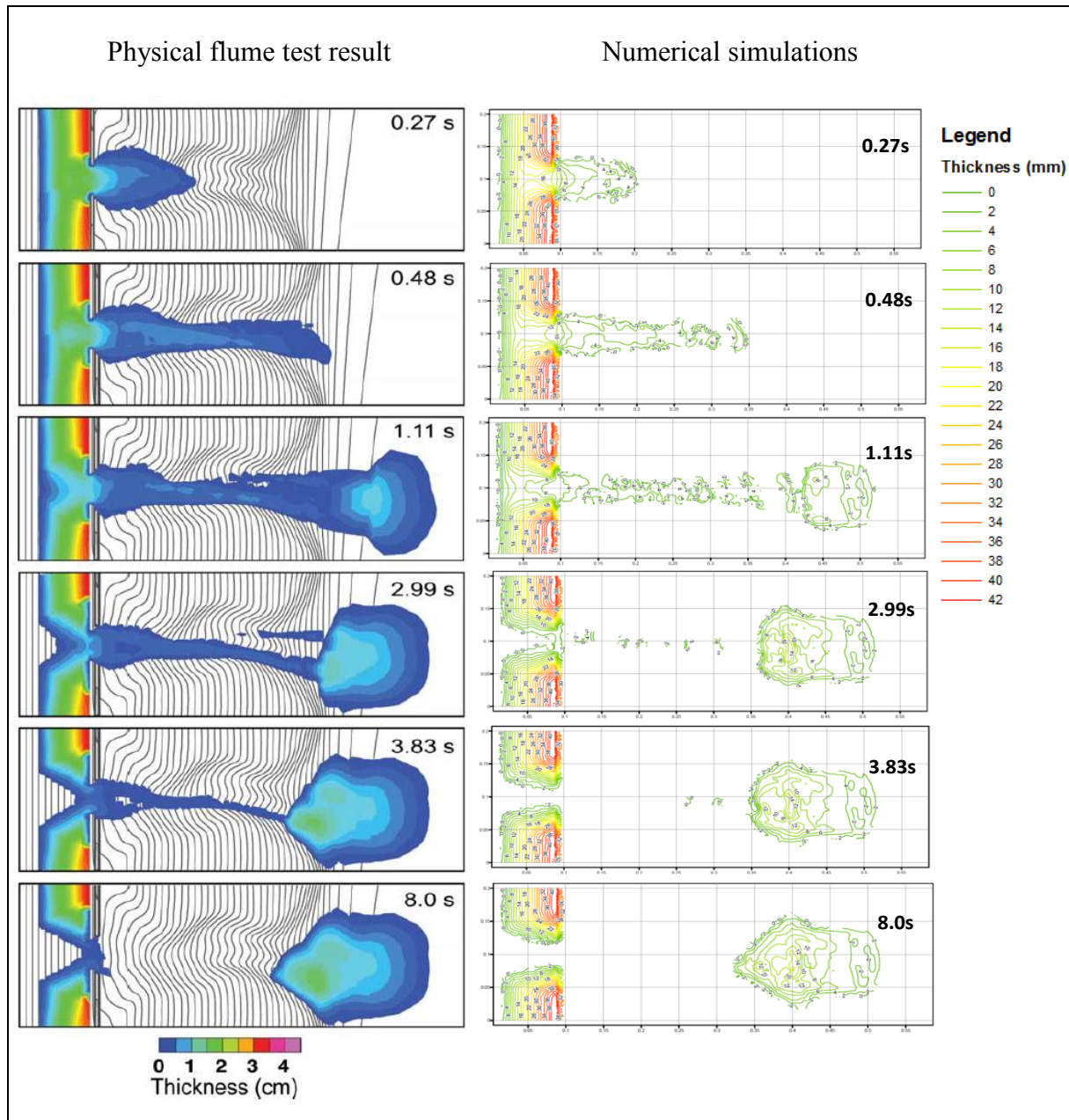


**Figure A6 Side-by-side Comparison of the USGS Flume Test Experiment Results and LS-DYNA Simulation for Experiment B**

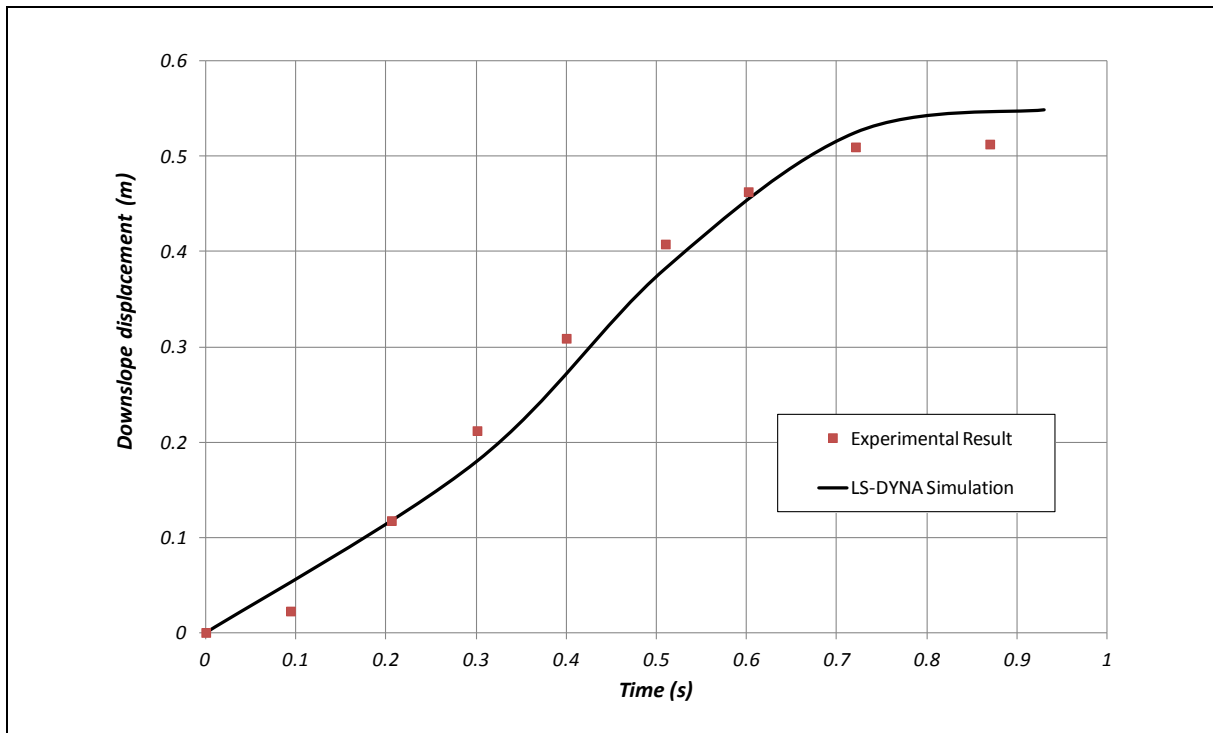


**Figure A7 Frontal Displacement-Time Curves of the Sand Flow Obtained from the Experiment Results and LS-DYNA Simulation for Experiment A**

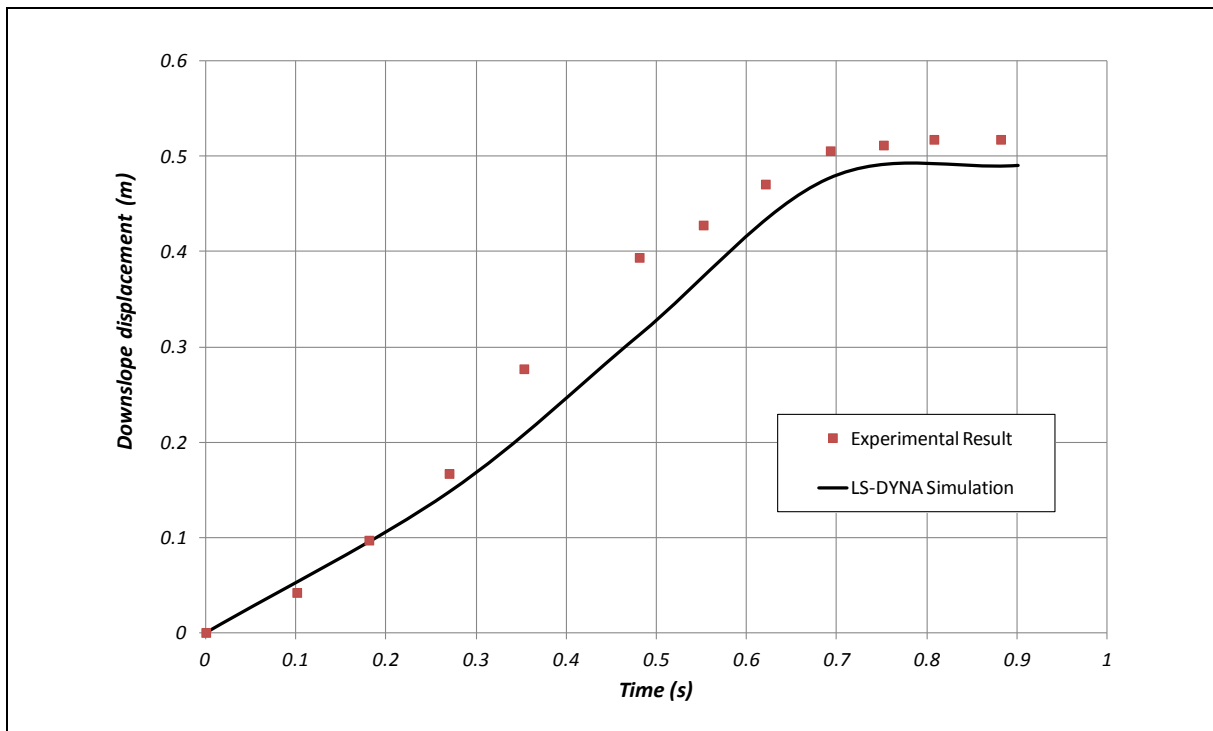


**Figure A8 Frontal Displacement-Time Curves of the Sand Flow Obtained from the Experiment Results and LS-DYNA Simulation for Experiment B**

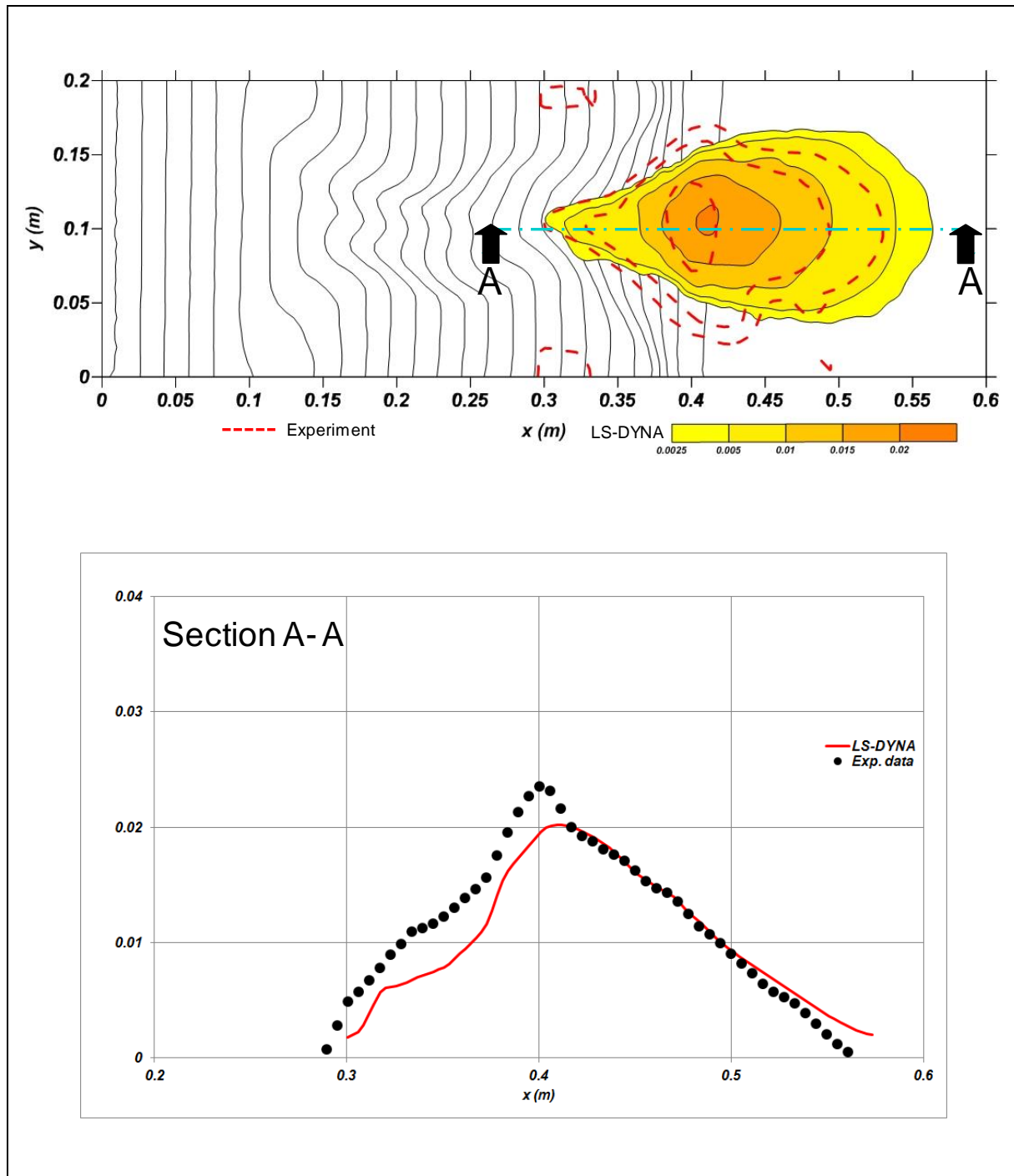


**Figure A9** Final Deposition of the Sand Flow Obtained from the LS-DYNA Simulation for Experiment A

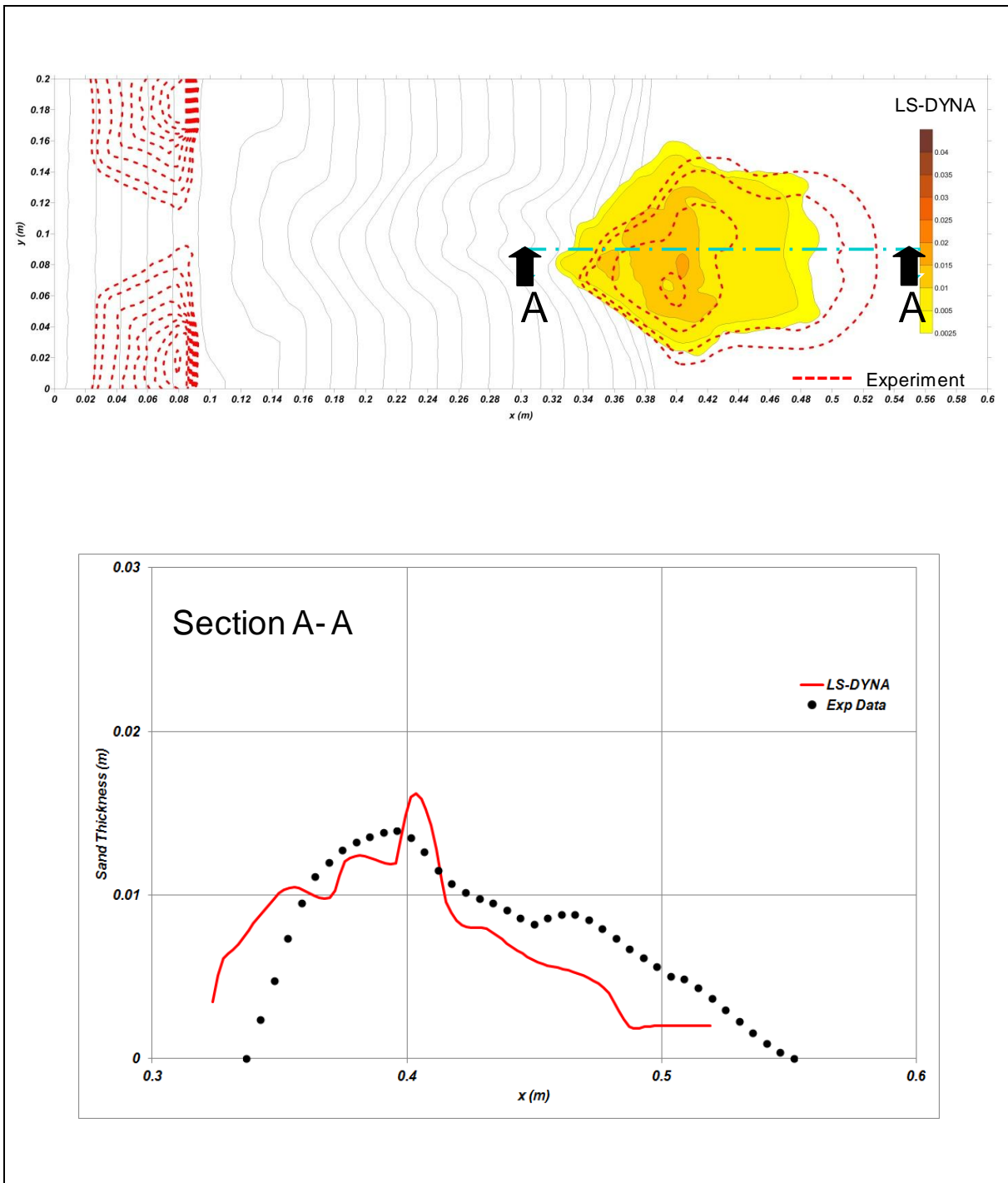


**Figure A10 Final Deposition of the Sand Flow Obtained from the LS-DYNA Simulation for Experiment B**

## A.2 Deflected Sand Flow

### A.2.1 Physical Test Setup

Manzella (2008) carried out a laboratory experiment of dry sand flow. In the experiment, dry sand was released from a box of dimensions 20 cm (high)  $\times$  40 cm (wide)  $\times$  65 cm (long) fixed on an inclined plane. This plane is inclined at  $37.5^\circ$  and it adjoins with another plane inclined at  $22.6^\circ$ . Figure A11 shows the experimental setup.

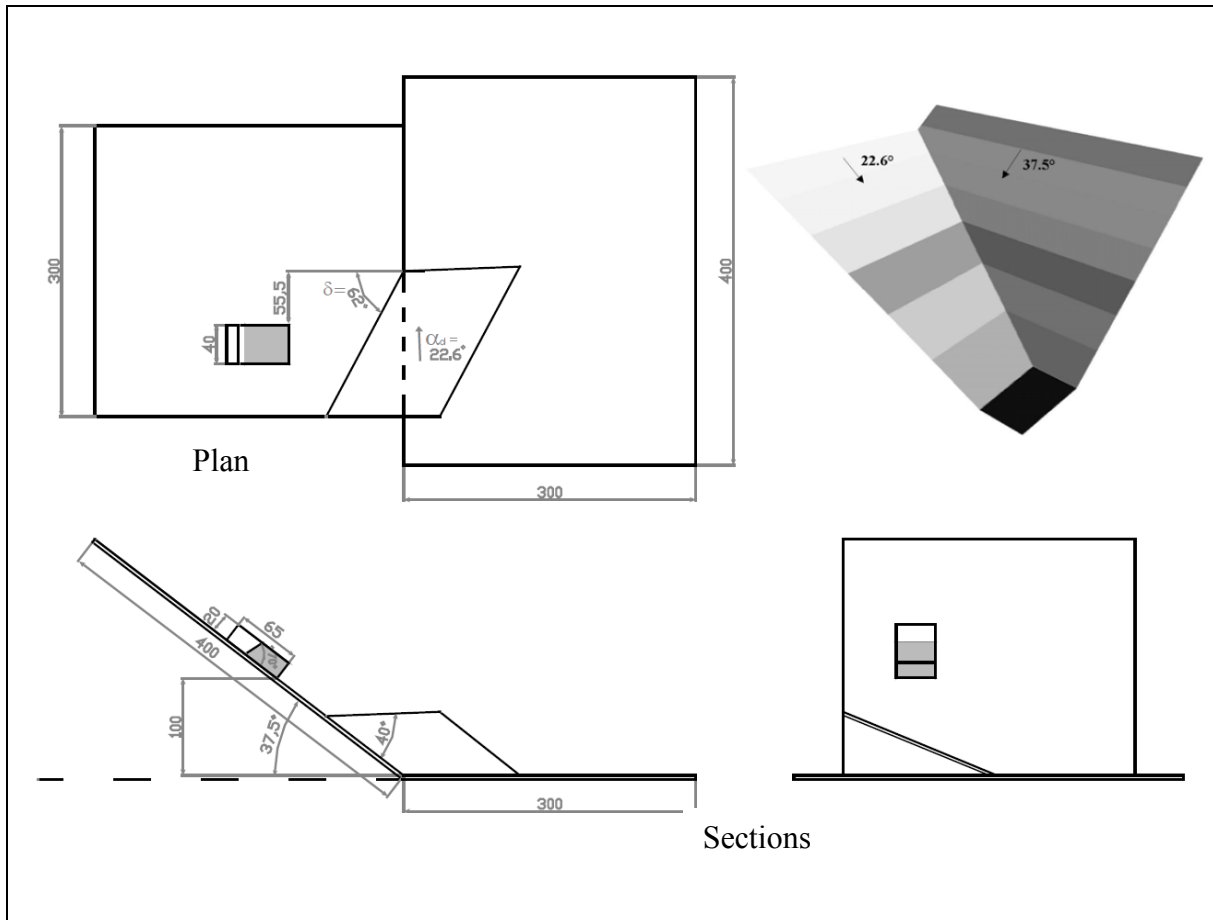


**Figure A11 Setup of the Deflected Sand Flow Experiment (extracted from Manzella, 2008)**

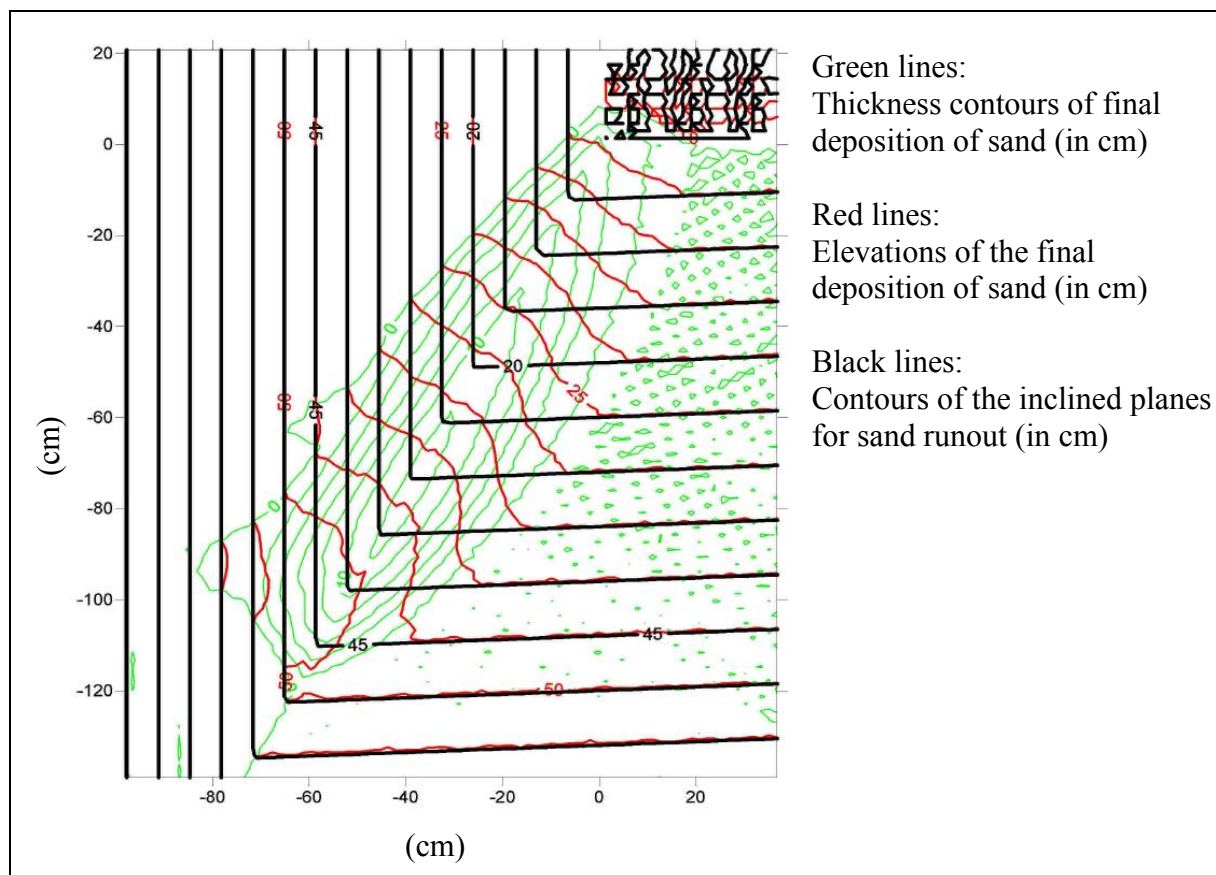
The basal friction of the sand was measured using a tilting test and the internal friction angle was estimated as the angle of repose of a sand pile. The density of the sand was  $1,260 \text{ kg/m}^3$ . The sand was released by a sudden removal of the downslope facing sidewall. Table A3 presents details of the experiment.

Manzella (2008) reported the thickness of the final deposition profile (see Figure A12).



**Table A3 Details of the Deflected Sand Flume Experiment**

Material	Hostun Sand (Fine)
Internal friction angle of sand	34°
Base material	Forex
Basal friction angle	32°
Volume of sand used	52 cm <sup>3</sup> (i.e. $5.2 \times 10^{-6}$ m <sup>3</sup> )

**Figure A12 Depth Contours of the Final Deposition of Sand****A.2.2 LS-DYNA Model Setup**

A LS-DYNA simulation has been carried out using the same internal frictional angle and base friction angle as measured in the laboratory, which are 34° and 32° respectively. The volume of sand is  $5.2 \times 10^{-6}$  m<sup>3</sup>. The flume is modelled using 2 mm thick quadrilateral rigid shell elements. The dimensions of the shell element are 10 mm by 10 mm. The ALE container mesh comprises regular tetrahedral solid elements. The resolution of the ALE container mesh is 20 mm cubic in shape. Vertical rigid shell elements are assigned at the

upslope of the flume to model the release box. Rigid boundaries are assigned on the two sides of the release box to prevent the ALE material from flowing out sideways. Figure A13 shows the setup of the LS-DYNA model.

The basal frictional angle and the internal friction angle of sand reported by Manzella (2008) are adopted in the analysis (see Table A3).

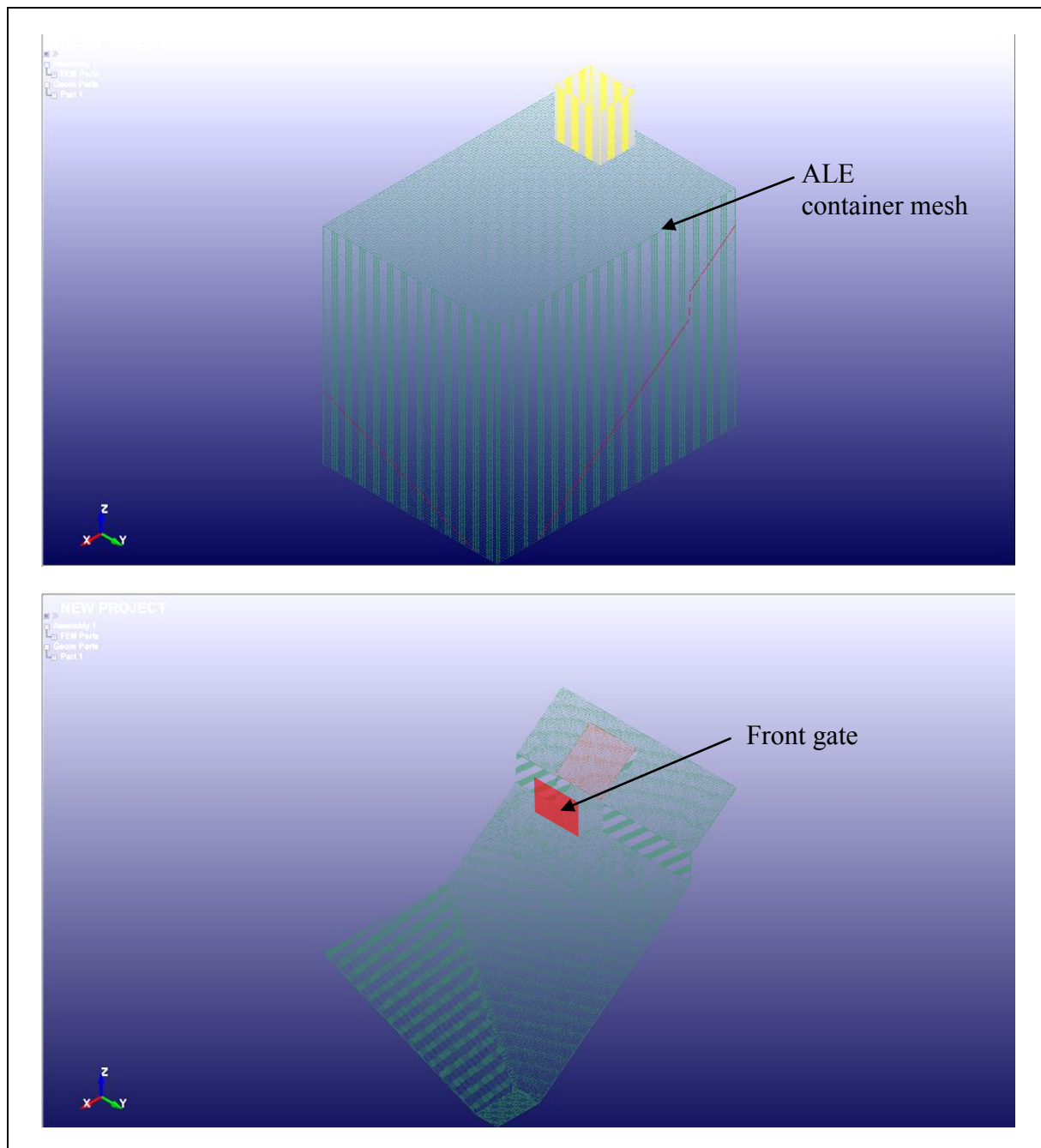


**Figure A13 Setup of the LS-DYNA Model of the Deflected Sand Flow Test**



### A.2.3 Simulations and Results

The LS-DYNA model was first initialised by applying gravity load to the ALE material for 1 second and the front gate was set to move upward by approximately 0.5 m, simulating the sudden release of the sand in the flume test. Figure A14 shows the final deposition profile produced by LS-DYNA. The calculated extent of sand deposition is largely comparable with the laboratory measurement. However, discrepancy is observed at the tail of the deposition profile. This may be caused by the thin layer of dispersed sand that cannot be simulated in the continuum analysis of LS-DYNA. Comparisons of the transverse and the longitudinal deposition profiles of the sand materials are shown in Figure A15. LS-DYNA slightly under-predicts the deposition thickness but the extent of the deposition is well predicted.

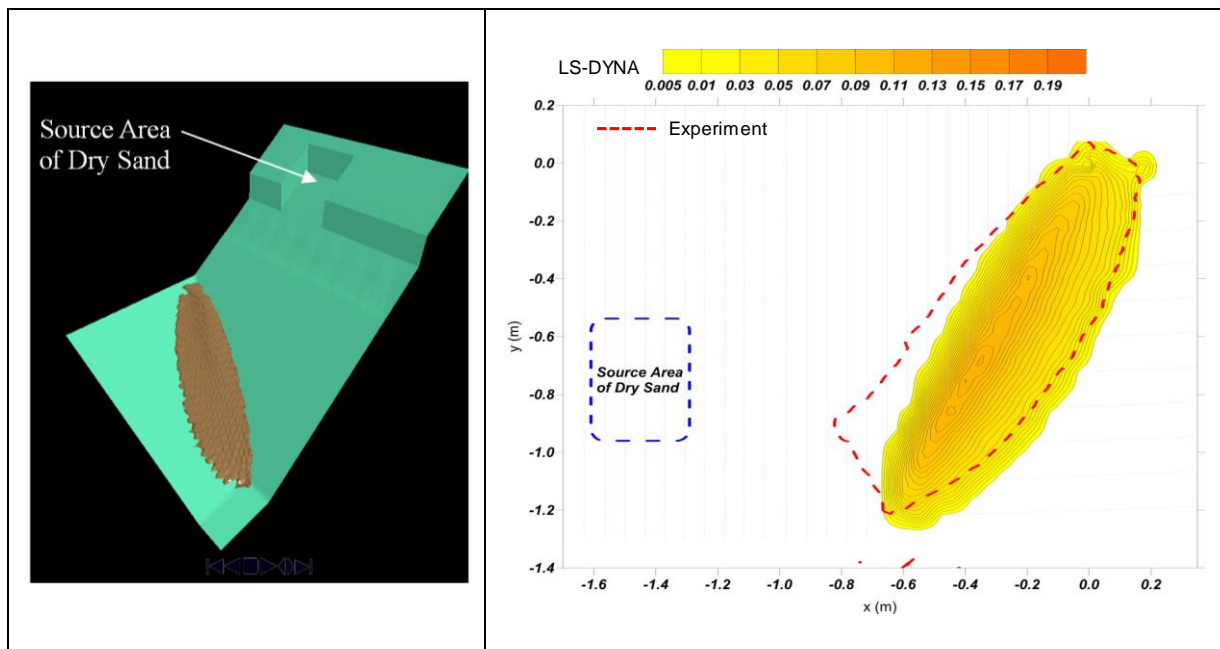


**Figure A14 Final Deposition of the Sand Flow of LS-DYNA Simulation**

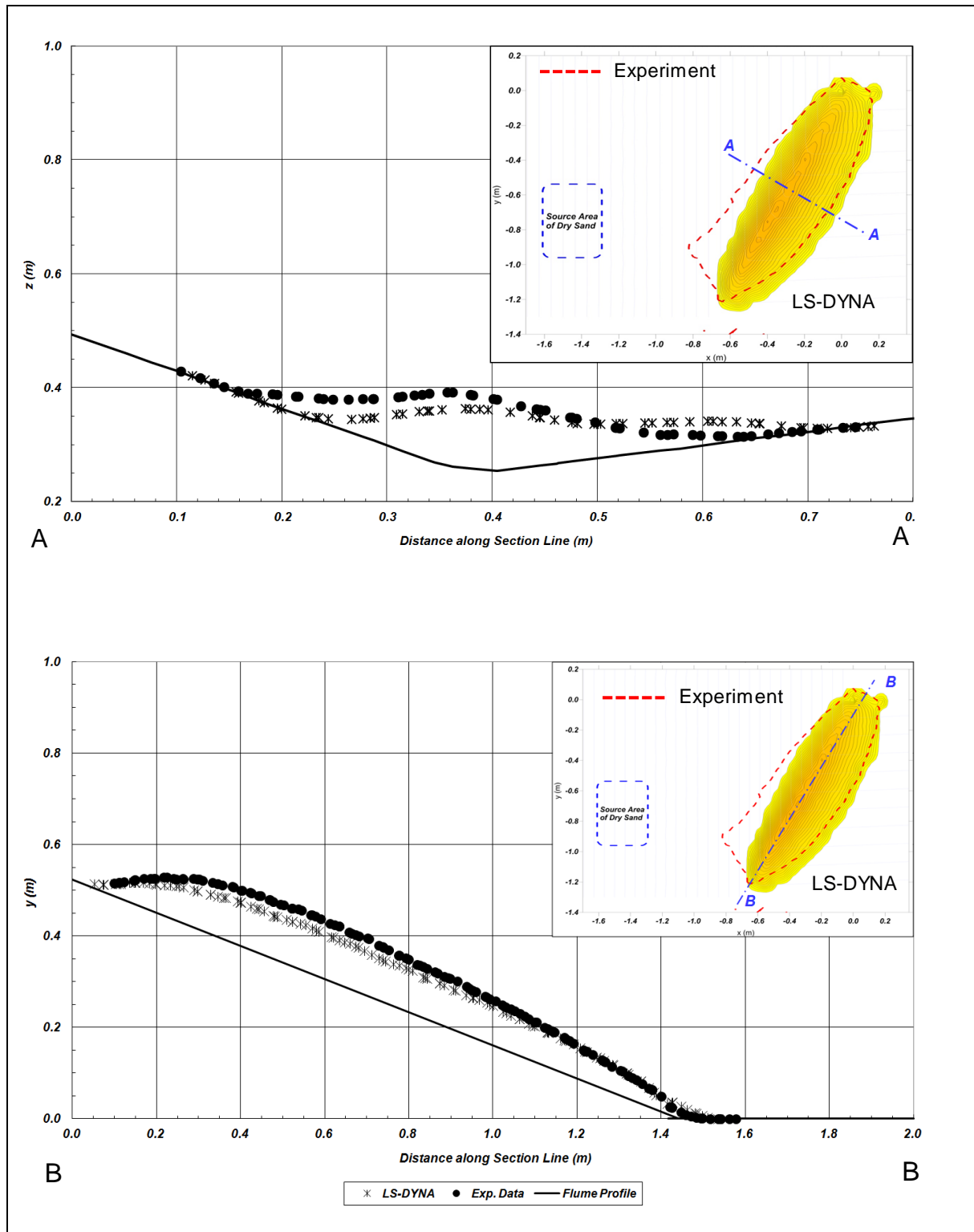


**Figure A15 Comparisons of the Deposition Profiles between the Experiment Results and the LS-DYNA Simulations**

### A.3 HKUST Flume Test

#### A.3.1 Physical Test Setup

HKUST was commissioned by the GEO to carry out a series of debris flow tests in a 5 m long flume with a channel base width of 0.2 m. Choi et al (2014) reported details of the experiments. Dry Leighton Buzzard Fraction C sand was composed of fairly uniform silica grains with specific gravity of 2,650 g/m<sup>3</sup> was used in the flume tests. The particle size of the sand ranged between 300 and 600 µm. The angle of repose of the sand is about 30° and the friction angle between the sand and flume bed is 22.6°. The initial bulk density of the sand mass was about 1,680 kg/m<sup>3</sup>. At the top end of the flume is a sand storage tank. Sand can be released into the flume by opening a flip gate that is attached to the tank. Details of the flume setup are shown in Figure A16.

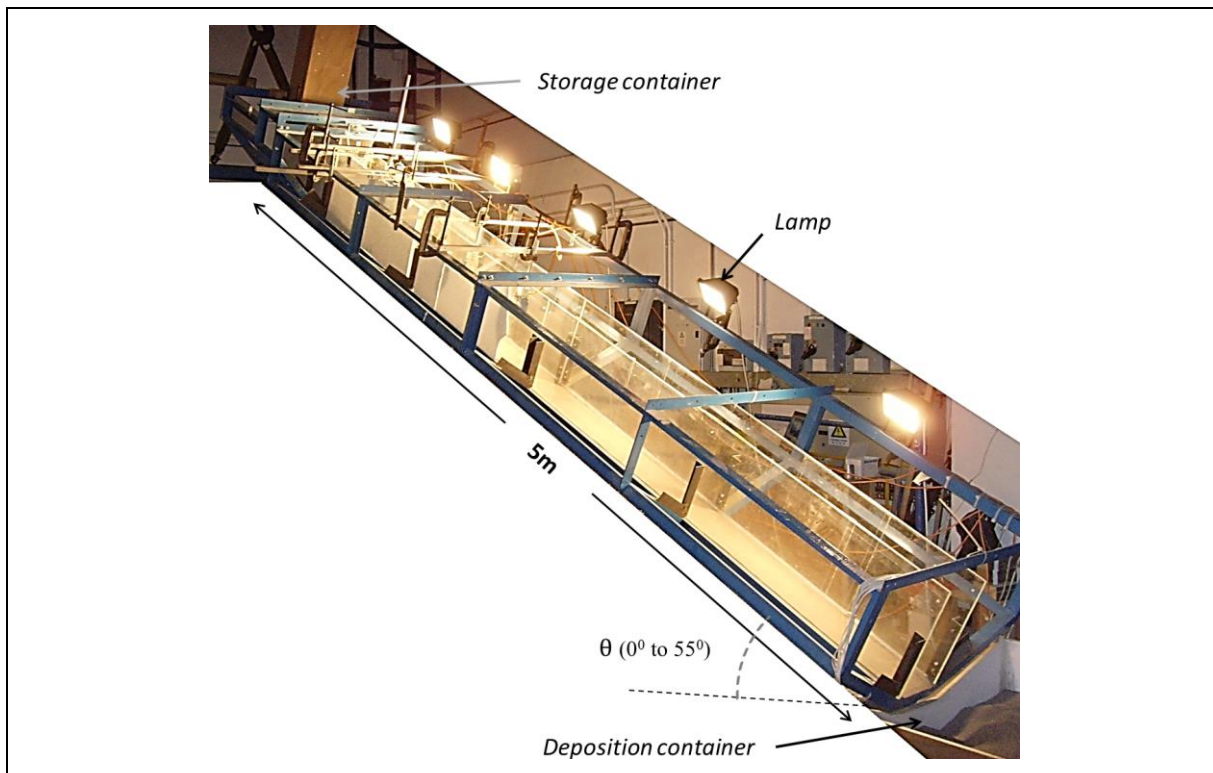


**Figure A16 The HKUST Flume Setup**

The flume inclination was selected to be 26° to facilitate development of sand flow corresponding to a Froude number of 2.6 ( $F_r = v / (g h)^{0.5}$ , where  $v$  is debris velocity,  $g$  is gravitational acceleration and  $h$  is debris depth normal to the flume bed), similar to the typical local design scenarios where  $F_r = 3$ . Instrumentation of the flume test included photo-sensors which measured debris frontal velocity along the flume, a laser sensor and high-speed camera installed at 0.8 m downstream of the flip gate which measured debris thickness and captured high-resolution images respectively. Figure A17 presents the images of the sand flow at the observation location, i.e. 1.0 m downstream of the flip gate. With the use of software ‘GeoPIV’ developed by White et al (2003), velocity hydrograph is determined (see Figure A18). The velocity presented in Figure A18 refers to the depth average velocity

at the observation position. Sand thickness hydrograph measured by the laser sensor at the observation location are also shown in the figure.

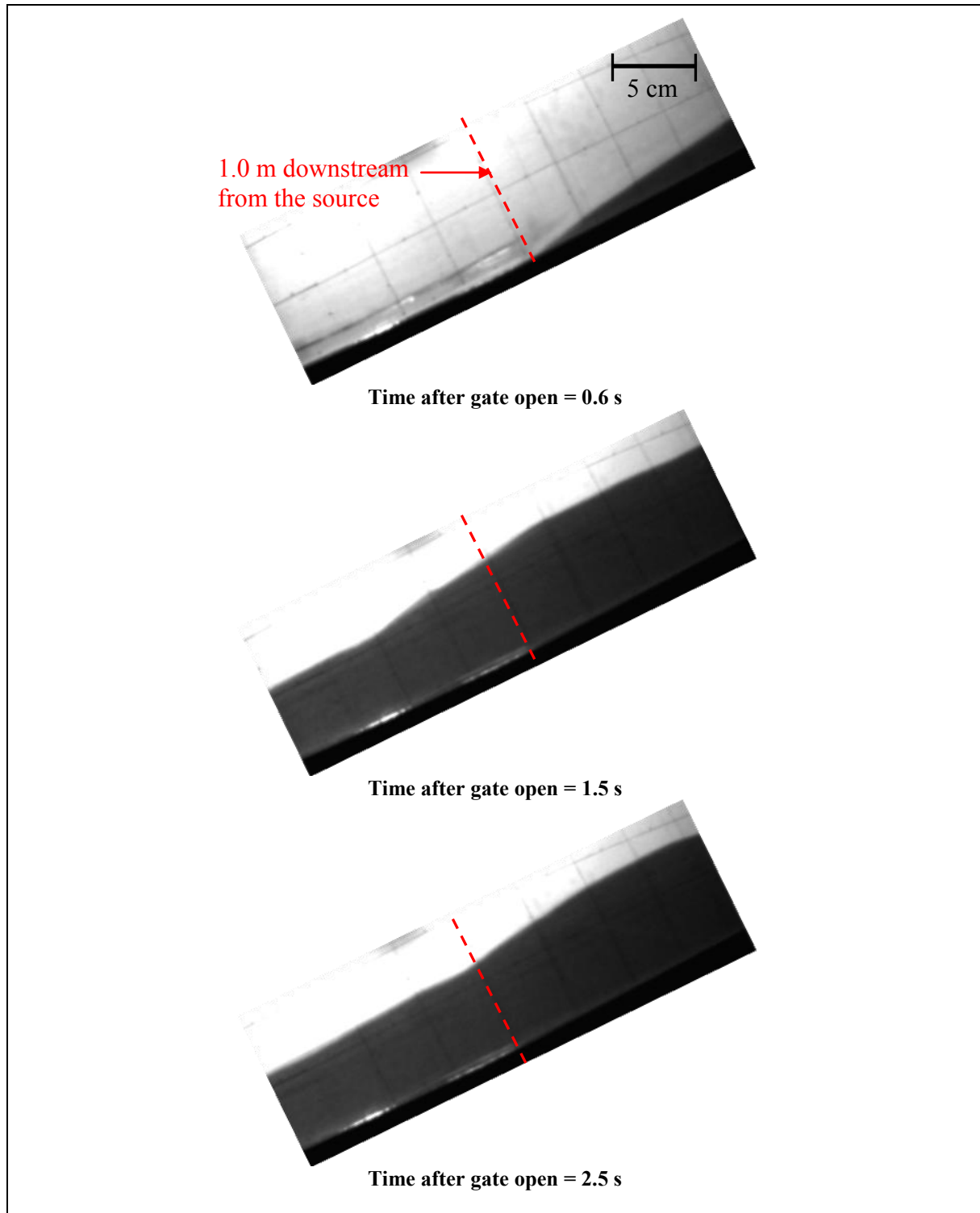


**Figure A17 The Debris Flow Images Captured by the High Speed Camera at the Observation Point of 1.0 m Downstream from the Source**

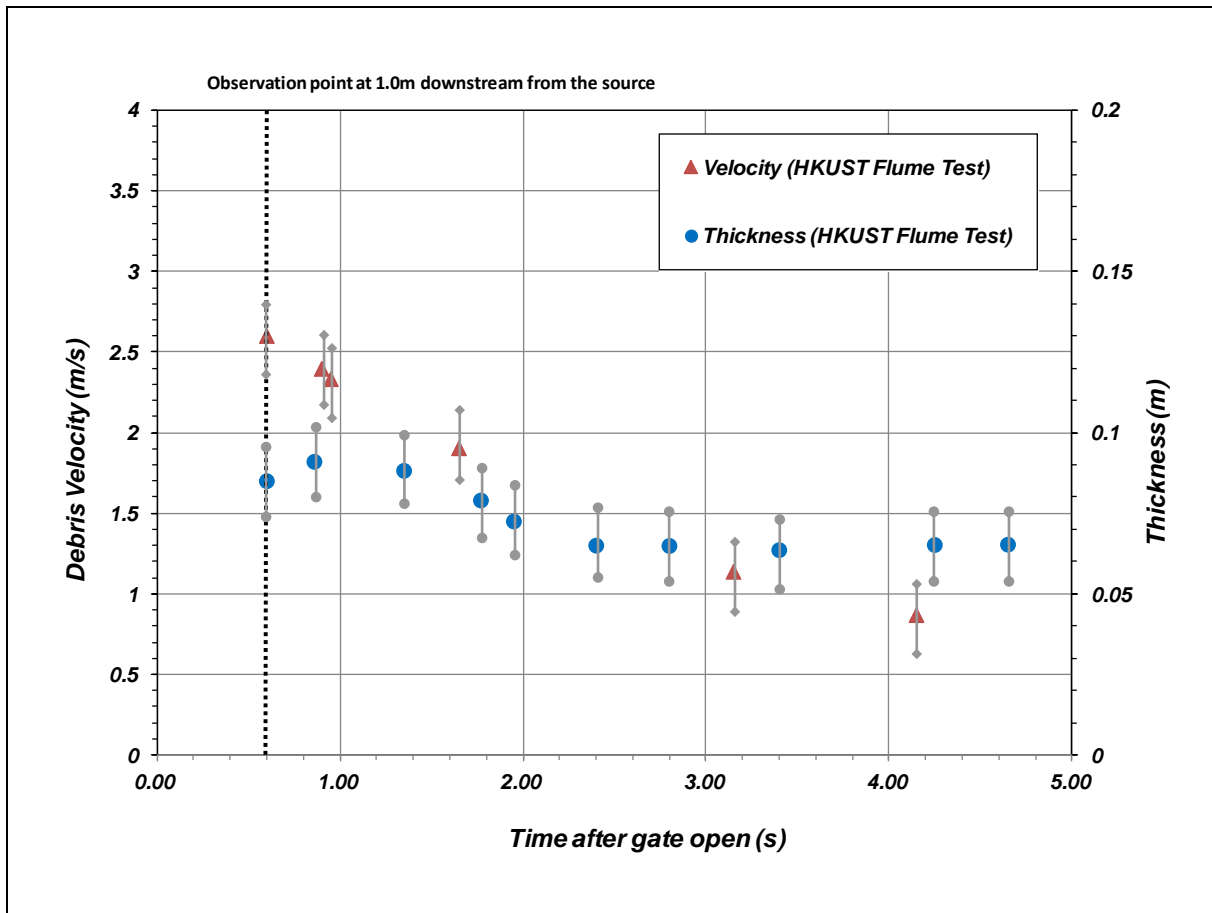


**Figure A18 Velocity and Thickness Hydrographs at 1.0 m Downstream from the Source**

### A.3.2 LS-DYNA Model Setup

The same internal frictional angle and base friction angle as measured in the laboratory, which are  $30^\circ$  and  $22.6^\circ$  respectively, are adopted in the LS-DYNA analysis. The side friction of the release box and flow channel is calibrated with the frontal velocity after the gate opened. The volume of ALE debris is  $0.06 \text{ m}^3$ , the same as the volume of sand used in the flume test. The floor and the side walls of the flume are modelled using rigid shell elements of dimensions 50 mm by 50 mm. The ALE container is made up of regular tetrahedral solid elements to cover the whole path of the sand flow. The resolution of the ALE container mesh is 25 mm (high)  $\times$  50 mm (long)  $\times$  50 mm (wide). Vertical rigid shell elements are assigned at the upslope of the flume to model the release box. The release box is set to move upward by 450 mm to mimic the effect of gate open (the gate used in the experiment was 450 mm high). Figure A19 shows the setup of the LS-DYNA model.

Table A4 presents the input parameters used. The measured density, basal friction and the internal friction angle of sand are adopted. The shear modulus and bulk modulus are the same as those used for modeling other flume tests (see Sections A.1 and A.2).

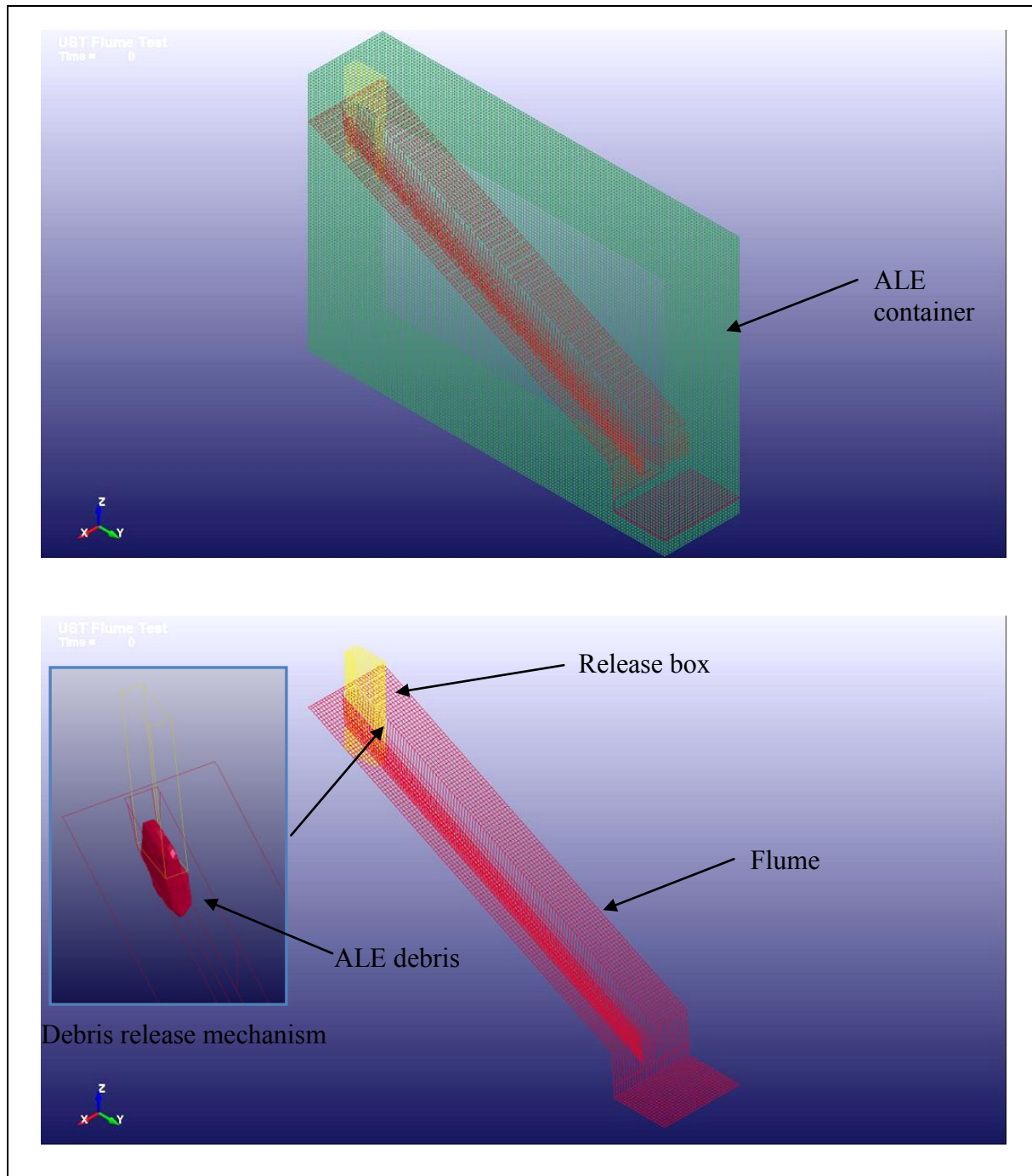


**Figure A19 Setup of the LS-DYNA Model for HKUST Flume Test**

**Table A4 Input Parameters Adopted in the LS-DYNA Models of the HKUST Tests**

Material Property	Adopted Input Parameters
Contact friction at the interface between sand and flume channel surface	22.6°
Internal friction angle	31°
Density of sand	1,680 kg/m <sup>3</sup>
Shear modulus	500 kPa
Bulk Modulus	1,000 kPa

### A.3.3 Simulation Results

The same technique of application of gravity load to the ALE material until 2 seconds is used. The simulations of sand flow with velocity vectors are presented in Figure A20. The average frontal velocity interpreted from photosensor data is compared with the simulated results in Figure A21. At upstream locations, LS-DYNA provides a better agreement with the measured data but it slightly overestimates at the downstream frontal velocity. In general, the simulation of LS-DYNA is in a good agreement with the measured data.

Figure A22 shows the comparison of the velocity and thickness hydrographs between the measurements and simulated results. The simulated velocity and thickness profiles are compared well with the test results.

### A.4 References

- Arup (2014). *Pilot Numerical Investigation of the Interactions between Landslide Debris and Flexible Debris-Resisting Barriers, Final Report*. Report prepared for Geotechnical Engineering Office, Hong Kong, 143 p.
- Choi, C.E., Ng, C.W.W., Song, D., Kwan, J.S.H., Shiu, H.Y.K., Ho, K.K.S. & Koo, R.C.H. (2014). Flume investigation of landslide debris-resisting baffles. *Canadian Geotechnical Journal*, vol. 51(5), pp 540-553.
- Iverson, R.M., Logan, M. & Denlinger, R.P. (2004). Granular avalanches across irregular three-dimensional terrain: 2. Experimental tests. *Journal of Geophysical Research*, vol. 109, F01015, doi:10.1029/2003JF000084, 16 p.
- Manzella, I. (2008). *Dry Rock Avalanche Propagation: Unconstrained Flow Experiments with Granular Materials and Blocks at Small Scale*. PhD Thesis, Ecole Polytechnique Federale De Lausanne, 220 p.
- White, D.J., Take, W.A. & Bolton, M.D. (2003). Soil deformation measurement using particle image velocimetry (PIV) and photogrammetry. *Geotechnique*, 53: 619-631.

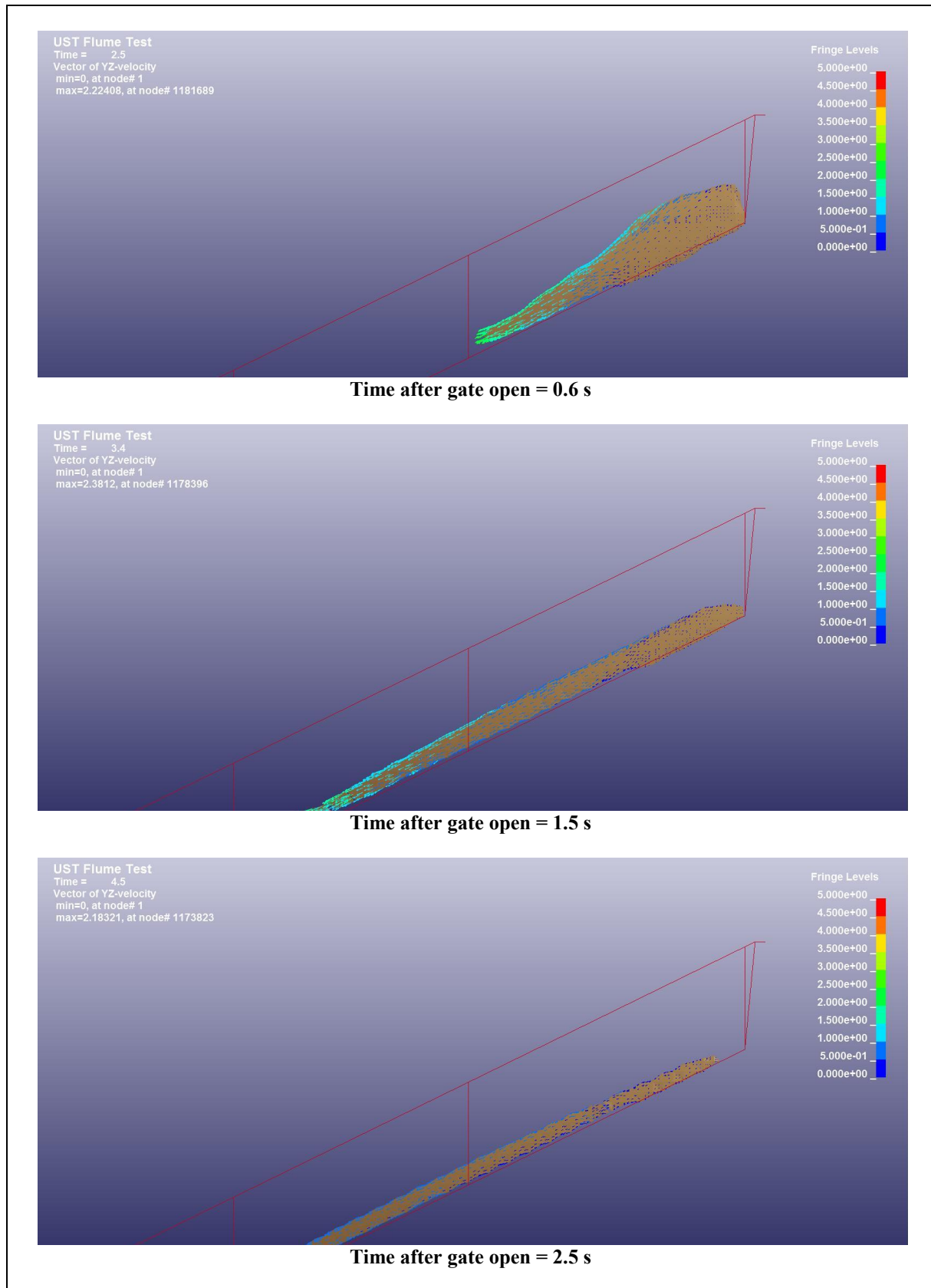


**Figure A20 Simulations of the LS-DYNA Model**



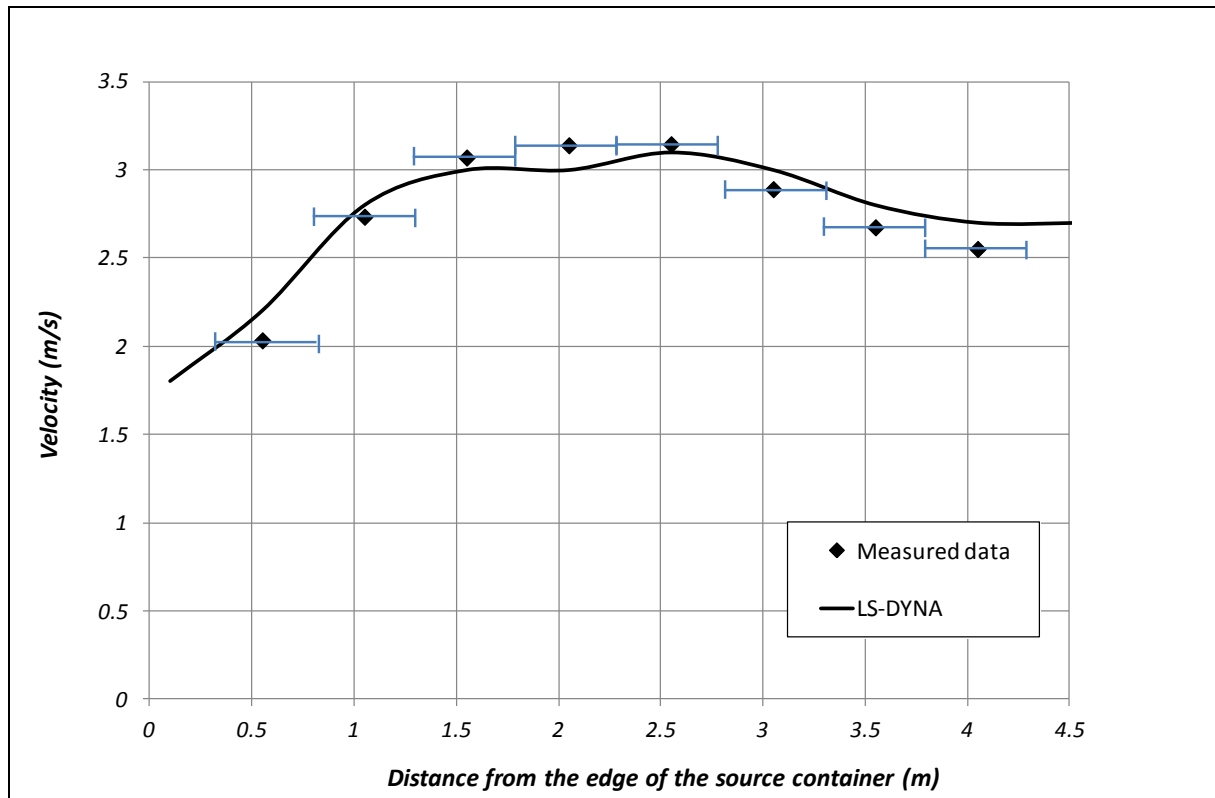


Figure A21 Frontal Velocity of the HKUST Test

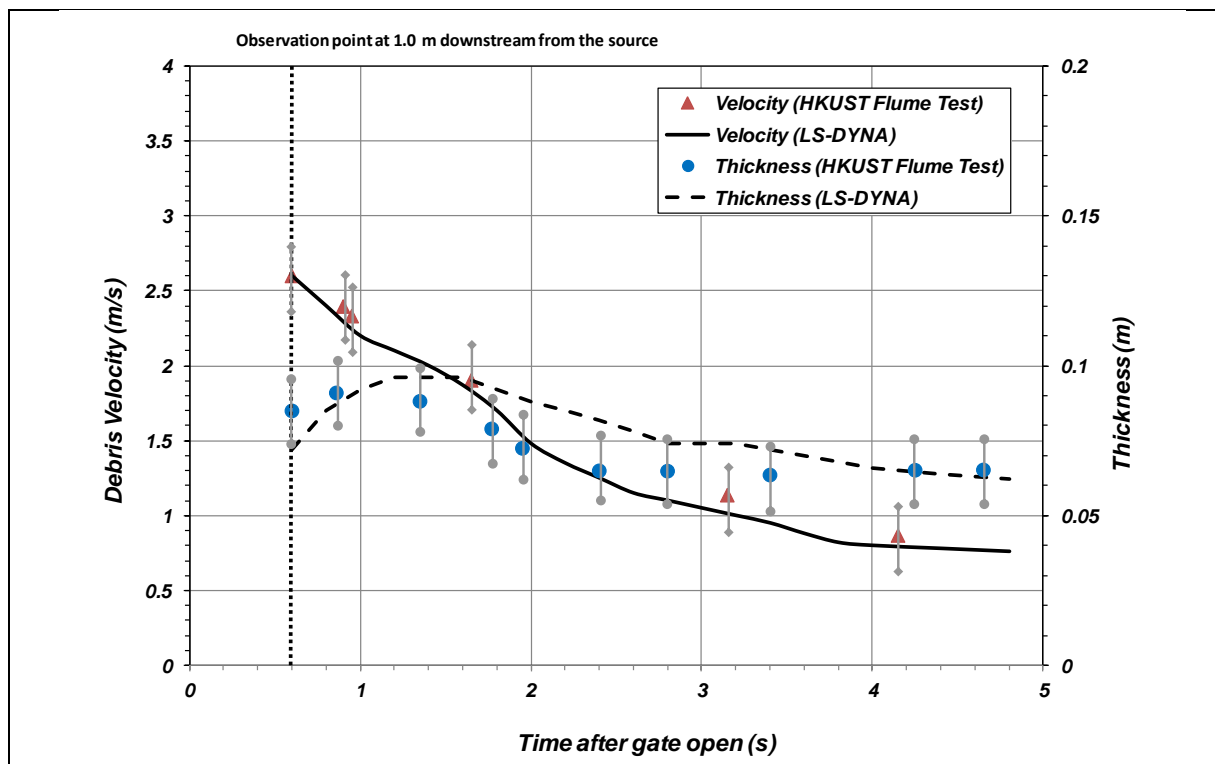


Figure A22 Velocity and Thickness Hydrographs of the HKUST Test

Appendix B  
Open Hillslope Failures

## Contents

	Page No.
Contents	50
List of Tables	51
List of Figures	52
B.1 Shum Wan Road Landslide on 13 August 1995	53
B.1.1 Background	53
B.1.2 LS-DYNA Model Setup	53
B.1.3 Simulation Results	55
B.2 Fei Tsui Road Landslide on 13 August 1995	55
B.2.1 Background	55
B.2.2 LS-DYNA Model Setup	55
B.2.3 Simulation Results	58
B.3 References	58

### List of Tables

Table No.		Page No.
B1	Input Parameters Adopted in the LS-DYNA Models of the Shum Wan Road Landslide	54
B2	Input Parameters Adopted in the LS-DYNA Models of the Fei Tsui Road Landslide	58

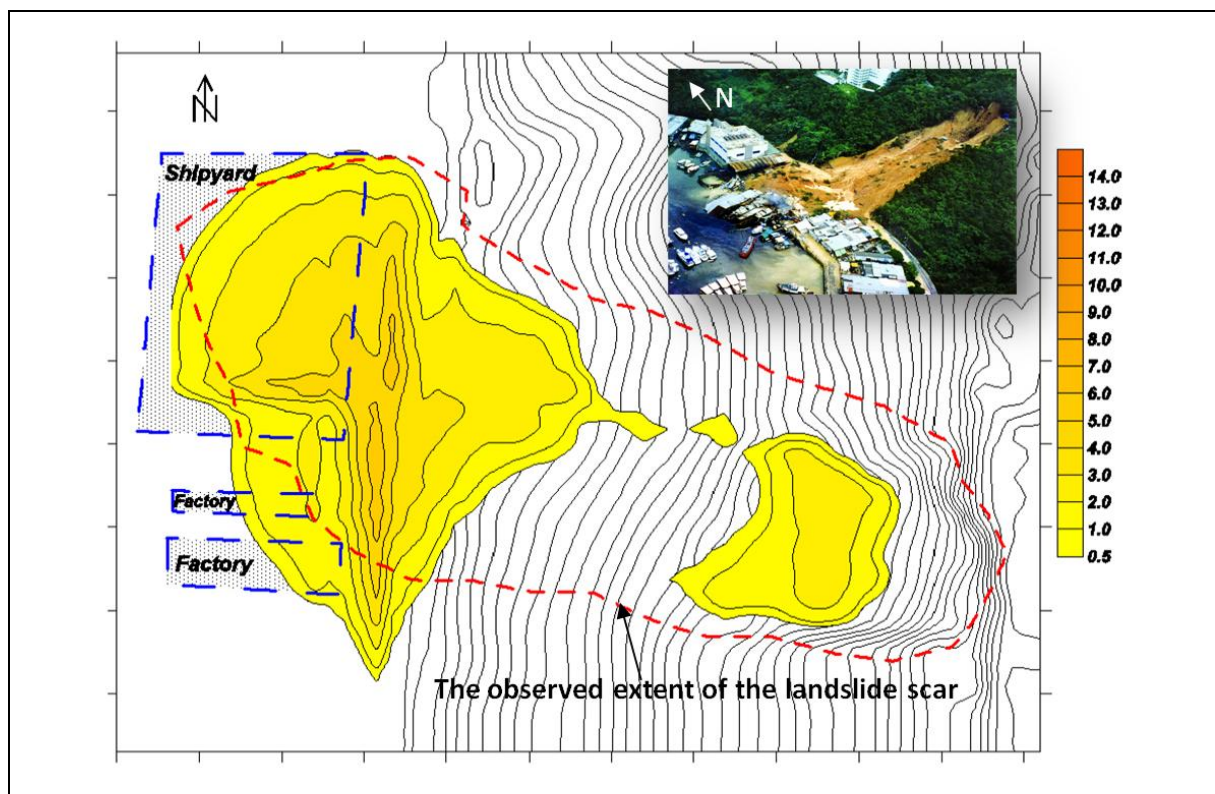
## List of Figures

Figure No.		Page No.
B1	Calculated Deposition Profile by 3d-DMM and the Observed Extent of the Scar of Shum Wan Road Landslide (Kwan & Sun, 2007)	53
B2	LS-DYNA Model of the Shum Wan Road Landslide	54
B3	LS-DYNA Simulation of the Shum Wan Road Landslide	56
B4	Comparison of Simulations between LS-DYNA and 3d-DMM of the Shum Wan Road Landslide	56
B5	Photograph of the Fei Tsui Road Landslide (Knill & GEO, 2006b)	57
B6	LS-DYNA Model of the Fei Tsui Road Landslide	57
B7	Plan and Cross Sectional Views of the Fei Tsui Road Landslide Simulation	59
B8	Velocity and Thickness Hydrographs Observed at the Southern Corner of the Church	60

## B.1 Shum Wan Road Landslide on 13 August 1995

### B.1.1 Background

The 1995 Shum Wan Road Landslide (Knill & GEO, 2006a) involved a landslide mass of 26,000 m<sup>3</sup>. It occurred on a 30° natural hillside during heavy rainfall. A planar, slab-like ground mass detached and slid down from the hillside. The landslide debris was stopped after hitting a shipyard at the slope toe up to around 7 m high. Site observations suggested that the landslide mass might remain intact during the sliding process. A series of back-analyses was carried out using 3d-DMM by Kwan & Sun (2007). The best match results were produced where frictional rheology with basal friction angle 20 degrees was adopted. The landslide density was taken as 2,000 kg/m<sup>3</sup>. The peak average velocity of debris was 10 m/s. Figure B1 shows the calculated deposition profile of the landslide debris by 3d-DMM (Kwan & Sun, 2007) with the observed extent of the landslide scar.



**Figure B1** Calculated Deposition Profile by 3d-DMM and the Observed Extent of the Scar of Shum Wan Road Landslide (Kwan & Sun, 2007)

### B.1.2 LS-DYNA Model Setup

The adopted basal friction angle is 20° to tally the back analysis by Kwan & Sun (2007). A 'landslide source container' is created in the model setup to hold landslide debris at the landslide source location. The dimensions of the topography shell elements are 2 m × 2 m. The ALE container mesh comprising regular tetrahedral solid elements is used to cover the whole runout path of the landslide. The resolution of the ALE container mesh is

approximately 1.5 m (high)  $\times$  5 m  $\times$  5 m (plan). Verticals wall that follow the outline of the landslide scar and a 'lid' that follows the pre-landslide profile over the landslide source location were set up to contain the debris material at the landslide source prior to the commencement of the mobility analysis. Similar to the analysis of the flume tests presented in Appendix A, gravity acceleration is applied to the debris materials before commencement of the mobility analysis. When the mobility analysis starts, the debris materials are released by moving the walls and the lid upwards for a distance of 10 m. Figure B2 shows the setup of the LS-DYNA model.

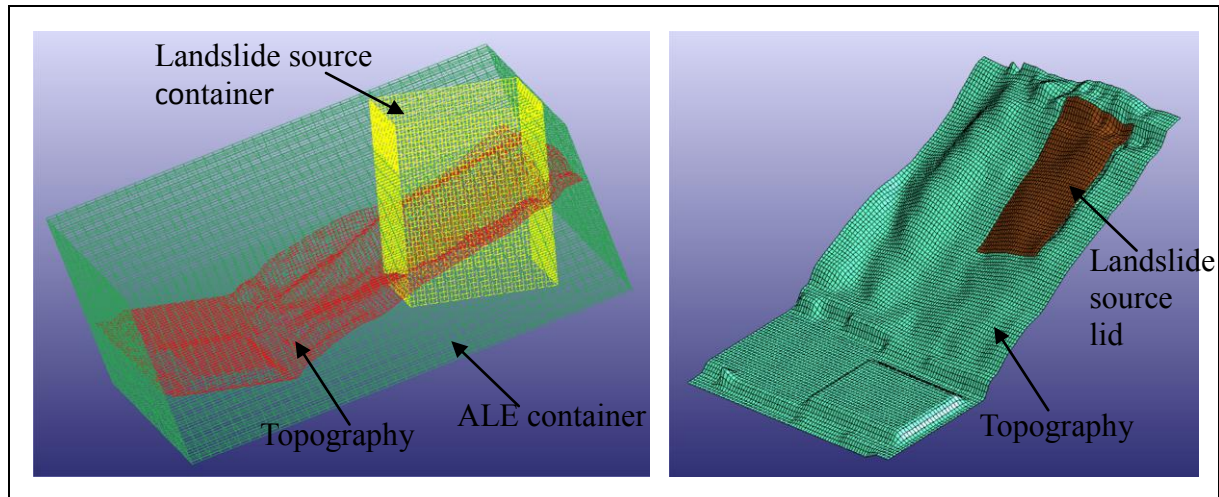


**Figure B2 LS-DYNA Model of the Shum Wan Road Landslide**

The parameters of the basal friction angle and the soil model are summarised in Table B1. The internal friction angle shown in the Table is back calculated to match the runout and the deposition profile observed on site. The shear stiffness and bulk stiffness do not have noticeable effect on the mobility analysis, values relevant to typical soil materials are therefore assumed.

**Table B1 Input Parameters Adopted in the LS-DYNA Models of the Shum Wan Road Landslide**

Material Property	Adopted Input Parameters
Basal friction angle	20°
Internal friction angle	25°
Material density	2,000 kg/m <sup>3</sup>
Shear modulus	6,000 kPa
Bulk Modulus	12,000 kPa

### **B.1.3 Simulation Results**

Figure B3 shows the calculated final landslide profiles. The extent of debris remained in the source area and the debris deposition profile at the slope toe area are comparable with the field observation. Further comparison between the simulations of LS-DYNA and 3d-DMM analyses is shown in Figure B4. The landslide extents produced by LS-DYNA and 3dDMM agree well. The maximum thickness of the debris deposition calculated by LS-DYNA matches the field observation closely, which is in an order of 7 m. Larger landslide extent is predicted by 3d-DMM, and this is probably due to the numerical dispersion at the non-constrained edge boundary. Both LS-DYNA and 3d-DMM estimate that debris motions could have come to rest in around 30 seconds. It is considered that the back analysed internal friction angle and basal friction angle adopted for the LS-DYNA analysis provide satisfactory simulation.

## **B.2 Fei Tsui Road Landslide on 13 August 1995**

### **B.2.1 Background**

The incident of Fei Tsui Road Landslide (Knill & GEO, 2006b) was a man-made cut slope failure along Fei Tsui Road, Chai Wan. The width and length of the landslide scar are 33 m and 90 m respectively. The maximum depth of the landslide mass is up to 15 m deposited at the slope toe. A corresponding landslide volume of 14,000 m<sup>3</sup> slid out from the scar crossing the fenced-off level ground and Fei Tsui Road. The landslide debris was brought to stop after hitting a reinforced concrete building on the opposite side of the road. The maximum height of debris abutting the building was 5 m. Figure B5 shows the photograph of the Fei Tsui Road Landslide (Knill & GEO, 2006b).

### **B.2.2 LS-DYNA Model Setup**

Based on the back analysis by Kwan & Sun (2007) using 3d-DMM, the basal resistance to movement of the landslide mass was calculated using frictional rheology. A low basal friction angle of 22° was used to account for the presence of the kaolinite-rich layer in the landslide source area. In contrast, a higher basal friction angle of 35° was used for the portion of runout path on Fei Tsui Road.

A LS-DYNA model is setup to simulate the landslide based on the site topography and the basal friction angle obtained from Kwan & Sun (2007). The resolution of the topography shell elements is 1 m × 1 m. ALE container mesh is placed over the entire landslide trail and the mesh dimensions are approximately 0.5 m (high) × 1 m × 1 m (plan). A 'lid' following the pre-landslide topography above the landslide source was established using rigid shell elements in the numerical model to retain the landslide debris material placed on the scar. The lid moved upwards for 10 m to release the source mass at the start of the analysis. Figure B6 shows the setup of the LS-DYNA model.



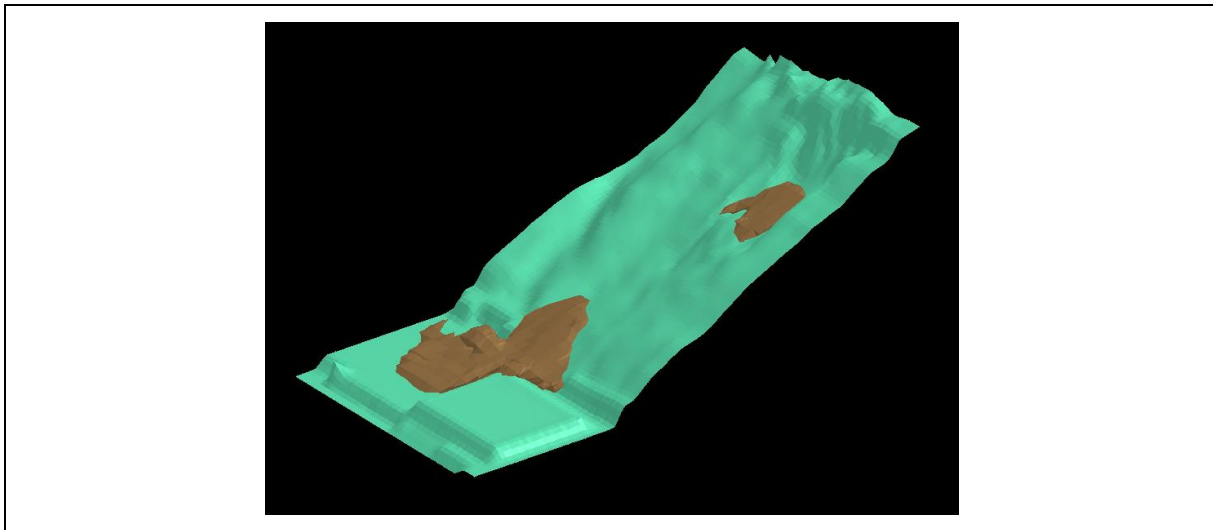


**Figure B3** LS-DYNA Simulation of the Shum Wan Road Landslide

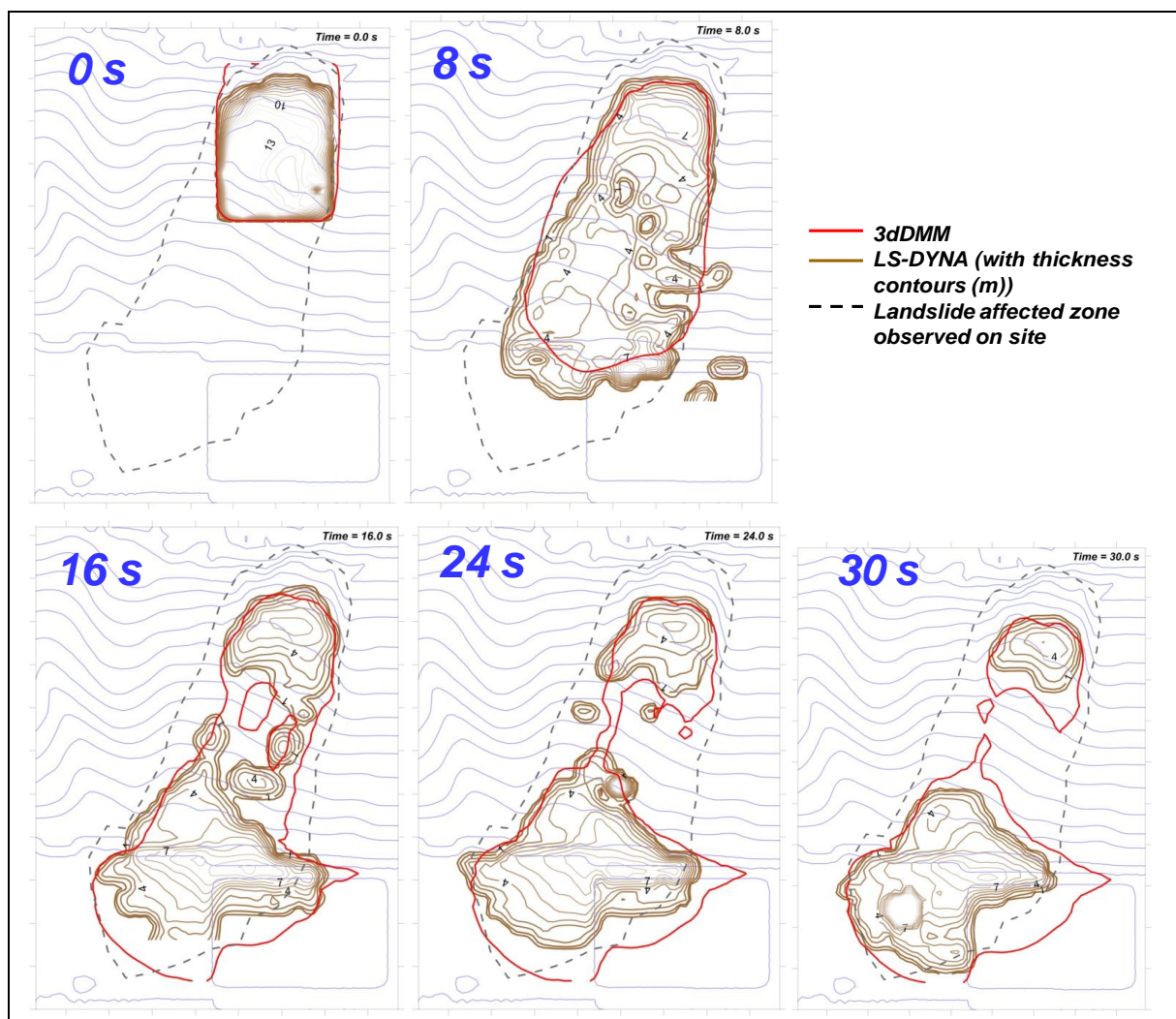


**Figure B4** Comparison of Simulations between LS-DYNA and 3d-DMM of the Shum Wan Road Landslide



**Figure B5 Photograph of the Fei Tsui Road Landslide (Knill & GEO, 2006b)**

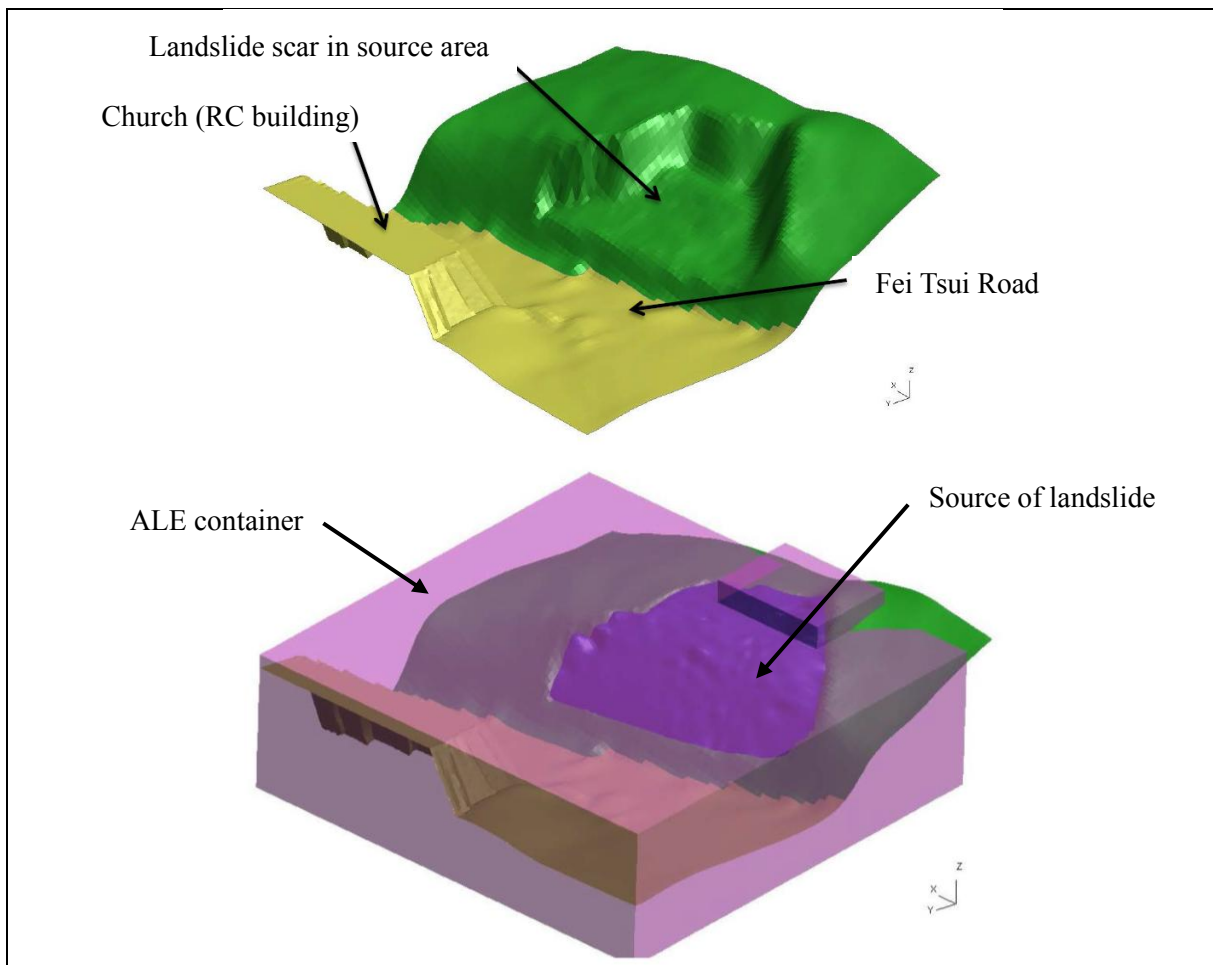


**Figure B6 LS-DYNA Model of the Fei Tsui Road Landslide**

The basal friction angle and the soil model are summarised in Table B2. The internal friction angle has been back analysed to match the runout distance and the deposition profile observed on site.

**Table B2 Input Parameters Adopted in the LS-DYNA Models of the Fei Tsui Road Landslide**

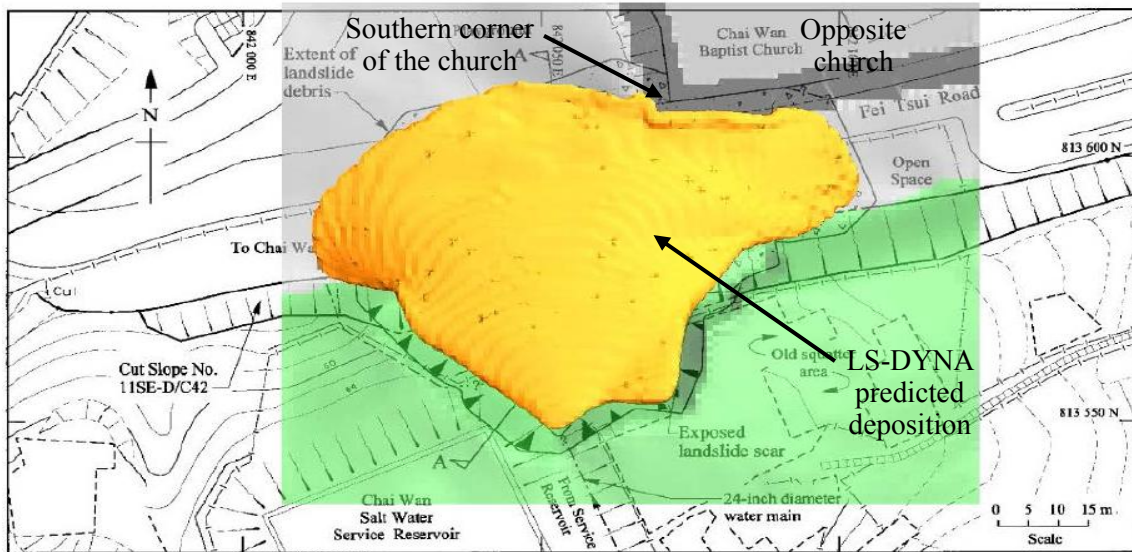
Material Property	Adopted Input Parameters
Basal friction angle of source area	22°
Basal friction angle of Fei Tsui Road	35°
Internal friction angle	30°
Material density	1,900 kg/m <sup>3</sup>
Shear modulus	6,000 kPa
Bulk Modulus	12,000 kPa

### B.2.3 Simulation Results

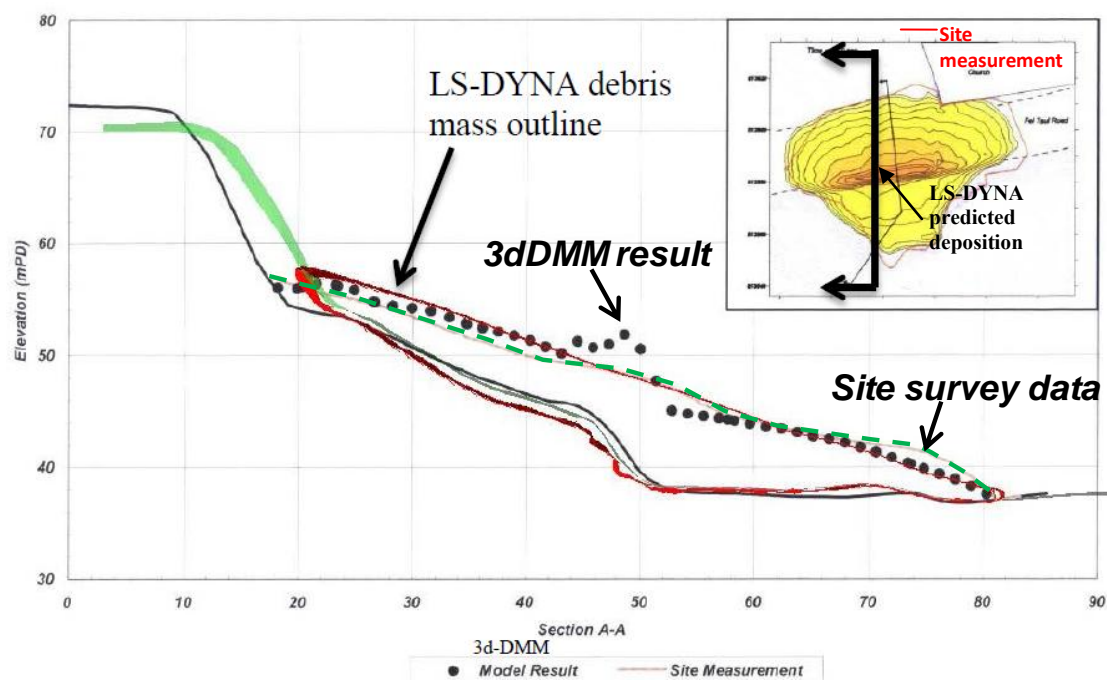
Figure B7 shows the simulated landslide debris profile and the topographic survey data of (Knill & GEO, 2006b). The deposition profile generated using 3d-DMM (Kwan & Sun, 2007) is also included in Figure B7 for comparison. The results of LS-DYNA are in good agreement with the field observation and the prediction of 3d-DMM. The debris is stopped and accumulated at the southern corner of the opposite church building. The velocity and thickness hydrographs at this location are plotted in Figure B8. They compared well with the results of 3d-DMM by Kwan & Sun (2007). It is shown that LS-DYNA gives a better result of debris height comparing with 3d-DMM. The debris height calculated by LS-DYNA is 4.4 m c.f. 5 m as observed on site. The velocity hydrographs shown in Figure B8 indicate that debris impacted on the church at a velocity of 3.8 m/s. Both LS-DYNA and 3d-DMM show similar results on velocity hydrographs and LS-DYNA predicted a closer match on maximum thickness of debris with the filed observation.

### B.3 References

- Knill, J. & GEO (2006a). *Report on the Shum Wan Road Landslide of 13 August 1995 (GEO Report No. 178)*. By Sir John Knill & Geotechnical Engineering Office. Geotechnical Engineering Office, Hong Kong, 177 p.
- Knill, J. & GEO (2006b). *Report on the Fei Tsui Road Landslide of 13 August 1995 (GEO Report No. 188)*. By Sir John Knill & Geotechnical Engineering Office. Geotechnical Engineering Office, Hong Kong, 147 p.
- Kwan, J.S.H. & Sun, H.W. (2007). Benchmarking exercise on landslide mobility modeling – runout analysis using 3dDMM. *Proceedings of the 2007 International Forum on Landslide Disaster Management*, vol. II, pp 945-966.



Plan View



Cross Sectional View

Figure B7 Plan and Cross Sectional Views of the Fei Tsui Road Landslide Simulation



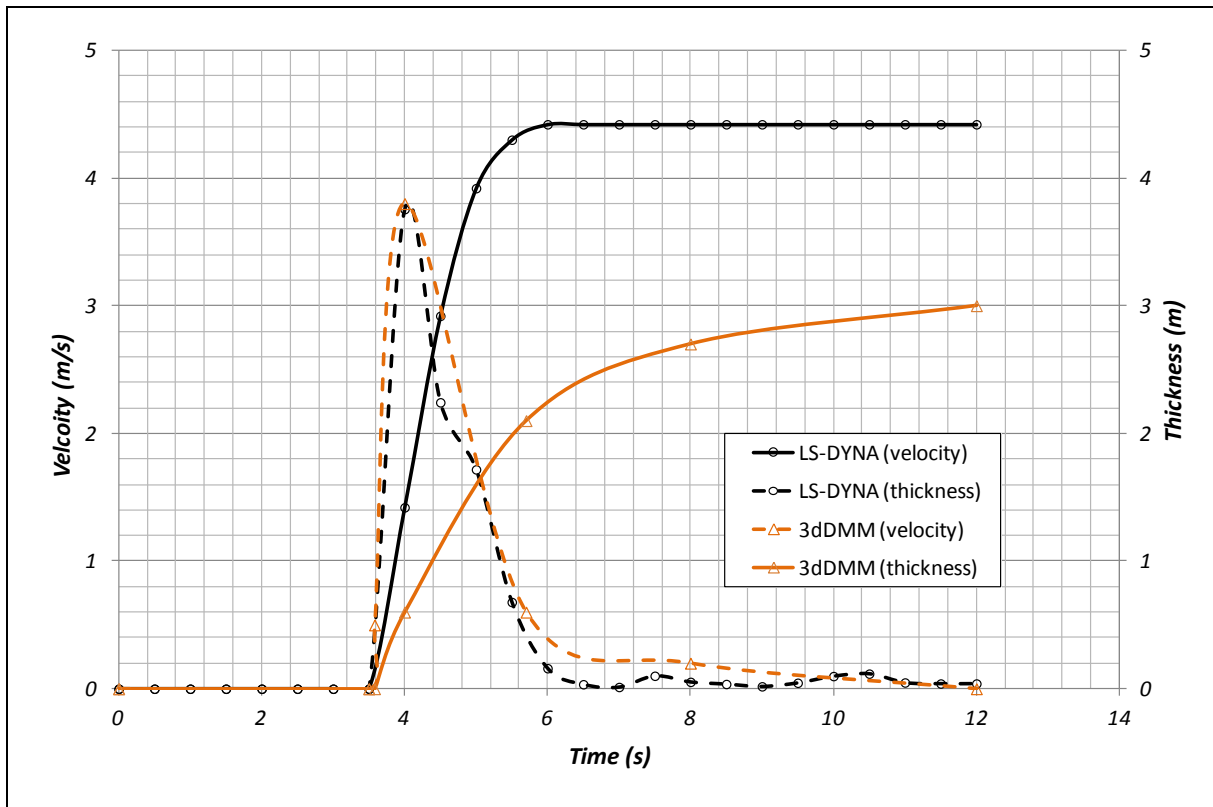


**Figure B8 Velocity and Thickness Hydrographs Observed at the Southern Corner of the Church**

Appendix C  
Channalised Debris Flows

## Contents

	Page No.
Contents	62
List of Tables	63
List of Figures	64
C.1 Yu Tung Road Debris Flow on 7 June 2008	65
C.1.1 Background	65
C.1.2 LS-DYNA Model Setup	66
C.1.3 Simulation Results	67
C.2 2005 Kwun Yam Shan Debris Flow	69
C.2.1 Background	69
C.2.2 LS-DYNA Model Setup	70
C.2.3 Simulation Results	71
C.3 Sham Tseng San Tsuen Debris Flow on 23 August 1999	74
C.3.1 Background	74
C.3.2 LS-DYNA Model Setup	75
C.3.3 Simulation Results	76
C.4 References	76

### List of Tables

Table No.		Page No.
C1	Input Parameters Adopted in the LS-DYNA Models of the Yu Tung Road Debris Flow	67
C2	Input Parameters Adopted in the LS-DYNA Models of the Kwun Yam Shan Debris Flow	71
C3	Input Parameters Adopted in the LS-DYNA Models of the Sham Tseng San Tsuen Debris Flow	75



## List of Figures

Figure No.		Page No.
C1	Catchment of the Yu Tung Road Debris Flow	65
C2	LS-DYNA Model of the Yu Tung Road Landslide	66
C3	Frontal Debris Flow Velocity against Chainage	67
C4	Simulation of Yu Tung Road Debris Flow Using LS-DYNA Analysis	68
C5	An Aerial Photograph of the Site (MGS, 2008)	69
C6	Longitudinal Profile of the Landslide Trail (MGS, 2008)	70
C7	LS-DYNA Model of the Kwun Yam Shan Debris Flow	71
C8	Simulations of LS-DYNA Run and Comparison with the Results of 3d-DMM by Kwan & Sun (2007)	72
C9	Debris Runout against Time	73
C10	Section at Sharp Bend (Ch 220 m)	73
C11	Site Layout Plan and the Aerial Photograph of Sham Tseng San Tsuen Debris Flow (FMSW, 2005)	74
C12	LS-DYNA Model of the Sham Tseng San Tsuen Debris Flow	75
C13	Debris Frontal Velocity	76

## C.1 Yu Tung Road Debris Flow on 7 June 2008

### C.1.1 Background

A large scale landslide occurred on the hillside above Yu Tung Road, Tung Chung Northern Lantau, on 7 June 2008 during a Black Rainstorm. Yu Tung Road was affected directly by the channelised debris flow which gave rise to about 3,500 m<sup>3</sup> of debris. Both westbound lanes of Yu Tung Road were closed for more than two months. A video showing the debris flow event is available online at <http://youtu.be/R2uTKyK1c9k>. A detailed geotechnical investigation of the event is reported in AECOM (2012). Figure C1 shows the catchment taken after the debris flow event. The debris flow was a result of a massive landslide with a 2,350 m<sup>3</sup> failure volume at the head of the drainage line. The landslide materials entered into the incised drainage line, mixed with surface runoff and developed into a debris flow with an additional volume of 1,000 m<sup>3</sup>. The debris flow travelled about 600 m and disrupted the traffic of Yu Tung Road immediately downstream of the drainage line outlet.

A detailed back-analysis of Voellmy parameters has been carried out by Kwan et al (2012) to fit the observation of the Yu Tung Road Landslide case. Voellmy rheological parameters comprising basal friction coefficient of 0.14 ( $= \tan \phi_b$ , where  $\phi_b$  is 8°) and turbulence coefficient of 500 m/s<sup>2</sup> were back obtained.



**Figure C1 Catchment of the Yu Tung Road Debris Flow**

### C.1.2 LS-DYNA Model Setup

The runout distance of Yu Tung Road debris flow exceeded 600 m and the width of some sections of the runout trail was over 30 m. The computational domain is discretised into an array of cells of dimensions 2 m (wide), 2 m (long) and 0.5 m (deep). Over 930,000 cells are used in the model. The topography is modelled using shell elements of  $2\text{ m} \times 2\text{ m}$ . The topography is established using the post-landslide topographic survey data. Again, in order to contain the debris mass at the initial position for internal stress initialisation, an artificial rigid tube and lid was specified in the model to restrict the debris mass movement before the debris mobility analysis. The tube and lid were modelled using rigid shell elements. A very low contact friction between debris materials and the shell elements was specified, such that there would be minimal disturbance to the debris when the “gate” was lift up for the release of the debris mass. The setup of the LS-DYNA model is shown in Figure C2.

The Yu Tung Road debris flow is watery as shown in the video record and the sedimentology of the event could mainly comprise sandy and coarse materials (AECOM, 2012). In theory, it is a cohesionless material. However, specification of a non-zero value of cohesion is required for LS-DYNA analysis. Therefore, a nominal value, or a very low value of cohesion, 1 kPa, is assumed. Drucker-Prager yield criteria are adopted. An internal friction angle ( $\phi$ ) of  $15^\circ$  has been back-calculated based on the velocity determined from the video record and the super-elevation data mapped on site (AECOM, 2012). Voellmy rheology is used. The basal friction coefficient ( $\tan\phi_b$ , where  $\phi_b$  is  $8^\circ$ ) of 0.14 same as the one used for 2d-DMM analysis was adopted. The turbulent friction of the Voellmy rheology was modelled as the damping force proportional to the square of the debris velocity as described in Section 2. A Voellmy turbulence coefficient  $\zeta$  of  $500\text{ m/s}^2$  is adopted. The average debris thickness was taken to be 2 m, therefore,  $\zeta_d$  for the LS-DYNA analysis is  $0.01\text{ m}^{-1}$  (see also Equation 2.3 in Section 2). Key parameters which define the properties of the debris flow materials are listed in Table C1.

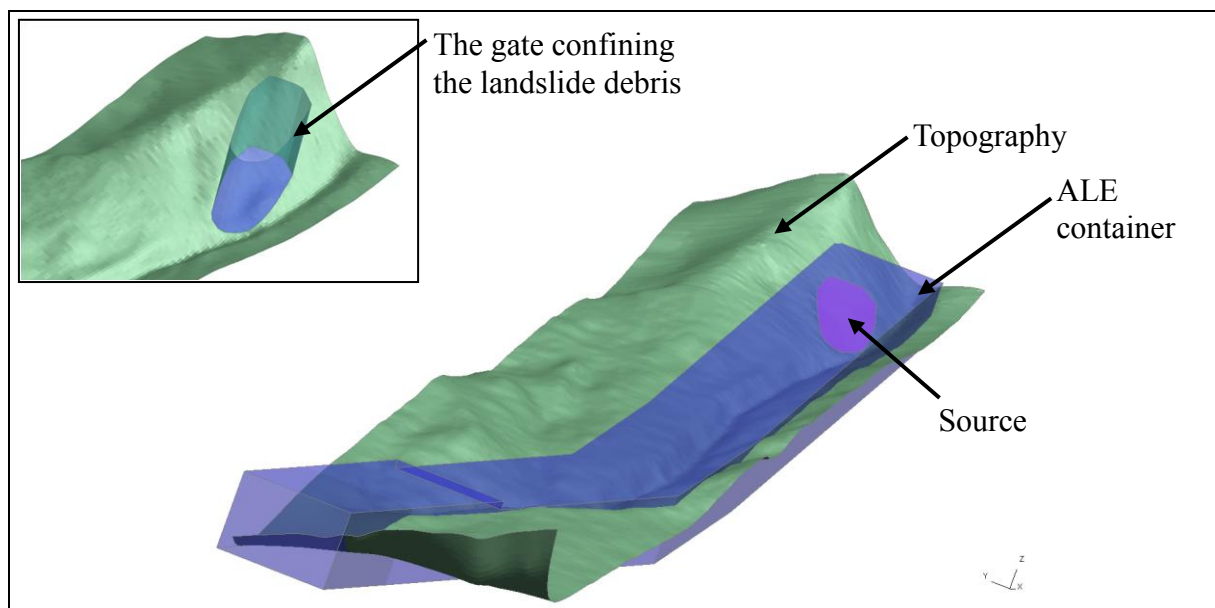


**Figure C2 LS-DYNA Model of the Yu Tung Road Landslide**

**Table C1 Input Parameters Adopted in the LS-DYNA Models of the Yu Tung Road Debris Flow**

Material Property	Adopted Input Parameters
Basal friction angle	8°
Voellmy turbulence coefficient	500 m/s <sup>2</sup>
Internal friction angle	15°
Material density	1,900 kg/m <sup>3</sup>
Shear modulus	6,000 kPa
Bulk Modulus	12,000 kPa

### C.1.3 Simulation Results

Figure C3 shows the frontal debris velocity of Yu Tung Road debris flow calculated by 2d-DMM and LS-DYNA. Both numerical models produce comparable results which generally match the observed debris velocity from the video record and super-elevation data mapped in the field. 2d-DMM and LS-DYNA adopt different numerical strategies. 2d-DMM is developed based on depth average approach, whereas LS-DYNA is a full 3-dimensional analysis with consideration of the yield criteria of the materials being modelled. The 2d-DMM analysis requires a pre-defined debris trail width whereas LS-DYNA does not. These factors may also contribute to the difference between the two simulation results. LS-DYNA conducts undrained analysis, the internal friction should be regarded as an apparent friction angle which incorporates the effects of pore water pressure. In view that the debris flow is watery, the back calculated internal friction angle (i.e. 15°) is of a reasonable order of magnitude.

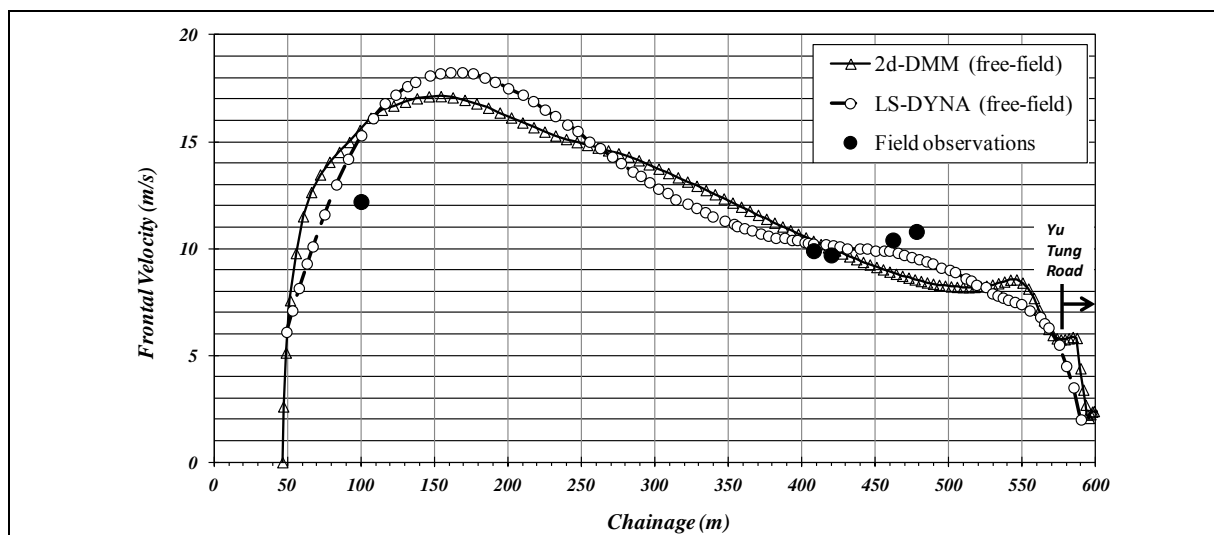
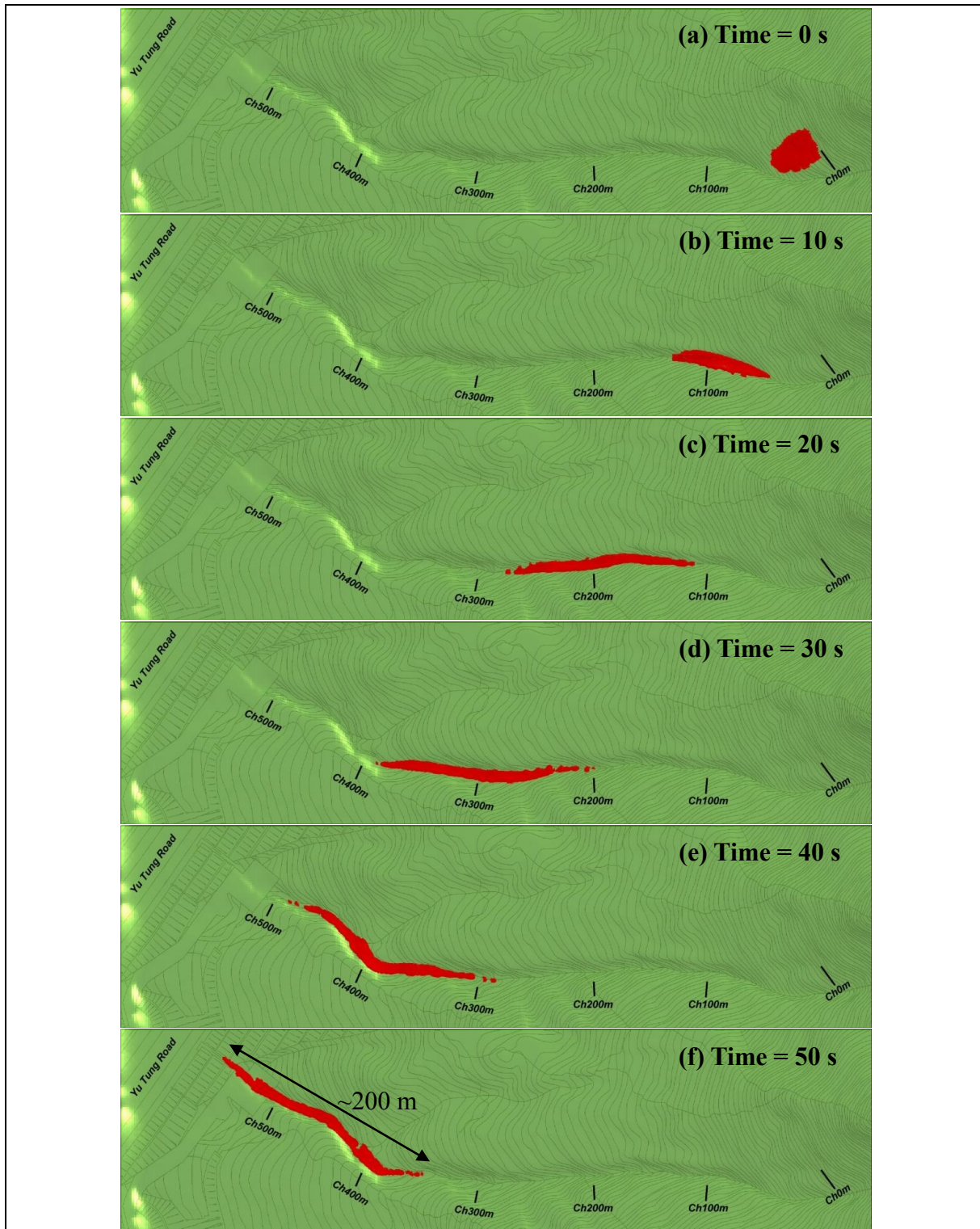
**Figure C3 Frontal Debris Flow Velocity against Chainage**

Figure C4 presents the calculated the travel of the debris flow extents at different times. The youtube video shows the progress of main debris pulse running down the channel. According to the footage of the debris flow, the debris flow front took about 20 seconds to



travel from Ch 320 m to Ch 530 m. This generally agrees with LS-DYNA's simulation. Figures C4(c) and C4(e) show that the debris front could have transported from about Ch 300 to Ch 500 in 20 seconds. Figure C4(f) shows that the calculated length of debris flow could have been about 200 m and this is generally consistent with the one determined from the footage.



**Figure C4 Simulation of Yu Tung Road Debris Flow Using LS-DYNA Analysis**

## C.2 2005 Kwun Yam Shan Debris Flow

### C.2.1 Background

A landslide incident (Incident No. 2005/08/0422) occurred on a natural hillside at Kwun Yam Shan, below Tate's Ridge. The landslide was reported in the early morning of 22 August 2005 following heavy rainfall on 19 and 20 August 2005. No casualties were reported as a result of the landslide. Figures C5 and C6 show the aerial photograph and the longitudinal profile of the landslide trail respectively. About 1,000 m<sup>3</sup> of material detached from the source and developed into a debris flow. The travel angle was about 22° and the runout path was inclined at an angle of about 35° to the horizontal. The inclination of the slope profile was gradually reduced to 12° at the debris deposition zone.

At about 220 m from the landslide source, landslide debris changed its direction of movement following a sharp bend of a drainage line with observed super-elevation of 6.8 m high. The debris travelled a total distance of about 330 m down the drainage line, finally coming to rest within the drainage line when it was blocked by two pre-existing boulder dams at about Chainage 270 m. Details of the incident are documented in the GEO Report No. 239 (MGS, 2008).

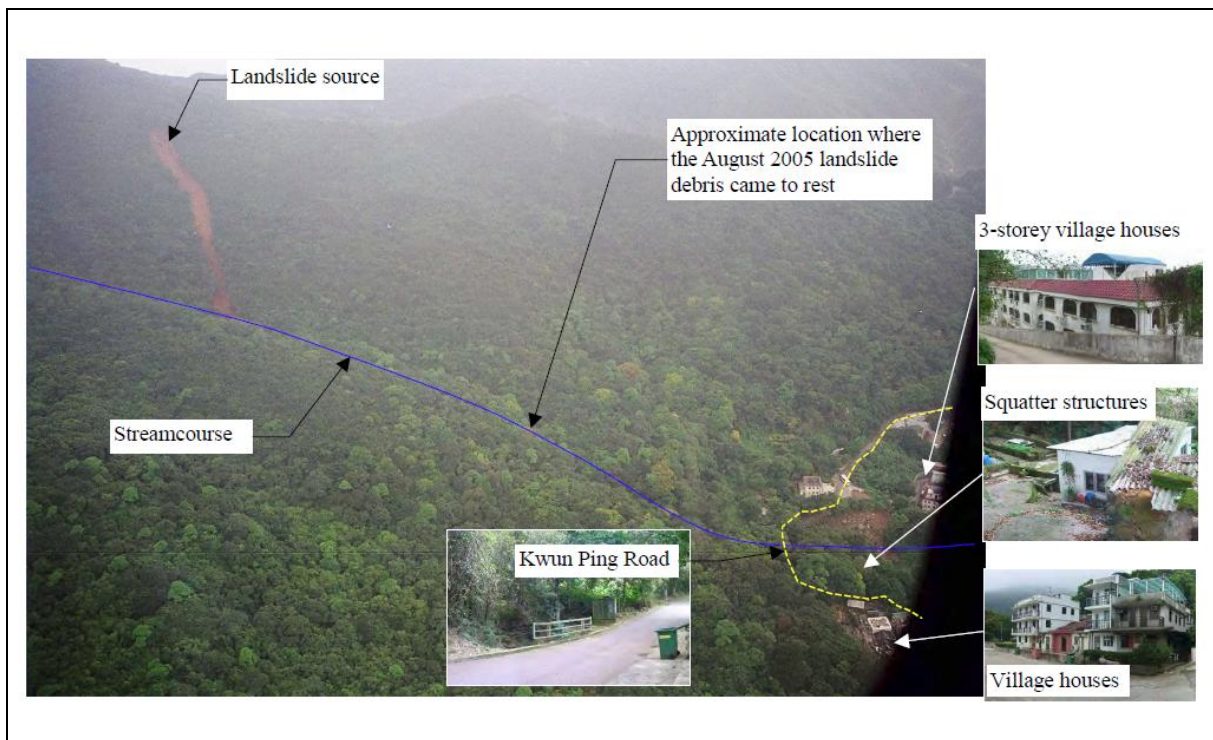


**Figure C5 An Aerial Photograph of the Site (MGS, 2008)**

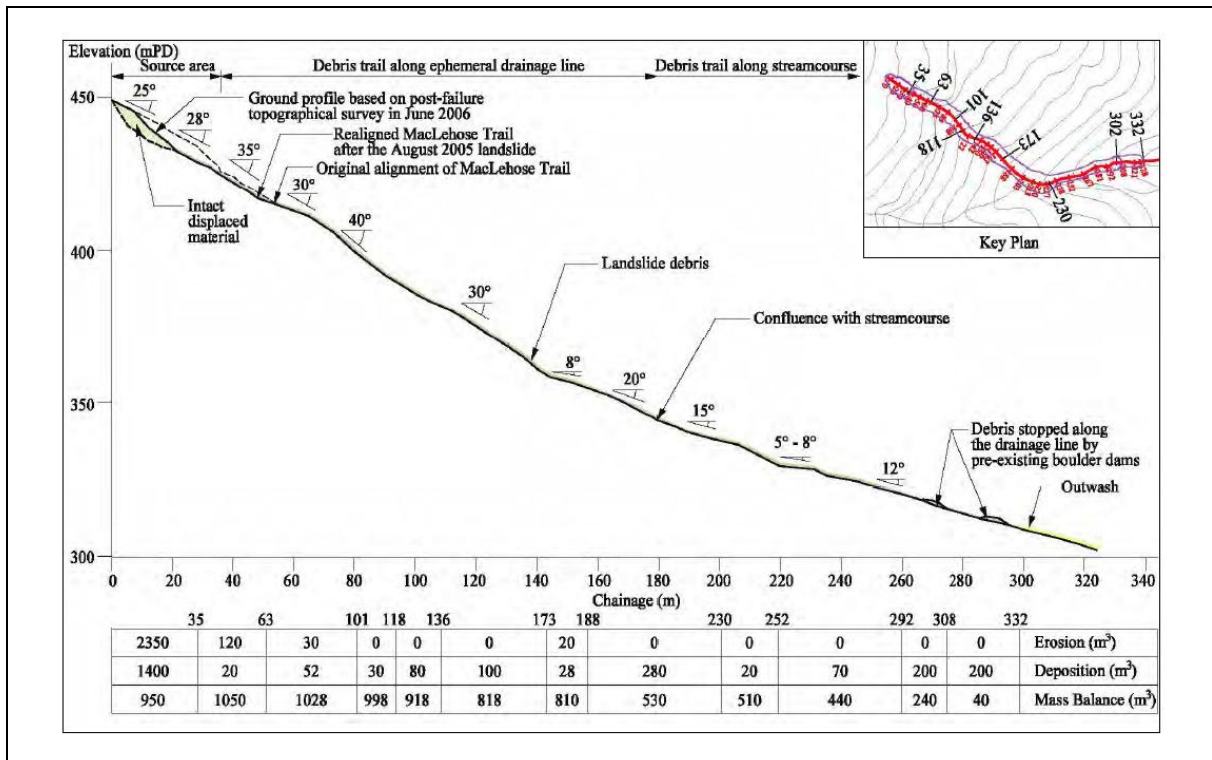


**Figure C6 Longitudinal Profile of the Landslide Trail (MGS, 2008)**

### C.2.2 LS-DYNA Model Setup

The dimensions of the ALE computational domain is 1 m (wide), 1 m (long) and 0.2 m (deep) and over 540,000 elements were used in the model. The topography was established using 1 m by 1 m shell elements. A relatively finer ALE computational domain was adopted when compared to the LS-DYNA model of the Yu Tung Road Landslide, since the length of the runout trail is shorter in this case history. The method of internal stress initialization and the use of an artificial rigid tube and lid to confine debris materials at landslide source are the same as other LS-DYNA runs. The setup of the LS-DYNA model is shown in Figure C7.

The turbulence coefficient of  $500 \text{ m/s}^2$  and the basal friction of  $15^\circ$  are adopted according to the back-analysis of 3d-DMM by Kwan & Sun (2007). Drucker-Prager yield criteria were also adopted. After a number of trials, it is found that LS-DYNA can produce a debris runout distance that best match the site observation when an internal friction angle of  $20^\circ$  was used. Key parameters which define the properties of the debris flow materials are listed in Table C2. The other input parameters (e.g. bulk modulus, density of debris flow, etc.) same as those of the 2008 Yu Tung Road Debris Flow were adopted (see Table C1).



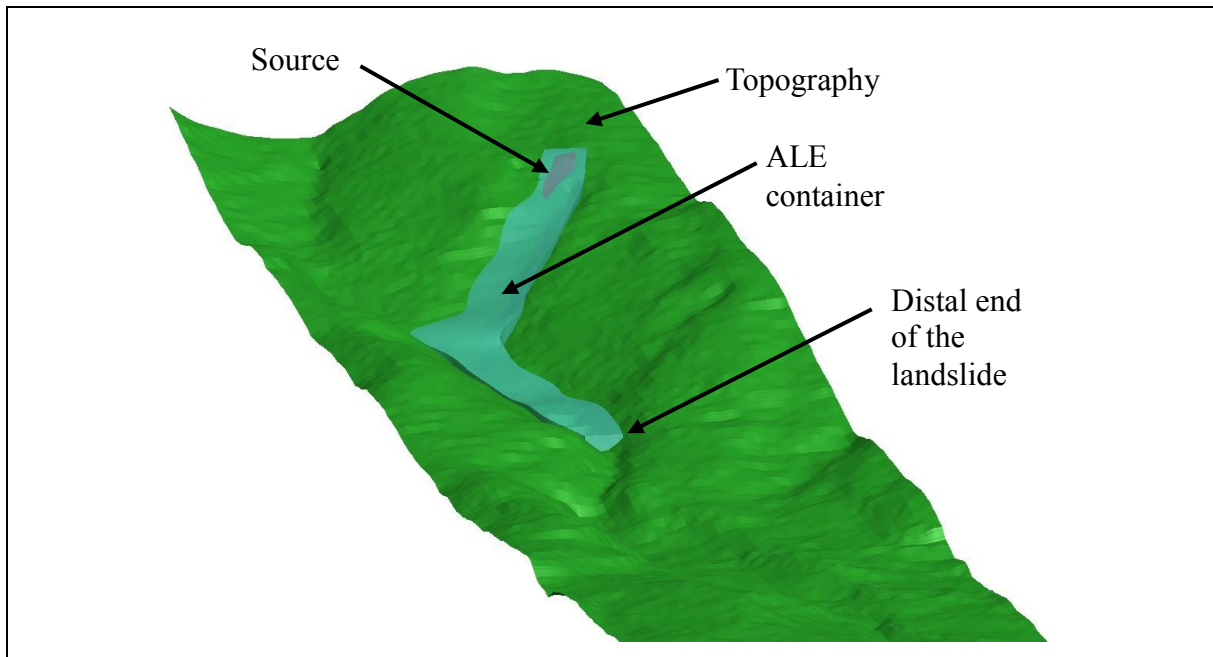


**Figure C7 LS-DYNA Model of the Kwun Yam Shan Debris Flow**

**Table C2 Input Parameters Adopted in the LS-DYNA Models of the Kwun Yam Shan Debris Flow**

Material Property	Adopted Input Parameters
Basal friction angle	15°
Voellmy turbulence coefficient	500 m/s <sup>2</sup>
Internal friction angle	20°

### C.2.3 Simulation Results

The LS-DYNA simulation with Voellmy resistance for the Kwun Yam Shan Debris Flow successfully predicted that the debris would stop at a location between the two pre-existing boulder dams. It calculated that debris could have reached this location at about 40 seconds after the landslide event. Figure C8 shows the simulation results of LS-DYNA, the results of 3d-DMM analysis by Kwan & Sun (2007) are also included for comparison. Figure C9 plots the calculated debris flow front location against time. The estimations of LS-DYNA and 3d-DMM are very similar.

At about 220 m from the landslide source, landslide debris changed its direction of movement following a sharp bend of the drainage line. MGS (2008) reports that a super-elevation of 6.8 m high was observed at this location. Figure C10 presents a cross-section at the location showing the calculated debris profile. LS-DYNA estimates that the super-elevation is 7.1 m high.



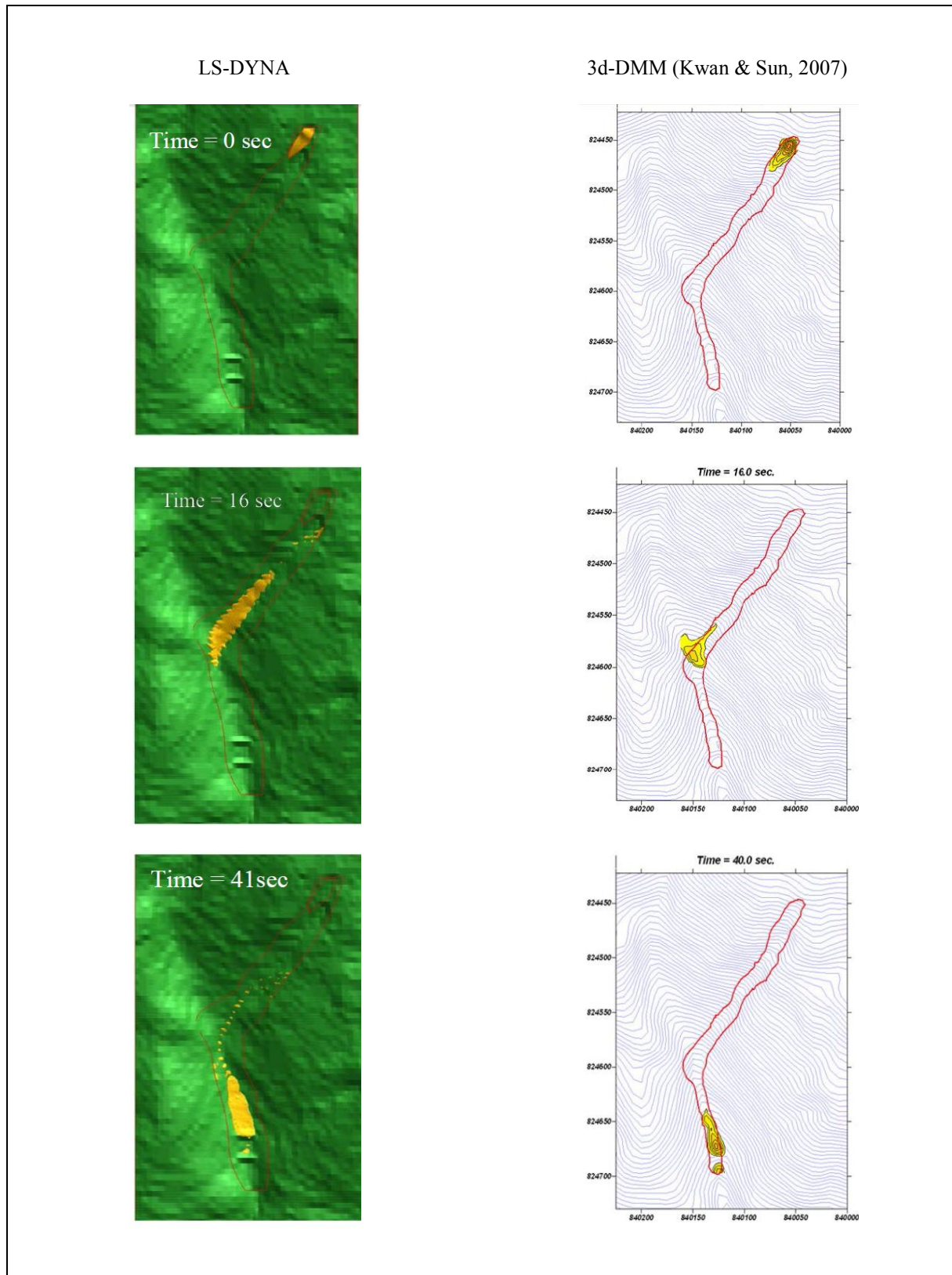


**Figure C8 Simulations of LS-DYNA Run and Comparison with the Results of 3d-DMM by Kwan & Sun (2007)**

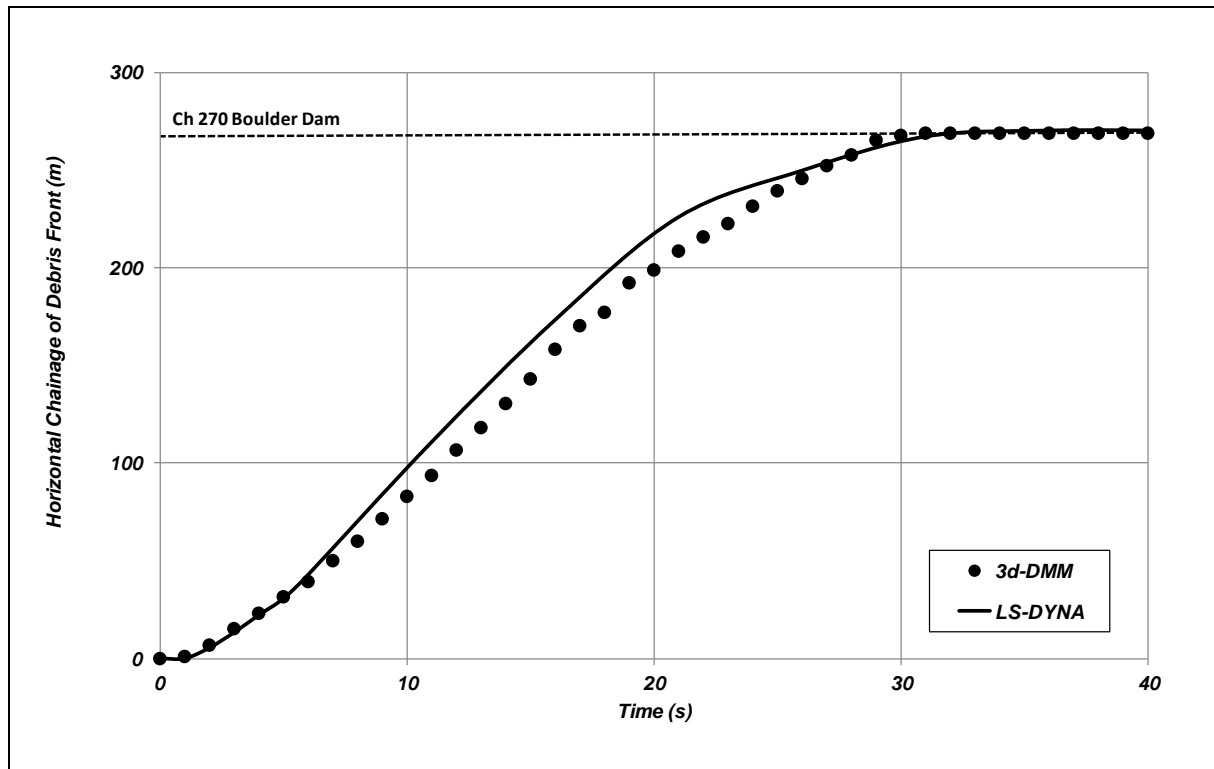


Figure C9 Debris Runout against Time

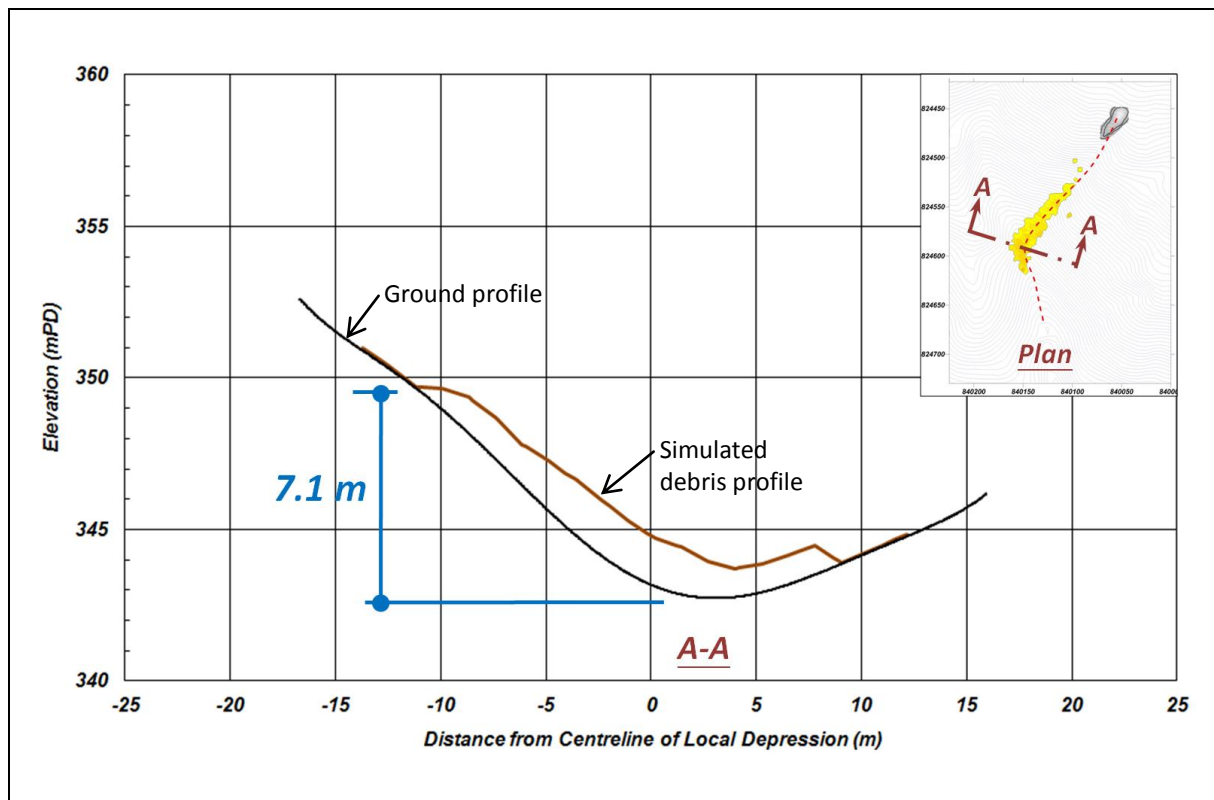
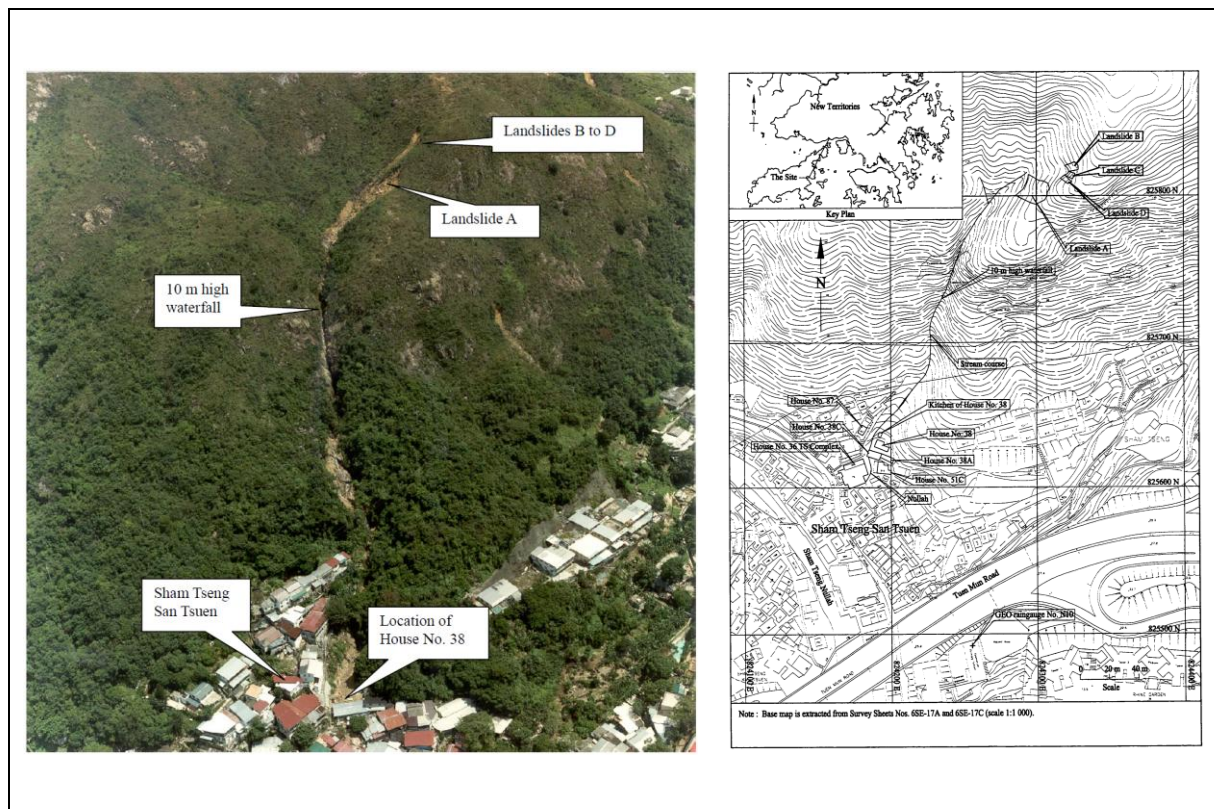


Figure C10 Section at Sharp Bend (Ch 220 m)

### C.3 Sham Tseng San Tsuen Debris Flow on 23 August 1999

#### C.3.1 Background

On 23 August 1999, landslides occurred at the natural hillside above Sham Tseng San Tsuen, giving rise to a debris flow down a stream course. The debris flow demolished a number of squatter dwellings constructed over, and in close proximity to, the stream course in Sham Tseng San Tsuen. One fatality was reported and 13 injured persons were rescued. Figure C11 shows the site layout plan and the aerial photograph after the incident. The landslide debris, of volume  $600 \text{ m}^3$ , ran into a streamcourse and developed into a channelised debris flow. The maximum gradient of some of the sections of the debris trail was over  $45^\circ$ . This could have resulted in a high degree of turbulence and low degree of basal friction within the debris flow. The landslides were probably caused by elevated water pressure within the slope-forming material following the severe rainfall that preceded the failures. Details of the incident were available in GEO Report No. 169 (FMSW, 2005).



**Figure C11 Site Layout Plan and the Aerial Photograph of Sham Tseng San Tsuen Debris Flow (FMSW, 2005)**

### C.3.2 LS-DYNA Model Setup

The dimensions of the ALE computational domain are 0.85 m (wide), 0.85 m (long) and 0.5 m (deep) and over 380,000 elements were used in the model. The topography was made up of shell materials of 1 m (wide)  $\times$  1 m (long). The method of internal stress initialization and the use of an artificial rigid tube and lid to confine debris materials at landslide source are the same as other LS-DYNA runs. The setup of the LS-DYNA model is shown in Figure C12.

A 2d-DMM mobility analysis of the debris flow has been carried out based on Voellmy rheology. Voellmy model with basal friction angle of  $9^\circ$  and turbulence coefficient of  $250 \text{ m/s}^2$  were adopted in the 2d-DMM analysis to match the debris frontal velocity determined from the super-elevations observed on site. Using the same basal friction angle and the same turbulence coefficient, a best fit internal friction angle of  $15^\circ$  for the LS-DYNA analysis was obtained. Key parameters which define the properties of the debris flow materials are listed in Table C3.

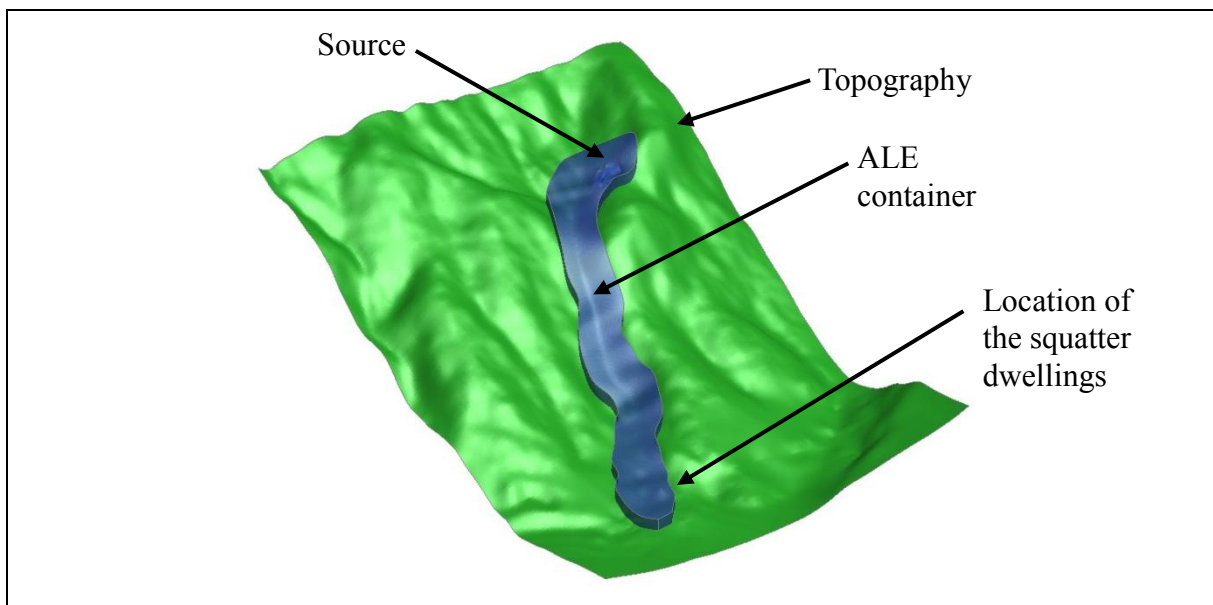


**Figure C12 LS-DYNA Model of the Sham Tseng San Tsuen Debris Flow**

**Table C3 Input Parameters Adopted in the LS-DYNA Models of the Sham Tseng San Tsuen Debris Flow**

Material Property	Adopted Input Parameters
Basal friction angle	$9^\circ$
Voellmy turbulence coefficient	$250 \text{ m/s}^2$
Internal friction angle	$15^\circ$



### C.3.3 Simulation Results

Figure C13 shows the calculated debris frontal velocity. Sensitivity runs using different combinations of rheological parameters are carried out. In all the runs, the average thickness of the debris flow for determining  $t$  was taken as 1.5 m to tally the field observation made by FMSW (2005). When using Voellmy turbulence coefficient of  $500 \text{ m/s}^2$ , the calculated debris frontal velocity exceeds the site observations (Run 13 and Run 16). It can be seen in general that LS-DYNA simulation Run 10 predicts a smoother debris velocity profile than the 2d-DMM results but both gave sufficiently close prediction of debris velocity as compared with the observed velocity at Ch 120 m and Ch 220 m. The results of Run 10 and Run 11 are similar, which indicate that basal friction angle in the range of  $9^\circ$  and  $11^\circ$  does not play a key role on varying the results.

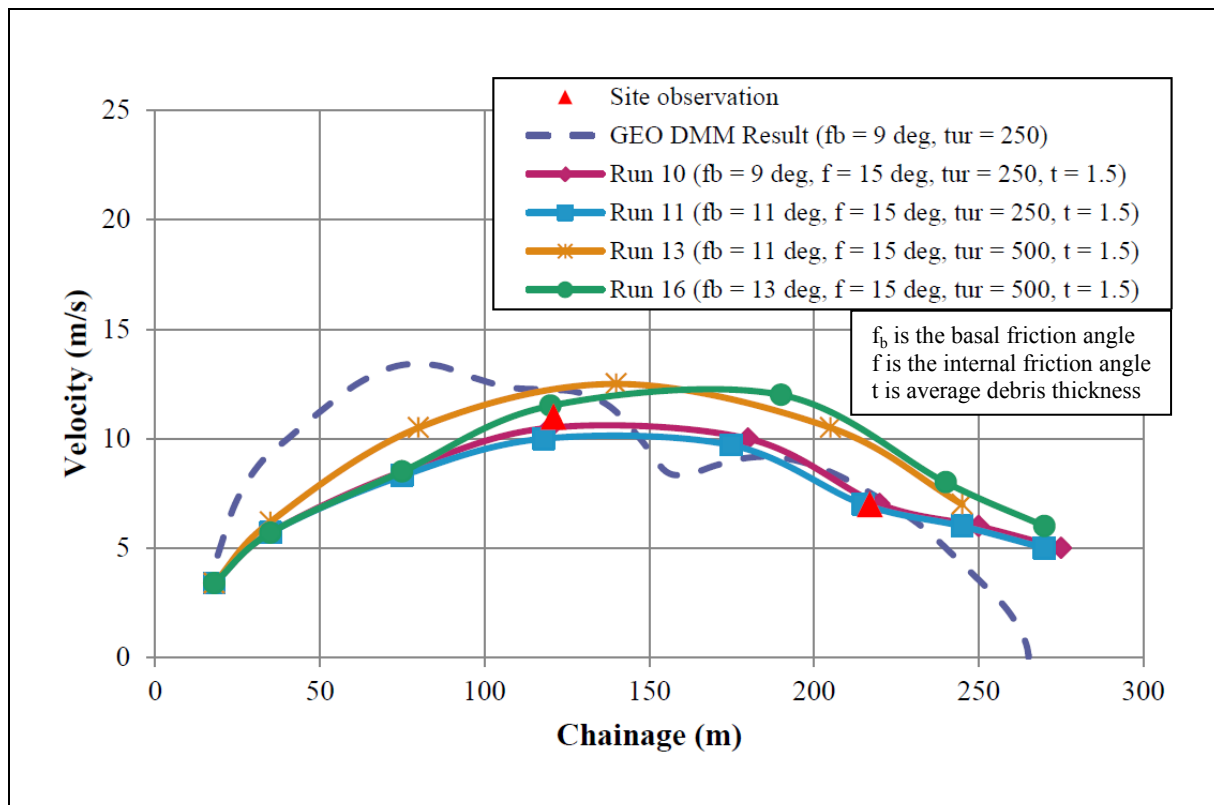


**Figure C13 Debris Frontal Velocity**

### C.4 References

- AECOM (2012). *Detailed Study of the 7 June 2008 Landslides on the Hillside above Yu Tung Road, Tung Chung (GEO Report No. 271)*. By AECOM Asia Company Limited. Geotechnical Engineering Office, Hong Kong, 124 p.
- FMSW (2005). *Report on the Debris Flow at Sham Tseng San Tsuen of 23 August 1999, Findings of the Investigation (GEO Report No. 169)*. By Fugro Maunsell Scott Wilson Joint Venture. Geotechnical Engineering Office, Hong Kong, 92 p.

- Kwan, J.S.H., Hui, T.H.H. & Ho, K.K.S. (2012). Modelling the motion of mobile debris flows in Hong Kong. *In Landslide Science and Practice, Volume 3: Spatial Analysis and Modelling*. Edited by C. Margottini, P. Canuti and K. Sassa. Springer-Verlag Berlin Heidelberg, pp 29-35.
- Kwan, J.S.H. & Sun, H.W. (2007). Benchmarking exercise on landslide mobility modeling – runout analysis using 3dDMM. *Proceedings of the 2007 International Forum on Landslide Disaster Management*, vol. II, pp 945-966.
- MGS (2008). *Detailed Study of the 22 August 2005 Landslide and Distress on the Natural Hillside at Kwun Yam Shan, below Tate's Ridge (GEO Report No. 239)*. By Maunsell Geotechnical Services Limited. Geotechnical Engineering Office, Hong Kong, 138 p.

## Appendix D

### Benchmarking with Other Advanced Programs

## Contents

	Page No.
Contents	79
List of Tables	80
List of Figures	81
D.1 Background of the Landslide	82
D.2 LS-DYNA Model Setup	82
D.3 Simulations and Results	84
D.4 References	86



**List of Tables**

Table No.		Page No.
D1	Input Parameters Adopted in the LS-DYNA Models of the Val Pola Landslide	83

**List of Figures**

Figure No.		Page No.
D1	Profile of the Val Pola Rock Avalanche (extracted from Crosta et al, 2003)	82
D2	LS-DYNA Model for the Val Pola Landslide	83
D3	LS-DYNA Simulation of the Landslide Deposition of the Val Pola Landslide	84
D4	Simulated Frontal Velocity Profiles against Time of the Val Pola Landslide by 3 Different Methods	85

## D.1 Background of the Landslide

The Val Pola landslide (Crosta et al, 2003 & 2004) occurred in Italy on 28 July 1987. Crosta et al (2004) reported that the velocity of the centre of mass determined using energy line approach was between 43 and 68 m/s. The landslide volume was in the order of 34 to 43 Mm<sup>3</sup>. It moved down the western valley flank to reach the valley bottom, raised for 300 m on the opposite valley flank and flowed both upstream and downstream (see Figure 4.1 of Section 4) along the valley. The landslide entrained 5 to 8 Mm<sup>3</sup> of debris along the track. The runout distance was about 1.5 km. The maximum debris deposit thickness was about 90 m (see Figure D1). Bulk weights between 19.8 and 21.6 kN/m<sup>3</sup> were determined and triaxial tests resulted indicated that the angle of internal friction ranged between 45° and 47°. The seismic motions associated with the landslide were recorded by a seismograph. Crosta et al (2004) conducted an interpretation of the seismic records and reported that the landslide could have reached the valley at 35 s after the landslide onset.

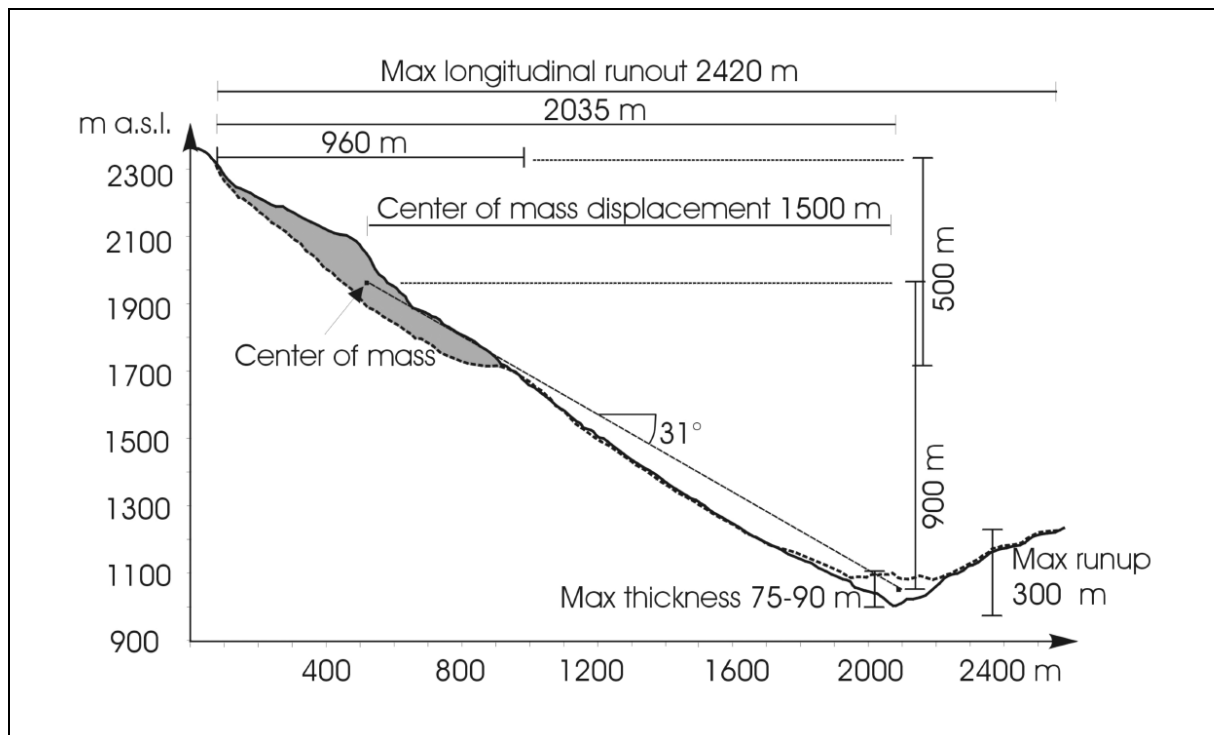


**Figure D1 Profile of the Val Polas Rock Avalanche (extracted from Crosta et al, 2003)**

## D.2 LS-DYNA Model Setup

A landslide source container is created to model the active volume of 40 million m<sup>3</sup>. The resolution of the topography shell elements is 20 m × 20 m. The resolution of the ALE container mesh is approximately 10 m (high) × 20 m × 20 m (plan) in rectangular shape. Vertical rigid shell elements are used to contain the volume of landslide debris at the source area. A lid is also created in the model to hold the landslide debris at the source area before debris mobility analysis started. Figure D2 shows the setup of the LS-DYNA model. The landslide source mass is released after the source container and the lid move upward by 50 m.

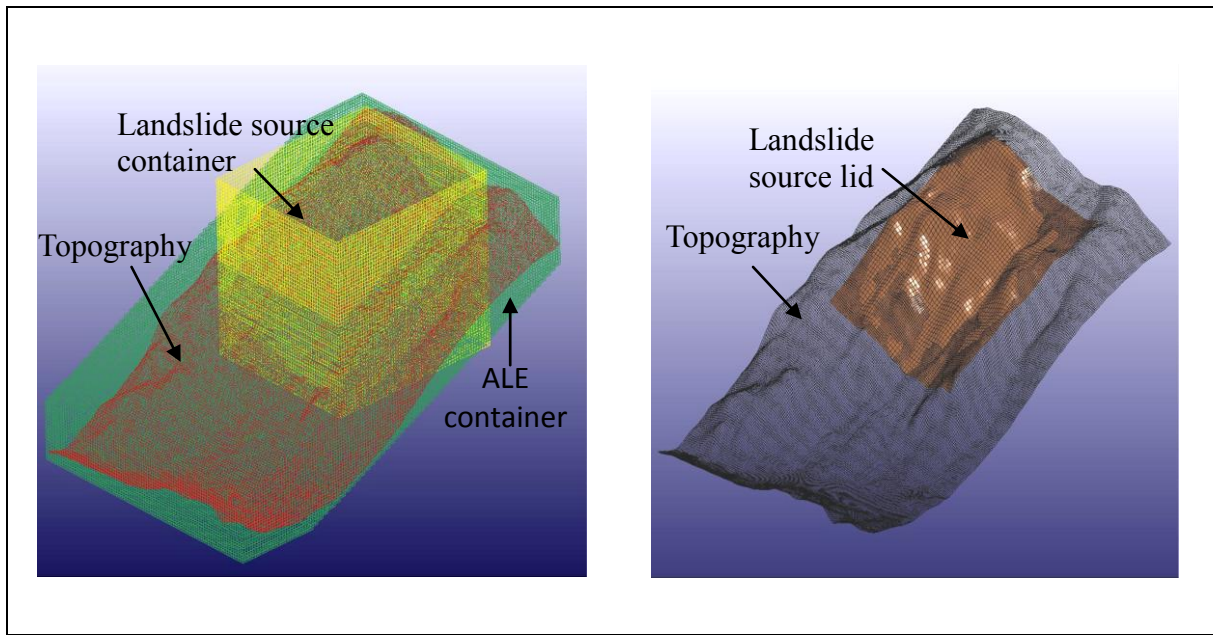


**Figure D2 LS-DYNA Model for the Val Pola Landslide**

Crosta et al (2003) used the program TOCHNOG to back-analyse the landslide. Drucker-Prager soil constitutive model was used. The back calculated basal friction angle of  $18^\circ$  and internal friction angle of  $45^\circ$  were reported. In the present study, the same basal friction angle and internal friction angle were adopted in the LS-DYNA model. Drucker-Prager soil constitutive model was also used. Other key input parameters adopted in the LS-DYNA analysis are summarised in Table D1.

**Table D1 Input Parameters Adopted in the LS-DYNA Models of the Val Pola Landslide**

Material Property	Adopted Input Parameters
Contact friction with the landslide	$18^\circ$
Internal friction angle	$45^\circ$
Material density	$2,100 \text{ kg/m}^3$
Shear modulus	6,000 kPa
Bulk Modulus	12,000 kPa

### D.3 Simulations and Results

Figure D3 shows the simulations of the landslide flow. The simulated debris slide down along the slope and reaches the valley and then spreads out laterally as observed in the field. LS-DYNA also replicates the flow separation observation at the southern flank of the landslide. The front of debris runs up to a maximum height of about 280 m on the opposite side of the valley in the LS-DYNA simulation which is consistent with the site measurement of about 300 m reported by Crosta et al (2003 & 2004).

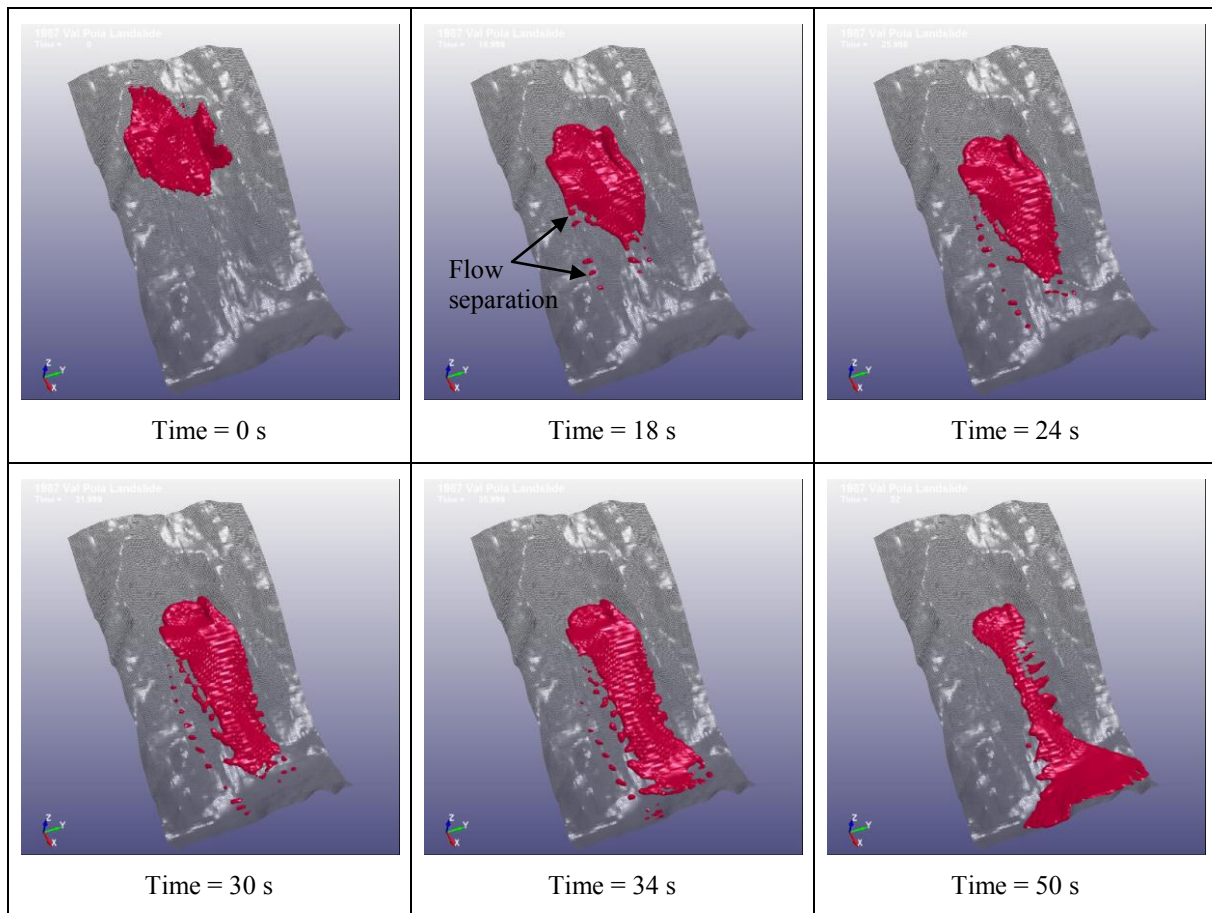


**Figure D3 LS-DYNA Simulation of the Landslide Deposition of the Val Pola Landslide**

Crosta et al (2003 & 2004) used TOCHNOG and MADflow respectively to simulate the Val Pola landslide. The TOCHNOG model adopted by Crosta et al (2003) is a type of combined Eulerian-Lagrangian method that can avoid large distortions of the finite element mesh. Crosta et al (2003) carried out a plain strain analysis (i.e. 2-dimensional analysis). Flow velocity along the debris depth had been calculated. However, debris width was not considered in the analysis.

The MADflow model adopted by Crosta et al (2004) referred to a (quasi) 3-dimensional dynamic model using the Lagrangian frame of reference. The model applies depth-integrated laws of mass and momentum conservation approach. In the MADflow

model, a finite moving mass is represented by a column connecting with the adjacent ones. The plan geometry of the columns is free to deform but volumes of debris column conserve when sliding down a slope. The properties of debris remain constant through material columns and no intra-column exchange of internal flow of debris material is considered.

Figure D4 shows the frontal velocity produced by using the three programs viz. TOCHNOG, MADflow and LS-DYNA. The plotted maximum velocity data refer to the depth average velocity along the centreline of the coherent frontal portion of the simulated landslide debris. The prediction by MADflow gives higher velocity than the other two methods before reaching the valley at about 34 s. This is caused by the use of the lowest internal friction angle of  $35^\circ$  in MADflow instead of  $45^\circ$  in the other programs LS-DYNA and TOCHNOG. TOCHNOG gives relatively lower velocity prediction than LS-DYNA and MADFlow. Crosta et al (2004) commented that the 2-dimensional plane-strain idealisation of the TOCHNOG analysis could have under-predicted the debris velocity, as the analysis ignored the effects of change in flow direction and lateral spreading. In general, LS-DYNA gives a good matching with the measured arrival time of debris at the toe of slope and reproduces a flow separation as observed at the southern flank of the landslide.

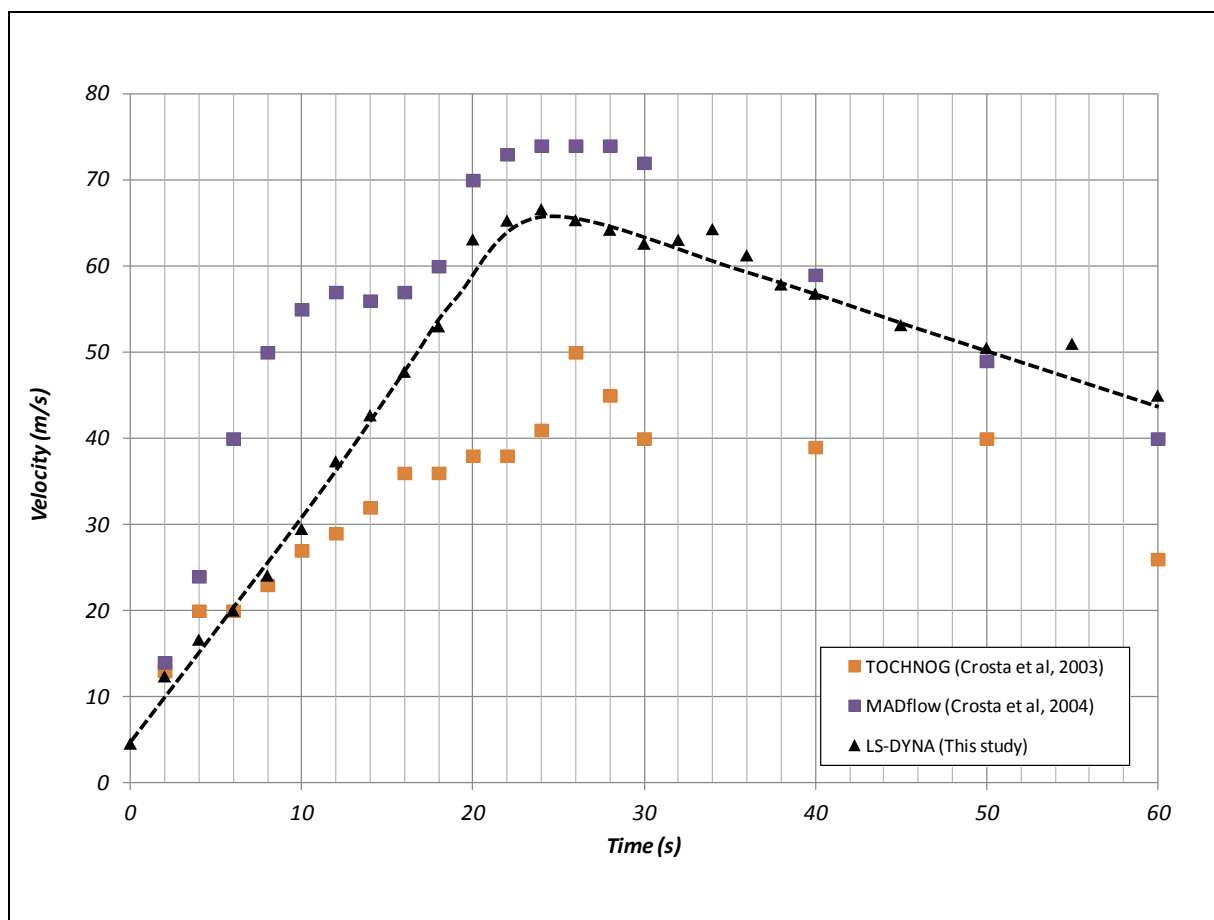


**Figure D4 Simulated Frontal Velocity Profiles against Time of the Val Pola Landslide by 3 Different Methods**

#### **D.4 References**

- Crosta, G.B., Chen, H. & Lee, C.F. (2004). Replay of the 1987 Val Pola Landslide, Italian Alps. *Geomorphology*, vol. 60, pp 127-146.
- Crosta, G.B., Imposimato, S. & Roddeman, D.G. (2003). Numerical modelling of large landslides stability and runout. *Natural Hazards and Earth System Sciences*, vol. 3, pp 523-538.

## Appendix E

### Yield Function Coefficients of Drucker-Prager Constitutive Model



**Contents**

	Page No.
Contents	88
E.1 Derivation of Drucker-Prager Model Input	89

### E.1 Derivation of Drucker-Prager Model Input

The Drucker-Prager (D-P) yield criterion can be expressed as:

$$\sqrt{J_2} = A + BI_1 \quad \text{..... (E.1)}$$

where  $I_1$  = the first invariant of the Cauchy stress  
 $J_2$  = the second invariant of the deviatoric part of the Cauchy stress  
 $A, B$  = material constants.

Equation E.1 can also be expressed in terms of Haigh-Westergaard coordinates:

$$\frac{1}{\sqrt{2}}\rho - \sqrt{3}B \zeta = A \quad \text{..... (E.2)}$$

where  $\rho = \sqrt{2J_2}$  and  $\zeta = \frac{1}{\sqrt{3}}I_1$ .

The Mohr-Coulomb (M-C) yield criterion expressed in Haigh-Westergaard coordinates is:

$$\left[ \sqrt{3} \sin\left(\theta + \frac{\pi}{3}\right) - \sin\phi \cos\left(\theta + \frac{\pi}{3}\right) \right] \rho - \sqrt{2} \sin(\phi) \zeta = \sqrt{6} c \cos\phi \quad \text{..... (E.3)}$$

where  $\theta$  = Lode angle and  $\phi$  = internal friction angle of the material.

If the D-P and M-C yield surfaces are assumed to coincide at pure shear mode, that is,  $\theta = \frac{\pi}{6}$ , Equation E.3 then becomes:

$$\sqrt{3}\rho - \sqrt{2} \sin(\phi) \zeta = \sqrt{6} c \cos\phi \quad \text{..... (E.4)}$$

Rearranging this equation to match the form of Equation E.3:

$$\frac{1}{\sqrt{2}}\rho - \frac{\sin(\phi)}{\sqrt{3}}\zeta = c \cos\phi \quad \text{..... (E.5)}$$

Thus,

$$A = c \cos(\phi)$$

$$B = \frac{\sin(\phi)}{3}$$

The back analyses conducted in this study adopt Material Model No. 5 (Soil and Foam) of LS-DYNA. The yield criterion of this material model is expressed as:

$$J_2 = a_0 + a_1 p + a_2 p^2 \quad \text{..... (E.6)}$$

Rearranging Equation E.1 gives:

$$J_2 = A^2 + 2AB + B^2 I_1^2$$

Since  $p = \frac{I_1}{3}$ ,

$$J_2 = A^2 + 6ABp + 9B^2 p^2 \dots\dots\dots (E.7)$$

Comparing Equations E.6 and E.7 gives:

$$a_0 = A^2 = c^2 \cos^2(\phi) \dots\dots\dots (E.8)$$

$$a_1 = 6AB = 2c \sin(\phi) \cos(\phi) \dots\dots\dots (E.9)$$

$$a_2 = 9B^2 = \sin^2(\phi) \dots\dots\dots (E.10)$$

where  $a_0$ ,  $a_1$  and  $a_2$  are the yield parameters to be input to LS-DYNA. They should be calculated following Equations E.8 to E.10 based on a specific  $\phi$  value.

## GEO PUBLICATIONS AND ORDERING INFORMATION

### 土力工程處刊物及訂購資料

A selected list of major GEO publications is given in the next page. An up-to-date full list of GEO publications can be found at the CEDD Website <http://www.cedd.gov.hk> on the Internet under "Publications". Abstracts for the documents can also be found at the same website. Technical Guidance Notes are published on the CEDD Website from time to time to provide updates to GEO publications prior to their next revision.

**Copies of GEO publications (except geological maps and other publications which are free of charge) can be purchased either by:**

Writing to  
Publications Sales Unit,  
Information Services Department,  
Room 626, 6th Floor,  
North Point Government Offices,  
333 Java Road, North Point, Hong Kong.

or

- Calling the Publications Sales Section of Information Services Department (ISD) at (852) 2537 1910
- Visiting the online Government Bookstore at <http://www.bookstore.gov.hk>
- Downloading the order form from the ISD website at <http://www.isd.gov.hk> and submitting the order online or by fax to (852) 2523 7195
- Placing order with ISD by e-mail at [puborder@isd.gov.hk](mailto:puborder@isd.gov.hk)

**1:100 000, 1:20 000 and 1:5 000 geological maps can be purchased from:**

Map Publications Centre/HK,  
Survey & Mapping Office, Lands Department,  
23th Floor, North Point Government Offices,  
333 Java Road, North Point, Hong Kong.  
Tel: (852) 2231 3187  
Fax: (852) 2116 0774

**Requests for copies of Geological Survey Sheet Reports and other publications which are free of charge should be directed to:**

For Geological Survey Sheet Reports which are free of charge:  
Chief Geotechnical Engineer/Planning,  
(Attn: Hong Kong Geological Survey Section)  
Geotechnical Engineering Office,  
Civil Engineering and Development Department,  
Civil Engineering and Development Building,  
101 Princess Margaret Road,  
Homantin, Kowloon, Hong Kong.  
Tel: (852) 2762 5380  
Fax: (852) 2714 0247  
E-mail: [jsewell@cedd.gov.hk](mailto:jsewell@cedd.gov.hk)

For other publications which are free of charge:  
Chief Geotechnical Engineer/Standards and Testing,  
Geotechnical Engineering Office,  
Civil Engineering and Development Department,  
Civil Engineering and Development Building,  
101 Princess Margaret Road,  
Homantin, Kowloon, Hong Kong.  
Tel: (852) 2762 5346  
Fax: (852) 2714 0275  
E-mail: [florenceko@cedd.gov.hk](mailto:florenceko@cedd.gov.hk)

部份土力工程處的主要刊物目錄刊載於下頁。而詳盡及最新的土力工程處刊物目錄，則登載於土木工程拓展署的互聯網網頁 <http://www.cedd.gov.hk> 的“刊物”版面之內。刊物的摘要及更新刊物內容的工程技術指引，亦可在這個網址找到。

**讀者可採用以下方法購買土力工程處刊物(地質圖及免費刊物除外):**

書面訂購  
香港北角渣華道333號  
北角政府合署6樓626室  
政府新聞處  
刊物銷售組

或

- 致電政府新聞處刊物銷售小組訂購 (電話: (852) 2537 1910)
- 進入網上「政府書店」選購，網址為 <http://www.bookstore.gov.hk>
- 透過政府新聞處的網站 (<http://www.isd.gov.hk>) 於網上遞交訂購表格，或將表格傳真至刊物銷售小組 (傳真: (852) 2523 7195)
- 以電郵方式訂購 (電郵地址: [puborder@isd.gov.hk](mailto:puborder@isd.gov.hk))

**讀者可於下列地點購買1:100 000、1:20 000及1:5 000地質圖：**

香港北角渣華道333號  
北角政府合署23樓  
地政總署測繪處  
電話: (852) 2231 3187  
傳真: (852) 2116 0774

**如欲索取地質調查報告及其他免費刊物，請致函：**

免費地質調查報告:  
香港九龍何文田公主道101號  
土木工程拓展署大樓  
土木工程拓展署  
土力工程處  
規劃部總土力工程師  
(請交:香港地質調查組)  
電話: (852) 2762 5380  
傳真: (852) 2714 0247  
電子郵件: [jsewell@cedd.gov.hk](mailto:jsewell@cedd.gov.hk)

其他免費刊物:  
香港九龍何文田公主道101號  
土木工程拓展署大樓  
土木工程拓展署  
土力工程處  
標準及測試部總土力工程師  
電話: (852) 2762 5346  
傳真: (852) 2714 0275  
電子郵件: [florenceko@cedd.gov.hk](mailto:florenceko@cedd.gov.hk)

## **MAJOR GEOTECHNICAL ENGINEERING OFFICE PUBLICATIONS**

### **土力工程處之主要刊物**

#### **GEOTECHNICAL MANUALS**

Geotechnical Manual for Slopes, 2nd Edition (1984), 302 p. (English Version), (Reprinted, 2011).

斜坡岩土工程手冊(1998)，308頁(1984年英文版的中文譯本)。

Highway Slope Manual (2000), 114 p.

#### **GEOGUIDES**

Geoguide 1 Guide to Retaining Wall Design, 2nd Edition (1993), 258 p. (Reprinted, 2007).

Geoguide 2 Guide to Site Investigation (1987), 359 p. (Reprinted, 2000).

Geoguide 3 Guide to Rock and Soil Descriptions (1988), 186 p. (Reprinted, 2000).

Geoguide 4 Guide to Cavern Engineering (1992), 148 p. (Reprinted, 1998).

Geoguide 5 Guide to Slope Maintenance, 3rd Edition (2003), 132 p. (English Version).

岩土指南第五冊 斜坡維修指南，第三版(2003)，120頁(中文版)。

Geoguide 6 Guide to Reinforced Fill Structure and Slope Design (2002), 236 p.

Geoguide 7 Guide to Soil Nail Design and Construction (2008), 97 p.

#### **GEOSPECS**

Geospec 1 Model Specification for Prestressed Ground Anchors, 2nd Edition (1989), 164 p. (Reprinted, 1997).

Geospec 3 Model Specification for Soil Testing (2001), 340 p.

#### **GEO PUBLICATIONS**

GCO Publication No. 1/90 Review of Design Methods for Excavations (1990), 187 p. (Reprinted, 2002).

GEO Publication No. 1/93 Review of Granular and Geotextile Filters (1993), 141 p.

GEO Publication No. 1/2006 Foundation Design and Construction (2006), 376 p.

GEO Publication No. 1/2007 Engineering Geological Practice in Hong Kong (2007), 278 p.

GEO Publication No. 1/2009 Prescriptive Measures for Man-Made Slopes and Retaining Walls (2009), 76 p.

GEO Publication No. 1/2011 Technical Guidelines on Landscape Treatment for Slopes (2011), 217 p.

#### **GEOLOGICAL PUBLICATIONS**

The Quaternary Geology of Hong Kong, by J.A. Fyfe, R. Shaw, S.D.G. Campbell, K.W. Lai & P.A. Kirk (2000), 210 p. plus 6 maps.

The Pre-Quaternary Geology of Hong Kong, by R.J. Sewell, S.D.G. Campbell, C.J.N. Fletcher, K.W. Lai & P.A. Kirk (2000), 181 p. plus 4 maps.

#### **TECHNICAL GUIDANCE NOTES**

TGN 1 Technical Guidance Documents